Effects of bending stiffness on localized bulging in a pressurized hyperelastic tube.

Geethamala Sarojini Francisco

Submitted in partial fulfilment of the requirements of the degree of PhD

School of Computing and Mathematics, Keele University.

June 2016

Acknowledgement

I am greatly indebted to Professor Yibin Fu in the Mathematics Department of Keele University for his support and guidance throughout my stay in the University. I have been greatly benefited from him in composing this thesis.

I would also like to thank everyone in the Mathematics Department, particularly Andrew for their friendship and help.

And finally I would like to thank my husband Aravinda Jayawardena for his endurance, patience and understanding and my son Upeshala Akalanka for his love. All of them gave me a pleasant and encouraging environment for me to complete the thesis.

Abstract

The problem of localised bulging in inflated thin-walled tubes has been studied by many authors. In all these studies, the strain-energy function is expressed only in term of principal stretches. However, there are some applications where the cylindrical tube concerned may have walls thick enough so that the membrane theory may become invalid. One such situation that motivates the present study is the mathematical modeling of aneurysm initiation; in that context the human arteries exhibit noticeable bending stiffness. The effects of bending stiffness on localized bulging are studied using two different approaches.

The first approach is related to the continuum-mechanical theory for three-dimensional finite deformations of coated elastic solids formulated by Steigmann and Ogden (1997, 1999). Strain-energy function has been defined in terms of the curvature of the middle surface and the principal stretches. The elasticity of the coating incorporates bending stiffness and generalizes the theory of Gurtin and Murdoch (1975). A bifurcation condition is derived using a weakly non-linear analysis and the near-critical behaviour is determined analytically. A finite difference scheme and a shooting method are formulated to determine the fully non-linear bulging solutions numerically.

The second approach is based on the exact theory of finite elasticity, and the tube concerned is assumed to have arbitrary thickness. The exact bifurcation condition is derived and used to quantify the effects of bending stiffness. A two-term asymptotic bifurcation condition that incorporates bending stiffness is also derived. Finally, it is shown that when the axial force is held fixed, the bifurcation pressure is equal to the maximum pressure in uniform inflation. However when the axial stretch is

fixed, localized solution is possible even if the pressure does not have a maximum in uniform inflation. This last result is particularly relevant to the continuum-mechanical modelling of the initiation of aneurysms in human arteries.

Contents

List of Figures

1 Introduction

1.1 Background and Motivations

This thesis is concerned with localized bulging in an elastic membrane, a thin-walled or thick-walled cylindrical tube that is subject to the combined action of internal inflation and axial extension. We shall assume that the tube is long enough so that the end effects can be neglected and we focus on the main section of the tube away from either of the two ends. Thus, for our purpose the tube is effectively infinitely long. We shall

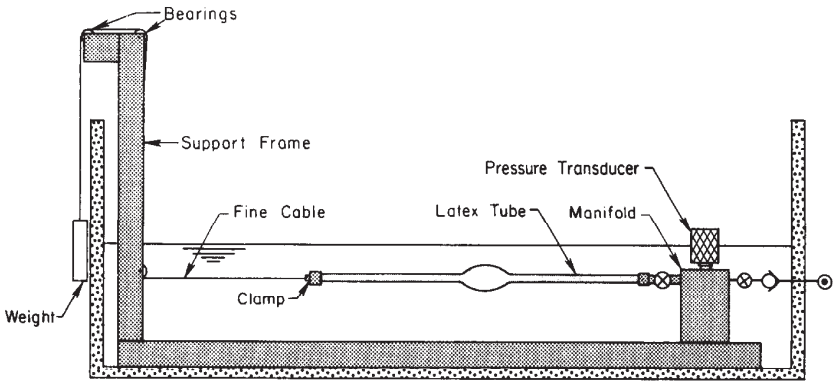

Fig. 2. Experimental set-up.

Figure 1.1.1: Experimental setup of Kyriakides and Chang (1991).

also assume that during inflation either the axial force or axial stretch is fixed. The former corresponds to the situation when one end is fixed but the other end is closed and free to move, and may or may not be subjected to the extra pulling of a dead

weight. Such a setup was used in the experiments of Kyriakides & Chang (1991); see Figure 1.1.1. This is also how one would usually inflate a tubular party balloon. The latter case of a fixed axial stretch corresponds to the situation when the tube is first subjected to an axial extension and then both ends are fixed. Such a setup was used in the experiments of Goncalves et al. (2008); see Figure 1.1.2. Our aim is to understand how bending stiffness affects the initiation pressure and the determination of the weakly non-linear and fully non-linear bulging solutions.

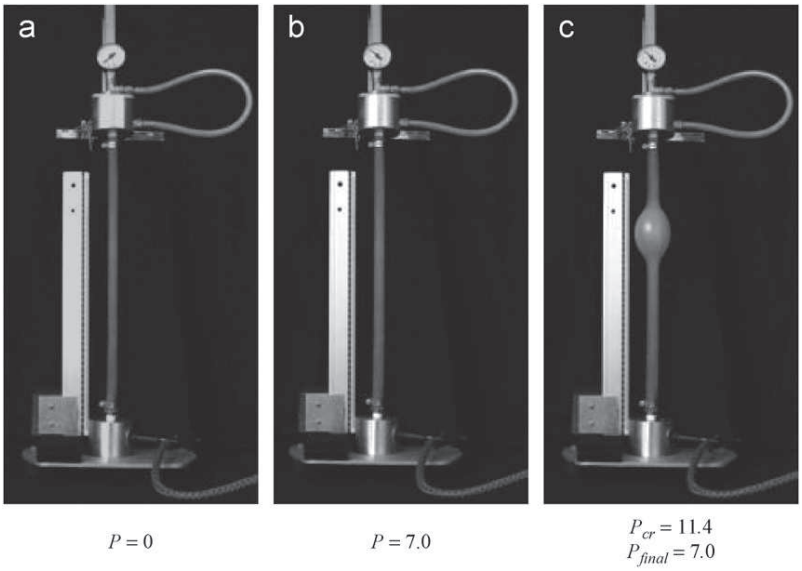

Figure 1.1.2: Experimental setup of Goncalves *et al.* (2008).

1.1.1 Inflation of a membrane tube

By a membrane tube we mean a tube that has no bending stiffness. In most applications, this assumption provides a good approximation and the theory based on this

assumption is able to capture most of the important features. When such an elastic membrane tube is inflated by an internal pressure, the tube inflates cylindrically until the pressure reaches a critical value. At this point, the cylindrical configuration becomes unstable and a bulge forms at one point of the tube. With continued inflation, the pressure drops gradually but the diameter of the bulge increases until it reaches the maximum size. Further inflation causes the bulge to spread laterally along the tube at a constant propagation pressure. The bulging solution before propagation is of solitary wave type whereas the propagating bulging solution is of the kink wave type. This process is well known and has been studied experimentally, analytically and numerically by many authors.

Localized bulging in inflated membrane tubes was first studied by Mallock (1891) and later studied experimentally and numerically by Kyriakides & Chang (1990, 1991), Pamplona et al. (2006), Goncalves et al. (2008), and Shi & Moita (1996). The propagation stage was recognized by Yin (1977) and Chater & Hutchinson (1984) as a two-phase deformation governed by Maxwell's equal area rule, but the character of the initiation stage, and its connection with the so-called limit-point instability, Alexander (1971) and Kanner and Horgan (2007) was not fully understood until more recently. In the early stability and buckling analysis of a hyperelastic cylindrical tube that is subjected to the combined action of internal inflation and axial stretching/compression, attention was mainly focused on periodic perturbations/patterns; see, for instance, Haughton & Ogden (1979a, b). The special case when the axial mode number is zero was thought to correspond to a bifurcation into another uniformly inflated configuration, and thus to have no relevance to localized bulging. However, it was recognized by Fu *et al* (2008) and Pearce & Fu (2010) that it is precisely this zero mode number case

that corresponds to localized bulging when non-linear effects are brought into play. It was further shown in Fu & Ilichev (2015) that in the case of fixed resultant axial force, the initiation pressure for localized bulging corresponds to the maximum pressure in uniform inflation, but this correspondence may no longer hold when other loading conditions are applied at the ends. In particular, when the axial stretch is fixed during inflation, localized bulging may occur even if the pressure in uniform inflation does not have a maximum.

The study by Kyriakides & Chang (1990) is performed under pressure control using compressed air, where the tube inflates cylindrically until a limiting pressure is reached. After this limiting pressure is reached, a bulge forms at one point of the tube with decrease in the radius elsewhere. After the bulge has filled the tube the inflation continues in a uniform manner, with an increasing pressure. While the non-uniformity is localized in this way, the remainder of the tube remains uniform. They named the initiation pressure at which bulging occurs as the limiting pressure corresponding to the first turning point of the pressure volume diagram for uniform inflation. However, the theoretical value was found to be slightly higher than what had been observed in their experiments. These experiments are consistent with those described by Alexander (1971). Pamplona et al. (2006) investigate the inflation of pre-stretched rubber tubes, showing the bulging behaviour as discussed above, along with the corresponding decrease in pressure.

In Kyriakides & Chang (1991), the deformation is volume controlled by filling the tube with water, where the tube was compressed internally with a fluid pressure and stretched externally by an axial tensile load at the two closed ends. They recognised that this process shared the same behaviour as described for the earlier pressure control

case of Kyriakides & Chang (1990). For the same problem, a stability study was carried out by Fu & Xie (2010). Their results were consistent with the experimental results of Kyriakides & Chang (1991). Stability studies are important because a bulge can be observed only if it is stable under environmental perturbations. Stability of an inflated membrane tube under pressure control has previously been studied by Pearce & Fu (2010). Recently, Fu & Xie (2012) showed that the initiation of localized bulging in inflated membrane tubes is more sensitive to material and geometrical imperfections than classical sub-critical bifurcations into sinusoidal patterns. Existence, persistence and the role of axial displacement on solitary waves in fluid filled elastic tubes was studied by Fu & IIichev (2015).

Goncalves et al. (2008) investigated the deformation of thick-walled cylindrical shells with $3/4 \leq H/R \leq 3/2$ under internal pressure where H and R are the wall thickness and radius respectively. In their experiment, the tube is first subjected to an axial extension, as illustrated in Figure 1.1.2. They extended their work to include a fixed axial stretch by fixing both ends of the tube.

Haughton & Ogden (1979a,1979b) examined the bifurcations in the cases where the bifurcation modes are either prismatic or axisymmetric. The deformation produced in a circular cylindrical configuration of an elastic tube of finite wall thickness subjected to a uniform axial loading combined with a uniform internal pressure was analysed by Haughton & Ogden (1979b). This extends the analysis given by Haughton & Ogden (1979a) for membrane tubes. Haughton & Ogden (1979b) stated that the bifurcation, if it exists, occurs before the pressure maximum, for the case of an infinite tube with fixed axial stretch. Kyriakides & Chang (1991) solve the differential equations for the membrane tube numerically for various strain-energy functions, and find good

agreement with their experimental results, where the ratio of thickness to radius for the rubber tubes involved was approximately one quarter.

An elastic shell is a three-dimensional body occupying a thin neighbourhood of a two-dimensional manifold, which resists deformation due to the material of which it is made, its shape, and boundary condition. Although the deformation of a shell arising in response to given internal or external loads and boundary conditions can be accurately captured by solving the three-dimensional elasticity equations, shell theory attempts to provide a two-dimensional representation of the three-dimensional phenomenon (Koiter & Simmonds 1973, Kaplunov et al. 1998, Goldenveizer 1961, Berdichevskii 1970, Le K.C. 1999).

There is a big literature devoted to dimensional reduction in elasticity theory. One approach starts with a priori assumptions on the displacement and stress fields based on mechanical considerations, such as the Kirchhoff-Love assumption on the displacements and the kinetic assumption on the stress fields that assumes that both the transverse shear and normal stresses are negligible. In 1888 Love proposed a theory of shells using the Kirchhoff assumptions that every straight line perpendicular to the mid-surface remain straight after deformation and perpendicular to the mid-surface, all elements of the mid-surface remain unstretched, and the thickness of the plate does not change during deformation. By this examination, Love was able to produce a set of linear equations of motion and boundary conditions for shells experiencing both infinitesimal extensional and bending strains from three-dimensional elasticity theory. This theory was known as the Kirchhoff-Love theory of shells, a two dimensional first order approximation theory, and at the time was the foremost complete and general linear theory of thin elastic shells. Loves shell theory and solutions to various shell

problems have been improved and justified using asymptotic analysis by Kaplunov et al. (1998), Green (1963), Kolos (1965), Friedrichs (1955a). Another approach is to view the thickness of the elastic body as a small parameter. The book by Ciarlet (1997) contains a comprehensive treatment of this approach. Throughout this thesis the second approach will be used. Libai & Simmonds (1998) defined membrane as a thin shell which has negligible resistance to bending, where bending moments and transverse shears are considered insignificant compared to in-plane loadings.

A non-linear theory for two or three-dimensional finite deformations of coated elastic solids was formulated by Steigmann & Ogden (1997,1999). The response of the coating was modelled by introducing a strain-energy function that depends on stretching and curvature of the coated part of the boundary curve/surface. This theory can be related to the engineering thin shell theory that takes into account bending stiffness. Plane strain deformation for such coated elastic solids was studied by Steigmann & Ogden (1997), whereas the deformation of an axisymmetric two-dimensional elastic surface embedded into three-dimensional space, subject to axisymmetric deformation was studied by Steigmann & Ogden (1999). These two authors identified that a surface model that does not account for bending stiffness cannot be used to simulate local surface features engendered by the response of the solids to compressive surface stress of any magnitude. Ogden et al. (1997) defined a two-dimensional theory for a thick-walled circular cylindrical tube which is subjected to an internal and external pressure. They showed that the maximum pressure was followed by a minimum during the inflation for an uncoated tube and it was a monotonic increasing function of the radius for the coated tube. The elasticity of the coating incorporates bending stiffness and in this sense generalizes the theory of Gurtin and Murdoch (1975).

Heil and co-workers investigated the steady deformations of the fully coupled three-dimensional system in another series of studies (Heil 1996, Heil & Pedley 1995, Heil & Pedley 1996) and the non-linear shell theory was used to describe the large non-axisymetric post-buckling deformations. The wall of the tube was modelled as a circular cylindrical shell and geometrically non-linear shell theory was used to describe the large non-axisymmetric post-buckling deformation.

For biological materials, large deformations often occur, and in this case a fully non-linear problem formulation is essential. To facilitate the solutions of such problems, simplifications are often made, such as the adoption of thin shell theories, which have been successful for describing thin-walled structures; see, e.g., Libai & Simmonds (1998), Yamaki (1969) and Yamaki (1984).

Erbay & Demiray (1995) considered the finite axisymmetric deformation of a circular cylindrical tube of Neo-Hookean material by using an asymptotic expansion method. Their perturbation solution is based on the smallness of the ratio of thickness to the inner radius of the tube. Normal and tangential tractions were applied on the inner surface of the tube but no boundary conditions were considered at the ends of the tube. Heil & Pedley (1995) performed a numerical simulation of the post-buckling behaviour of tubes under external pressure.

1.1.2 Aneurysms and its mathematical modelling

An aneurysm is a bulge in a blood vessel that is caused by a weakness in its wall. The pressure of the blood passing through the weakened blood vessel causes it to

bulge outward like a balloon. Aneurysms can happen in any part of the body but the most common place is the brain or part of the aorta, the largest blood vessel in the body. Our current study is particularly relevant to explaining the initial formation of abdominal aortic aneurysms (AAAs). The abdominal aorta is the section of the aorta in the abdomen, between the rental arteries that supplied blood to the kidney. Once an aneurysm has formed, it may grow in diameter with time at a mean rate that is initially slow and then increases exponentially, terminating in a rupture when the arterial wall's structure can no longer support the stress and causing a huge internal bleeding. The bulging occurs when the wall of the aorta weakens. The most common symptoms of an aortic aneurysm are sudden and sever stomach or back pain. Smoking, hypertension, excessive alcohol consumption and high blood pressure are the main factors that increase the risk of an aneurysm. AAAs occur most commonly in men aged over 65.

The clinical study of aneurysm behaviour has been investigated for 250 years (McGloughlin 2011). However, the parameters of aneurysm geometry which can serve as reliable factors in changing the mechanical behaviour of arteries before aneurysm formation is still not clearly understood. Both fluid dynamicists and solid mechanicians have attempted to provide an explanation for aneurysm formation. Some studies by fluid dynamicists on the mechanics of aneurysm growth and rapture have focused on the role of blood flow and loading in terms of blood pressure using oversimplified models for the arterial wall which do not account precisely the elastic properties of the wall; see, e.g., Lasheras (2007) and Duclaux et al (2010). On the other hand, the non-linear behaviour of the arterial walls and the growth of an aneurysm once it has already formed were studied by solid mechanicians by ignoring the existence of blood flows;

see, e.g., Humphrey (2004), Watton et al (2004) and, Vorp (2007). Localized standing waves in a hyperelastic membrane tube and their stabilization by a mean flow was studied by Fu & Ilichev (2015).

Aneurysm formation is geometrically similar to the localized bulge that forms when a cylindrical tube was inflated by an internal pressure. This motivated Akkas (1990) to attribute the initial formation of aneurysms to the pressure volume curve having a maximum. This connection has recently been explored more fully by Fu *et al* (2011) and Fu & Ilichev (2015) by assuming that the initial formation of aneurysms is a bifurcation phenomenon, just as localized bulging in inflated rubber balloons. They have shown that when the artery has no localized weakening, the bifurcation pressure is extremely high, but as soon as localized wall weakening is introduced the actual bifurcation pressure will come down. Recent numerical studies on this problem have focussed on the effect of fibre-reinforcement; see Alhayani et al. (2013, 2014) and Rodriguez-Martinez et al. (2015). Fung et al. (1979) and Gasser et al. (2006) show that human arteries exhibit noticeable bending stiffness in contrast with party balloons. Horgan and Saccomandi (2003) use the Gent strain-energy function to model arteries, giving values of J_m in the range between 0.422 and 3.93 for healthy human arteries, corresponding to a maximum stretch ratio between 1.4 and 1.8, which is considerably smaller than that for rubber. Another popular model in the biomechanics literature, which reflects a less pronounced strain-stiffening effect than the Gent model, is the Fung model (1993). Horgan and Saccomandi (2003) use the Fung strain-energy function to model arteries with values Γ between 1.067 and 5.5.47. The Gent model, which introduces a limiting chain parameter and thus an upper bound for the range of possible stretches, and the Fung model, which exhibits an exponential increase of stress with respect to

strain but no maximal stretch. Finally, we note that the case of fixed axial stretch is particularly relevant to arteries. For human arteries Learoyd & Taylor (1996) gave the axial stretch as 1.28 to 1.67 for people under 35, and 1.14 and 1.32 for people over 35, while Humphrey et al. (2009) states that it is 1.5 for various mammals.

1.2 Organization of the Thesis

We start by considering the inflation of a cylindrical, isotropic, incompressible elastic tube subject to an internal pressure, looking in particular for solutions which are localized in their non-uniformity along the length of the tube. Bending stiffness is incorporated in the model and assess the effect of bending stiffness on the initiation of localised bulging in inflated thin-walled and thick-walled elastic tubes.

In Chapter 2, we introduce the theory of continuum mechanics and a number of mathematical methods, which will be used throughout the thesis.

In Chapter 3, we consider the inflation of an isotopic, incompressible, elastic cylindrical membrane subject to an internal pressure. We re-derive the bifurcation condition given by Fu et al. (2008) using a weakly non-linear analysis. A finite difference scheme and a shooting method are formulated that can be used to determine fully non-linear solutions. The main objective of this Chapter is to test these techniques and numerical methods on a known case so that they can be used in the next Chapter with full confidence.

In Chapter 4, the axisymmetric deformation of a thin-walled cylindrical shell of an

incompressible hyper-elastic material subject to an internal pressure is formulated. We consider the inflation of the shell by including contributions to the strain-energy from stretching as well as the bending of the shell. The bifurcation condition is derived using two methods, a weakly non-linear analysis and a perturbation theory. A system of five first-order ordinary differential equations that describe the deformation of the shell is derived. We find an expression for the critical value of the pressure at which a localized bulging solution may exist. The system of five equations is solved numerically using the finite difference method. Results for shells with different aspects, such as tubes with fixed axial force or axial stretch, are presented to show how the bending stiffness affects the localization behaviour. The main findings are that for a tube with fixed axial force, the bifurcation points occur at the turning points of the pressure volume curve. For a tube with fixed axial stretch, if a bifurcation point exist, it must come before the maximum of the pressure volume curve, and localized bulging can take place even if the latter maximum does not exist at all.

In Chapter 5, we consider the fully non-linear and fully 3D problem of localized bulging in a cylindrical tube of arbitrary thickness that is subject to the combined action of internal inflation and axial extension. An exact bifurcation condition is derived and used to quantify the effect of bending stiffness on localized bulging. Finally, we derive a two-term approximate bifurcation condition for computing the initiation pressure. We show that the first term corresponds to the membrane approximation while the second term corresponds to the effect of bending stiffness.

2 Mathematical Preliminaries

2.1 Continuum Mechanics

2.1.1 Introduction

In this section we outline the theory of non-linear elasticity including the deformation of a body, fundamental principles of mechanics, constitutive law of Cauchy elastic material and a short description of strain-energy functions for non-linear materials and arterial walls. For a thorough description of the mathematical theory of non-linear elasticity with application to the analysis of the large elastic deformation of hyperelastic materials, the book by Ogden (1997) should be consulted. Similar description based on modern topics in this field is presented in Fu & Ogden (2011).

2.1.2 Bodies and configurations

In continuum mechanics, a body B is a collection of elements which can be put into one-to-one correspondence with some region of Euclidean point space. We consider two configurations B_r and B_t, where B_r is the reference configuration and B_t is the current configuration of the body respectively. The corresponding position vectors of an arbitrary material point $\boldsymbol{X} \in B_r$ and $\boldsymbol{x} \in B_t$ are relative to an origin O in a coordinate system with orthonormal basis vectors $(\boldsymbol{E}_i)$ and $(\boldsymbol{e}_i)$ respectively. The deformation of

the body from the reference configuration to the current configuration is described by a mapping

$$\boldsymbol{x} = \chi(\boldsymbol{X}), \tag{2.1.1}$$

which takes $B_r \rightarrow B_t$. We assume that χ is twice-continuously differentiable with respect to position here. The displacement of a particle is defined by $\boldsymbol{u} = \boldsymbol{x} - \boldsymbol{X}$, and therefore $\boldsymbol{x} = \boldsymbol{X} + \boldsymbol{u}$. Then the deformation gradient tensor $\boldsymbol{F}$ is defined by

$$\boldsymbol{F} = \mathrm{Grad}\boldsymbol{x}. \tag{2.1.2}$$

With respect to the orthonormal bases $\boldsymbol{E}_i$ and $\boldsymbol{e}_i$, we have

$$\boldsymbol{F} = \frac{\partial(x_i \boldsymbol{e}_i)}{\partial X_j} \otimes \boldsymbol{E}_j = \frac{\partial x_i}{\partial X_j} \boldsymbol{e}_i \otimes \boldsymbol{E}_i, \quad i, j = 1, 2, 3, \tag{2.1.3}$$

where $\otimes$ denotes the tensor product between two vectors. To gain a full understanding of tensor analysis, we refer to Ogden (1997), Spencer (1980), Chadwick (1999) or Bertram (2008). In a cylindrical polar coordinate system, the deformation gradient $\boldsymbol{F}$ can be written as

$$\boldsymbol{F} = \frac{\partial}{\partial R}(r\boldsymbol{e}_r + z\boldsymbol{e}_z) \otimes \boldsymbol{E}_R + \frac{1}{R}\frac{\partial}{\partial \Theta}(r\boldsymbol{e}_r + z\boldsymbol{e}_z) \otimes \boldsymbol{E}_\Theta + \frac{\partial}{\partial Z}(r\boldsymbol{e}_r + z\boldsymbol{e}_z) \otimes \boldsymbol{E}_Z, \tag{2.1.4}$$

with reference to the basis vectors $\{\boldsymbol{E}_R, \boldsymbol{E}_\Theta, \boldsymbol{E}_Z\}$ and $\{\boldsymbol{e}_r, \boldsymbol{e}_\theta, \boldsymbol{e}_z\}$ in the reference and current configurations respectively.

Thus

$$\boldsymbol{F} = \begin{pmatrix} \frac{\partial r}{\partial R} & \frac{1}{R}\frac{\partial r}{\partial \Theta} & \frac{\partial r}{\partial Z} \\ r\frac{\partial \theta}{\partial R} & \frac{r}{R}\frac{\partial \theta}{\partial \Theta} & r\frac{\partial \theta}{\partial Z} \\ \frac{\partial z}{\partial R} & \frac{1}{R}\frac{\partial z}{\partial \Theta} & \frac{\partial z}{\partial Z} \end{pmatrix}. \tag{2.1.5}$$

The relation for the deformation of line elements between the two configurations are

given by $d\boldsymbol{x} = \boldsymbol{F}d\boldsymbol{X}$, where $d\boldsymbol{X}$ and $d\boldsymbol{x}$ are infinitesimal line elements in the reference and current configurations, respectively. The deformation gradient therefore carries the undeformed line element into the deformation configuration. Physically, $\boldsymbol{F}$ must be a one-to-one relation between $d\boldsymbol{X}$ and $d\boldsymbol{x}$ and thus $\boldsymbol{F}$ must be non-singular with a positive determinant given by

$$J = \det\boldsymbol{F} \neq 0, \tag{2.1.6}$$

where J is the local volume change between the two configurations. Therefore we find the relation $dv = JdV$, where dV and dv are the infinitesimal volume elements in the reference and current configuration, respectively. For an incompressible material we have $J = \det\boldsymbol{F} = 1$. As the deformation gradient tensor $\boldsymbol{F}(\boldsymbol{X})$ completely characterises the deformation in the vicinity of the particle $\boldsymbol{X}$, the polar decomposition theorem (Chadwick 1999, Antman 2005) enables us to write it uniquely as

$$\boldsymbol{F} = \boldsymbol{R}\boldsymbol{U} = \boldsymbol{V}\boldsymbol{R}, \tag{2.1.7}$$

where $\boldsymbol{R}$ is a proper orthogonal vector so that $\boldsymbol{R}\boldsymbol{R}^T = \boldsymbol{R}^T\boldsymbol{R} = \boldsymbol{I}$, and $\boldsymbol{I}$ is the identity tensor. $\boldsymbol{U}$, $\boldsymbol{V}$ are positive definite symmetric tensors. $\boldsymbol{R}$ represents the rotational part of $\boldsymbol{F}$ while the decomposition (2.1.7) represents a stretch $\boldsymbol{U}$, followed by $\boldsymbol{R}$ or $\boldsymbol{R}$ followed by a stretch $\boldsymbol{V}$. Since $\boldsymbol{U}$ is symmetric, it has three real eigenvalues λ_1, λ_2 and λ_3 and a corresponding triplet of orthonormal eigenvectors $\boldsymbol{r}_1, \boldsymbol{r}_2, \boldsymbol{r}_3$. Since $\boldsymbol{U}$ is positive definite, all three eigenvalues are positive. Thus the matrix of components of $\boldsymbol{U}$ relative to principal basis $\{\boldsymbol{r}_1, \boldsymbol{r}_2, \boldsymbol{r}_3\}$ is

$$[U] = \begin{pmatrix} \lambda_1 & 0 & 0 \\ 0 & \lambda_2 & 0 \\ 0 & 0 & \lambda_3 \end{pmatrix}. \tag{2.1.8}$$

It is easy to show that the eigenvalues λ_1, λ_2 and λ_3 of $\boldsymbol{U}$ are identical to those of $\boldsymbol{V}$. Moreover, the eigenvectors $\{\boldsymbol{r}_1, \boldsymbol{r}_2, \boldsymbol{r}_3\}$ of $\boldsymbol{U}$ are related to the eigenvectors $\{\boldsymbol{l}_1, \boldsymbol{l}_2, \boldsymbol{l}_3\}$ of $\boldsymbol{V}$ by $\boldsymbol{l}_i = \boldsymbol{R}\boldsymbol{r}_i, \;\; i = 1, 2, 3$. The common eigenvalues of $\boldsymbol{U}$ and $\boldsymbol{V}$ are known as the principal stretches associated with the deformation at $\boldsymbol{X}$. The stretch tensors $\boldsymbol{U}$ and $\boldsymbol{V}$ can be expressed in terms of their eigenvalues and eigenvectors by

$$\boldsymbol{U} = \sum_{i=1}^{3} \lambda_i \boldsymbol{r}_i \otimes \boldsymbol{r}_i, \quad \boldsymbol{V} = \sum_{i=1}^{3} \lambda_i \boldsymbol{l}_i \otimes \boldsymbol{l}_i. \tag{2.1.9}$$

As there is a one-to-one relation between $\boldsymbol{U}$ and $\boldsymbol{U}^2$, and similarly between $\boldsymbol{V}$ and $\boldsymbol{V}^2$, the right and left Cauchy-Green deformation tensors, introduced by George Green in 1839, can be written as

$$\boldsymbol{C} = \boldsymbol{F}^T\boldsymbol{F} = \boldsymbol{U}^2, \quad \boldsymbol{B} = \boldsymbol{F}\boldsymbol{F}^T = \boldsymbol{V}^2, \tag{2.1.10}$$

where a superscript T denotes the transport of a tensor. $\boldsymbol{C}$ is symmetric as $(\boldsymbol{F}^T\boldsymbol{F})^T = \boldsymbol{F}^T(\boldsymbol{F}^T)^T = \boldsymbol{F}^T\boldsymbol{F}$ and positive definite as, for a non-zero arbitrary vector $\boldsymbol{a}$, $\boldsymbol{a}\cdot\boldsymbol{C}\boldsymbol{a} = \boldsymbol{a}\cdot\boldsymbol{F}^T\boldsymbol{F}\boldsymbol{a} = \boldsymbol{F}\boldsymbol{a}\cdot\boldsymbol{F}\boldsymbol{a} = |\boldsymbol{F}\boldsymbol{a}|^2 > 0$. Physically, the tensor $\boldsymbol{C}$ gives us a measure of local change in length of an line element due to deformation. The eigenvalues of $\boldsymbol{C}$ and $\boldsymbol{B}$ are λ_1^2, λ_2^2 and λ_3^2, and the eigenvectors of $\boldsymbol{C}$ and $\boldsymbol{B}$ are the same as those of $\boldsymbol{U}$ and $\boldsymbol{V}$ respectively. The two Cauchy-Green tensors admit the spectral representation

$$\boldsymbol{C} = \sum_{i=1}^{3} \lambda_i^2 \boldsymbol{r}_i \otimes \boldsymbol{r}_i, \quad \boldsymbol{B} = \sum_{i=1}^{3} \lambda_i^2 \boldsymbol{l}_i \otimes \boldsymbol{l}_i. \tag{2.1.11}$$

The particular scalar-valued functions of $\boldsymbol{C}$

$$I_1(\boldsymbol{C}) = \mathrm{tr}\boldsymbol{C}, \;\; I_2(\boldsymbol{C}) = \frac{1}{2}[\mathrm{tr}(\boldsymbol{C})^2 - (\mathrm{tr}\ \boldsymbol{C})^2], \;\; I_3(\boldsymbol{C}) = \det\boldsymbol{C}, \tag{2.1.12}$$

are called the principal scalar invariants of $\boldsymbol{C}$. The principal scalar invariants can be written in terms of the principal stretches as

$$I_1(\boldsymbol{C}) = \lambda_1^2 + \lambda_2^2 + \lambda_3^2, \quad I_2(\boldsymbol{C}) = \lambda_1^2\lambda_2^2 + \lambda_2^2\lambda_3^2 + \lambda_3^2\lambda_1^2, \quad I_3(\boldsymbol{C}) = \lambda_1^2\lambda_2^2\lambda_3^2. \tag{2.1.13}$$

The Green strain tensor, $\boldsymbol{E}$, is defined by

$$\boldsymbol{E} = \frac{1}{2}(\boldsymbol{U}^2 - I) = \frac{1}{2}(\boldsymbol{F}^T\boldsymbol{F} - I), \tag{2.1.14}$$

where I is the identity tensor. The velocity of a point $\boldsymbol{x}$ is given by

$$\boldsymbol{v} \equiv \dot{\boldsymbol{x}} = \frac{\partial}{\partial t}\boldsymbol{x}(\boldsymbol{X}, t), \tag{2.1.15}$$

where a superimposed dot represents differentiation with respect to t. We also define the velocity gradient tensor $\boldsymbol{L}$ as

$$\boldsymbol{L} = \text{grad } \boldsymbol{v}. \tag{2.1.16}$$

Since Grad $\boldsymbol{v}$ = (grad $\boldsymbol{v}$)$\boldsymbol{F}$ = $\boldsymbol{L}\boldsymbol{F}$, and Grad $\boldsymbol{v}$ = $\frac{\partial}{\partial t}$Grad $\boldsymbol{x}$ = $\dot{\boldsymbol{F}}$, we have

$$\dot{\boldsymbol{F}} = \boldsymbol{L}\boldsymbol{F}. \tag{2.1.17}$$

We also have

$$\text{tr}\boldsymbol{L} = \text{tr}(\text{grad}\boldsymbol{v}) = \text{div}\boldsymbol{v}, \tag{2.1.18}$$

which follows from the definition (2.1.16).

2.1.3 Mechanical balance laws

In this section we will consider the fundamental principles of mechanics: the conservation of mass, conservation of linear momentum, equation of motion and conservation of energy.

2.1.3.1 Conservation of mass

Let R_t be an arbitrary region in the current configuration. Given any material in this region, its mass m is a positive, scalar valued property, whose dimension is independent of length and time. In terms of the mass density $\rho(> 0)$

$$m = \int_{R_t} \rho dv. \tag{2.1.19}$$

Conservation of mass states that the mass of any material does not depend on the motion or time. Since m is time independent, we differentiate (2.1.19) with respect to t to get the following equation which represents the conservation of mass.

$$\frac{d}{dt} \int_{R_t} \rho dv = 0. \tag{2.1.20}$$

By transferring the integral over R_t to their respective integral in the equivalent region in the reference configuration, R_r, we may take the derivative with respect to time inside the integral as R_r does not depend on time. Therefore (2.1.20) becomes

$$\frac{d}{dt} \int_{R_t} \rho \, dv = \int_{R_r} \frac{d(\rho J)}{dt} dV = \int_{R_t} (\dot{\rho} + \rho \text{ div } \boldsymbol{v}) dv = 0. \tag{2.1.21}$$

As the region R_t is arbitrary and the integrand is continuous, it can be localised to get the the equation

$$\dot{\rho} + \rho \text{ div } \boldsymbol{v} = 0, \tag{2.1.22}$$

which holds for all $\boldsymbol{x} \in R_t$ and all t. Recall that the dot represents the material time derivation. If the density is constant, (2.1.22) reduces to div$\boldsymbol{v} = 0$, where $\boldsymbol{v}$ is a particle velocity.

2.1.3.2 Conservation of momentum

We consider the forces acting on a small region in the current configuration. We assume that there are two types of forces, body forces that act at each point in the region R_t, and tractions that act at points on the boundary of R_t. Body forces are denoted by $\boldsymbol{b}$ and tractions which depend on the position in the configuration, along with a normal to the excised surface $\boldsymbol{n}$, are denoted by $\boldsymbol{t}(\boldsymbol{x}, \boldsymbol{n})$. The resultant body force in the current configuration R_t is given by $\int_{R_t} \rho \boldsymbol{b} dv$ while the resultant tractions in the current configuration ∂R_t is given by $\int_{\partial R_t} \boldsymbol{t} da$. Then using Newton's second law, in the form Force $= \frac{d}{dt}$(Momentum), along with the previous considerations, we have,

$$\int_{R_t} \rho \boldsymbol{b} \; dv + \int_{\partial R_t} \boldsymbol{t}(\boldsymbol{x}, \boldsymbol{n}) da = \frac{d}{dt} \int_{R_t} \rho \boldsymbol{v} dv. \tag{2.1.23}$$

The right hand side of (2.1.23) may be written, by transferring from R_t to R_r, taking the derivative inside and transferring back to R_t, as

$$\frac{d}{dt} \int_{R_t} \boldsymbol{\rho} v \; dv = \int_{R_t} \frac{d}{dt} (\rho \boldsymbol{v} J \; dV) = \int_{R_t} \frac{d}{dt} (\rho v J) \frac{dv}{J} =$$

$$\int_{R_t} (\rho \dot{\boldsymbol{v}} + \boldsymbol{v} \dot{\rho} + \rho \frac{\dot{J}}{J} \boldsymbol{v}) dv = \int_{R_t} \rho \boldsymbol{a} dv, \tag{2.1.24}$$

where the conservation of mass has been used in the last equality and $\boldsymbol{a} = \dot{\boldsymbol{v}}$. Therefore (2.1.24) may be written as,

$$\int_{\partial R_t} \boldsymbol{t}(\boldsymbol{x}, \boldsymbol{n}) \; da = \int_{R_t} \rho (\boldsymbol{a} - \boldsymbol{b}) dv. \tag{2.1.25}$$

2.1.3.3 Equation of motion

Let $\boldsymbol{t}(\boldsymbol{x}, \boldsymbol{n})$ denote the traction vector, per unit deformed area, which depend on $\boldsymbol{x}$ and $\boldsymbol{n}$ as defined earlier. Then Cauchy's theorem, as given in Ogden (1997) or Holzapfel

(2000), states that if $\boldsymbol{t}(\boldsymbol{x}, \boldsymbol{n})$ is continuous in $\boldsymbol{x}$, then there exists a second order tensor field $\boldsymbol{\sigma}$ such that

$$\boldsymbol{t}(\boldsymbol{x}, \boldsymbol{n}) = \boldsymbol{\sigma}^T(\boldsymbol{x}, t)\boldsymbol{n}, \tag{2.1.26}$$

where the tensor $\boldsymbol{\sigma}$ is called the Cauchy stress tensor and is independent of $\boldsymbol{n}$. The equation of linear momentum, (2.1.25), therefore becomes,

$$\int_{\partial R_t} \boldsymbol{\sigma}^T \boldsymbol{n} da = \int_{R_t} \rho(\boldsymbol{a} - \boldsymbol{b}) dv. \tag{2.1.27}$$

Using the divergence theorem, (2.1.27) may be written as,

$$\int_{\partial R_t} \boldsymbol{\sigma}^T \boldsymbol{n} da = \int_{R_t} \text{div}\boldsymbol{\sigma} dv, \tag{2.1.28}$$

and therefore we find the equation of motion,

$$\text{div}\boldsymbol{\sigma} + \rho\boldsymbol{b} = \rho\boldsymbol{a}, \tag{2.1.29}$$

where ρ is the mass density of the material of the body in current configuration, $\boldsymbol{b}$ is the body forces, measured per unit volume, and $\boldsymbol{a}$ is the acceleration. If there are no body forces the local equilibrium equation for the body has the form

$$\text{div}\boldsymbol{\sigma} = \boldsymbol{0}. \tag{2.1.30}$$

2.1.3.4 Conservation of energy

We now derive the law of conservation of energy, following the method presented in Ogden (1997). In equation of motion (2.1.29), taking the dot product with the velocity $\boldsymbol{v}$,

$$(\text{div}\boldsymbol{\sigma}) \cdot \boldsymbol{v} + \rho(\boldsymbol{b}.\boldsymbol{v}) = \boldsymbol{a}.\boldsymbol{v}, \tag{2.1.31}$$

or equivalently

$$\operatorname{div}(\boldsymbol{\sigma v}) - \operatorname{tr}(\boldsymbol{\sigma L}) + \rho(\boldsymbol{b}.\boldsymbol{v}) = \boldsymbol{a}.\boldsymbol{v}, \tag{2.1.32}$$

where $\boldsymbol{a}$ is the acceleration and $\boldsymbol{L}$ is the velocity gradient as defined earlier. Integrating (2.1.32) over the current configuration, and using the divergence theorem, we have

$$\int_{B_t} \rho \boldsymbol{b} \cdot \boldsymbol{v} dv + \int_{\partial B_t} \boldsymbol{t} \cdot \boldsymbol{v} dv = \frac{d}{dt} \int_{B_t} \frac{1}{2} \rho \boldsymbol{v} \cdot \boldsymbol{v} dv + \int_{B_t} \operatorname{tr}(\boldsymbol{\sigma L}) dv. \tag{2.1.33}$$

This represents the equation of mechanical energy balance.

2.1.4 Cauchy elastic material

A simple elastic material is one for which the Cauchy stress depends only on the deformation gradient without depending on the history or the path taken to reach the point $\boldsymbol{F}$. The constitutive equation for a homogeneous elastic material can be written as

$$\boldsymbol{\sigma} = \boldsymbol{g}(\boldsymbol{F}). \tag{2.1.34}$$

for some symmetric tensor valued function g, with $g(\boldsymbol{I}) = 0$ so that the reference configuration is stress free.

2.1.4.1 Objectivity

The principle of objectivity requires that material properties should be independent of superposed rigid-body motions. This means the constitutive law $\boldsymbol{g}$ must satisfy

$$\boldsymbol{g}(\boldsymbol{QF}) = \boldsymbol{Q}\boldsymbol{g}(\boldsymbol{F})\boldsymbol{Q}^T, \tag{2.1.35}$$

for each $\boldsymbol{F}$ and any rotation $\boldsymbol{Q}$, which is a proper orthogonal second-order tensor.

2.1.4.2 Isotropy

A body is isotropic with respect to B_r if the response of any small section of material cut from B_r is independent of its orientation in B_r. This means the material properties have no preferred direction. For example, rubber is isotropic, but rubber reinforced with metal strips in a specific direction is anisotropic. For isotropic materials, we have

$$\boldsymbol{g}(\boldsymbol{FP}) = \boldsymbol{g}(\boldsymbol{F}), \tag{2.1.36}$$

where $\boldsymbol{P}$ is an arbitrary orthogonal tensor. In equation (2.1.36), with $\boldsymbol{P}$ replaced by $\boldsymbol{R}^T$ and use of polar decomposition (2.1.7), we get

$$\boldsymbol{g}(\boldsymbol{F}) = \boldsymbol{g}(\boldsymbol{VRR}^T) = \boldsymbol{g}(\boldsymbol{V}). \tag{2.1.37}$$

With the further use of material objectivity (2.1.35) we obtain

$$\boldsymbol{g}(\boldsymbol{QFP}) = \boldsymbol{g}(\boldsymbol{QF}) = \boldsymbol{Qg}(\boldsymbol{F})\boldsymbol{Q}^T = \boldsymbol{Qg}(\boldsymbol{V})\boldsymbol{Q}^T. \tag{2.1.38}$$

On taking $\boldsymbol{P} = \boldsymbol{Q}^T$, we have

$$\boldsymbol{g}(\boldsymbol{QVQ}^T) = \boldsymbol{Qg}(\boldsymbol{V})\boldsymbol{Q}^T. \tag{2.1.39}$$

which shows that the tensor-valued function $\boldsymbol{g}$ is an isotropic tensor function of $\boldsymbol{V}$. It can be shown that the Cauchy stress $\boldsymbol{\sigma}$ may be written in the form

$$\boldsymbol{\sigma} = \phi_0\boldsymbol{I} + \phi_1\boldsymbol{V} + \phi_2\boldsymbol{V}^2, \tag{2.1.40}$$

where ϕ_i are functions of the three principal invariants of a three dimensional second-order tensor, given by $\mathrm{tr}\boldsymbol{V}$, $\frac{1}{2}[(\mathrm{tr}\boldsymbol{V})^2 - \mathrm{tr}(\boldsymbol{V}^2)]$ and $\det\boldsymbol{V}$ (Spencer 1980). Using $(2.1.9)_2$, these invariants may be written as

$$\begin{aligned} i_1 &= \mathrm{tr}(\boldsymbol{V}) = \lambda_1 + \lambda_2 + \lambda_3, \\ i_2 &= \frac{1}{2}(I_1(\boldsymbol{C})^2 - \mathrm{tr}(\boldsymbol{V}^2)) = \lambda_1\lambda_2 + \lambda_2\lambda_2 + \lambda_3\lambda_1, \\ i_3 &= \det\boldsymbol{V} = \lambda_1\lambda_2\lambda_3. \end{aligned} \tag{2.1.41}$$

Two sets of invariants i_1, i_2, i_3 and $I_1(\boldsymbol{C}), I_2(\boldsymbol{C}), I_3(\boldsymbol{C})$ may be connected using $I_1(\boldsymbol{C}) = i_1^2 - 2i_2$, $I_2(\boldsymbol{C}) = i_2^2 - 2i_1i_3$, $I_3(\boldsymbol{C}) = i_3^2$.

2.1.5 Strain energy functions

The strain energy function represents the stored elastic energy per unit undeformed volume of the material. A material is said to be hyperelastic if there exists a strain-energy function $W(\boldsymbol{F})$ such that

$$\frac{\partial}{\partial t}W(\boldsymbol{F}) = J\mathrm{tr}(\boldsymbol{\sigma}\boldsymbol{L}), \tag{2.1.42}$$

where $\boldsymbol{L}$ the velocity gradient tensor. We also have

$$\frac{\partial}{\partial t}W(\boldsymbol{F}) = \mathrm{tr}(\frac{\partial W}{\partial \boldsymbol{F}}\dot{\boldsymbol{F}}). \tag{2.1.43}$$

We may then write

$$\frac{\partial}{\partial t}W(\boldsymbol{F}) = \mathrm{tr}(\frac{\partial W}{\partial \boldsymbol{F}}\boldsymbol{L}\boldsymbol{F}) = \mathrm{tr}(\boldsymbol{F}\frac{\partial W}{\partial \boldsymbol{F}}\boldsymbol{L}), \tag{2.1.44}$$

where we have used $\dot{\boldsymbol{F}} = \boldsymbol{L}\boldsymbol{F}$.

Comparing (2.1.42) and (2.1.44) we find a relation between the strain-energy function and the Cauchy stress,

$$\boldsymbol{\sigma} = J^{-1}\boldsymbol{F}\frac{\partial W}{\partial \boldsymbol{F}}. \tag{2.1.45}$$

For an isotopic material, W is either a function of three stretches, $W(\lambda_1, \lambda_2, \lambda_3)$, or the three invariants defined in (2.1.13), $W(I_1, I_2, I_3)$. In the former case, the strain-energy function must be a symmetric function of the three principal stretches and hence

$$W(\lambda_1, \lambda_2, \lambda_3) = W(\lambda_2, \lambda_3, \lambda_1) = W(\lambda_3, \lambda_2, \lambda_1). \tag{2.1.46}$$

In this case (2.1.45) may be written as

$$\sigma_i = J^{-1}\lambda_i\frac{\partial W}{\partial \lambda_i}, \quad i = 1, 2, 3 \quad \text{(no summation)}, \tag{2.1.47}$$

showing that the strain-energy function is a potential function for the three principal stresses σ_i $(i = 1, 2, 3)$. The connection between the Cauchy stress $\boldsymbol{\sigma}$ and the nominal stress $\boldsymbol{S}$ can be written as

$$\boldsymbol{S} = J\boldsymbol{F}^{-1}\boldsymbol{\sigma}. \tag{2.1.48}$$

Then we obtain the simple formula

$$\boldsymbol{S} = \frac{\partial W}{\partial \boldsymbol{F}}, \quad S_{ij} = \frac{\partial W}{\partial F_{ij}}. \tag{2.1.49}$$

2.1.5.1 Neo-Hookean strain-energy function

The most fundamental non-linear elastic model is the Neo-Hookean relation given by

$$W(\lambda_1, \lambda_2, \lambda_3) = \frac{1}{2}\mu(I_1(\boldsymbol{C}) - 3) = \frac{1}{2}\mu(\lambda_1^2 + \lambda_2^2 + \lambda_3^2 - 3), \tag{2.1.50}$$

where $\mu(>0)$ is a material constant referred to as the shear modulus of the material. This is an extension of Hooke's law (Boulanger and Hayes 2001) for the case of large deformations and can be applied to plastics and rubber-like substances at small to moderate stretches of up to approximately 1.5. In particular, Muller and Strehlow (2004) show that (2.1.50) is inappropriate for biaxial stretching above this range.

2.1.5.2 Mooney-Rivlin strain-energy function

Another fundamental non-linear isotropic model is the Mooney-Rivlin model, which was introduced by Melvin Mooney and Ronald Rivlin (Selvadurai 2006), is one of the benchmark models for describing isotropic rubber-like materials (Muller and Strehlow 2004). The Mooney-Rivlin strain-energy function, a generalization of the Neo-Hookean strain-energy function, is defined by

$$W(\lambda_1, \lambda_2, \lambda_3) = \frac{1}{2}\mu_1(I_1(\boldsymbol{C}) - 3) - \frac{1}{2}\mu_2(I_2(\boldsymbol{C}) - 3), \tag{2.1.51}$$

where $\mu_1(\geq 0)$ and $\mu_2(\leq 0)$ are material constants such that $\mu_1 - \mu_2 = \mu(>0)$.

2.1.5.3 Fung strain-energy function

The strain energy function for the passive arterial wall was constructed by Fung et al. (1979) as a strain energy equation for two-dimensional problems. Fung (1993) presented a generalized three-dimensional model that assumed that the principal directions of the stress tensor coincide with the radial, circumferential, and axial directions of the artery.

Fung type strain energy function is given by

$$W = \frac{\mu(e^{\Gamma(I_1(\boldsymbol{C})-3)} - 1)}{\Gamma}, \tag{2.1.52}$$

where Γ is a positive parameter representing the degree of strain stiffening. Destrade et al. (2009) gave $1.0 \leq \Gamma \leq 5.5$ as the typical range for arteries. In the limit as Γ approaches zero, (2.1.53) reproduces the Neo-Hookean strain-energy function (2.1.50).

2.1.5.4 Ogden strain-energy function

For complex materials such as rubbers, polymers, and biological tissue subject to even larger deformation, more sophisticated models are necessary. The Ogden strain-energy function, which was developed by Ogden (1972), is given by

$$W = \sum_{n=1}^{3} \frac{\mu_n}{\alpha_n}(\lambda_1^{\alpha_n} + \lambda_2^{\alpha_n} + \lambda_3^{\alpha_n} - 3), \tag{2.1.53}$$

where μ_n and α_n are material constants that satisfy the constraint

$$\sum_{n=1}^{N} \mu_n \alpha_n = 2\mu. \tag{2.1.54}$$

Based on experimental measurements of rubber, the material constants of the Ogden model are given by $\mu_1 = 1.491,\ \mu_2 = 0.003,\ \mu_3 = -0.023,\ \alpha_1 = 1.3,\ \alpha_2 = 5.0,\ \alpha_3 = -2.0$, (Ogden 1972).

2.1.5.5 Varga strain-energy function

The Varga strain-energy function proposed by Varga (1966) to model rubber for small stretches. As a function of the stretches it is given by

$$W(\lambda_1, \lambda_2, \lambda_3) = 2\mu(i_1 - 3), \tag{2.1.55}$$

where μ is the shear modules. The Varga strain-energy function is useful for theoretical work due to its simple linear mathematical structure, but does not model many physical behaviours observed in elastic materials.

2.1.5.6 Gent strain-energy function

The simplified Gent strain-energy function was first introduced by Gent (1996) to model rubbers which are strain-hardening. The Gent strain-energy function is given by

$$W(\lambda_1, \lambda_2, \lambda_3) = -\frac{1}{2}\mu J_m \log\left(1 - \frac{J_1}{J_m}\right), \tag{2.1.56}$$

where J_m represents the maximum value of $J_1 = I_1(\boldsymbol{C}) - 3$ beyond which the hydrocarbon chains may not extend any further. For rubber-like materials, the values for the dimensionless parameter J_m for simple extension range from 30 to 100 (Gent 1996). In particular, Gent (1996) suggests that $J_m = 97.2$ is the typical value of the parameter J_m for rubber. Later studies showed that $J_m = 30$ is also a realistic value for rubber. Detailed review of some of the possibilities of the limiting chain extensibility J_m, may be found in the paper by Horgan and Saccomandi (2002). For biological tissue, much smaller values of J_m are appropriate. For human arteries Horgan and Saccomandi

(2003) give a range for J_m between 0.422 and 3.93. Kanner & Horgan (2007) showed that for known values of J_m for arterial tissue, pressure does not have a maximum in uniform inflation.

2.1.5.7 Arterial model

A simple arterial model is given by

$$W = \frac{\mu}{2(1-k+k\alpha)}\left\{(1-k)J_1 + k\mathrm{e}^{\alpha J_1} - k\right\}, \tag{2.1.57}$$

where k, α are material constants. Without the first term $(1-k)J_1$ on the right hand side, equation (2.1.57) has been used by Delfino et al. (1997) as a possible model for arteries. This first term is added to represent the contribution from the matrix material. This model is used in Chapter 5 in order to discuss the behaviour of initiation of critical pressure in uniform inflation.

2.2 Compound Matrix Method and Evans Function

We consider the linear homogeneous system of n first order differential equations,

$$\frac{d\mathbf{y}}{dZ} = A(Z,\lambda)\mathbf{y}, \quad a \leq Z \leq b, \tag{2.2.1}$$

where $\mathbf{y}(Z) = (y_1(Z), y_2(Z), ...y_n(Z))$ is a n-dimensional vector, A is a $n \times n$ matrix whose entries are functions of the independent variable Z and a parameter λ. The boundary conditions at $Z = a$ and $Z = b$ are expressed as

$$B(Z,\lambda)\mathbf{y} = \mathbf{0}, \quad \text{at } Z = a \tag{2.2.2}$$

$$C(Z,\lambda)\mathbf{y} = \mathbf{0}, \quad \text{at} \;\; Z = b \tag{2.2.3}$$

where B and C are $m \times n$ and $(n-m) \times n$ matrices respectively, and are both known functions of the independent variable Z and a parameter λ. One or both of the boundaries $Z = a, b$ may be infinite.

The aim is to determine the values of the parameter λ such that the system has a non trivial solution which satisfies the boundary conditions, where the values of λ will be called the eigenvalues. It is possible to use a standard shooting technique for finding these eigenvalues but it tends to be inaccurate for stiff problems. In the next section we introduce the determinant base method to solve the eigenvalue problem (2.2.1).

2.2.1 Determinant based method

First, for a given value of λ, assuming B has rank m, we must be able to find m linearly independent solutions to (2.2.2) which are denoted by $\mathbf{y}_0^{(1)}, \mathbf{y}_0^{(2)}, ...\mathbf{y}_0^{(m)}$. Using these vectors as initial values at $Z = a$, we may integrate (2.2.1) from $Z = a$, to obtain a set of m linearly independent solutions $\mathrm{y}^{(i)}(Z),\ i = 1, 2, ...m$. Therefore a general solution that satisfies (2.2.1) and the boundary condition (2.2.2) is then given by

$$\mathbf{y} = \sum_{i=1}^{m} k_i \mathbf{y}^{(i)}(Z), \tag{2.2.4}$$

where $k_1,\ k_2, ...k_m$ are arbitrary constants. We define $M^-(Z,\lambda)$ to be the $n \times m$ matrix given by

$$\boldsymbol{M}^-(Z,\lambda) = \begin{bmatrix} y_1^{(1)}(Z) & y_1^{(2)}(Z) & . & . & y_1^{(i)}(Z) & . & . & y_1^{(m)}(Z) \\ y_2^{(1)}(Z) & y_2^{(2)}(Z) & . & . & y_2^{(i)}(Z) & . & . & y_2^{(m)}(Z) \\ . & . & . & . & . & . & . & . \\ . & . & . & . & . & . & . & . \\ y_n^{(1)}(Z) & y_n^{(2)}(Z) & . & . & y_n^{(i)}(Z) & . & . & y_n^{(m)}(Z) \end{bmatrix}. \tag{2.2.5}$$

Then equation (2.2.4) can be written as

$$\boldsymbol{y} = M^-(Z,\lambda)\boldsymbol{k}, \tag{2.2.6}$$

where $\boldsymbol{k} = [k_1, k_2, ...k_m]^T$. We now use the same procedure to obtain a general solution that satisfies the boundary condition (2.2.3). Let $\boldsymbol{y}^{(i)}(Z),\ i = m+1, m+2, ...n$, be the $n-m$ solutions obtained by shooting from $Z = b$. Then a general solution that satisfies (2.2.1) and the boundary condition (2.2.3) is given by

$$\mathbf{y} = \sum_{i=m+1}^{n} k_i \mathbf{y}^{(i)}(Z), \tag{2.2.7}$$

where $k_{m+1},\ k_{m+2}, ...k_n$ are another set of constants. Proceeding in the same way, (2.2.7) can be written as

$$\boldsymbol{y} = M^+(Z,\lambda)\boldsymbol{k}, \tag{2.2.8}$$

where $\boldsymbol{k} = [k_{m+1},\ k_{m+2}, ...k_n]^T$ and $M^+(Z,\lambda)$ be the $n \times (n-m)$ matrix whose i^{th} column is $[y_1^{(m+i)}(Z), y_2^{(m+i)}(Z), ...y_n^{(m+i)}(Z)]^T$. We then impose that these two solutions (2.2.6) and (2.2.8) or equivalently (2.2.4) and (2.2.7) must match at some intermediate point $Z = d$. Thus,

$$\mathbf{y} = \sum_{i=1}^{m} k_i \mathbf{y}^{(i)}(Z) = \sum_{i=m+1}^{n} k_i \mathbf{y}^{(i)}(Z), \quad \text{at } Z = d, \tag{2.2.9}$$

or equivalently

$$\mathbf{N}(d,\lambda)\mathbf{c} = \mathbf{0}, \tag{2.2.10}$$

where

$$N(d,\lambda) = [\mathbf{y}^{(1)}, \mathbf{y}^{(2)}, ...\mathbf{y}^{(m)}, \mathbf{y}^{(m+1)}, \mathbf{y}^{(m+2)}, ...\mathbf{y}^{(n)}], \tag{2.2.11}$$

$$c = (k_1, k_2, ...k_m, -k_{m+1}, -k_{m+2}, ... - k_n)^T.$$

Therefore we need to iterate on λ until the matching condition,

$$|\mathbf{N}(d,\lambda)| = 0 \tag{2.2.12}$$

is satisfied. The function $D(\lambda)$ is known as Evans function; it is an invariant of the differential equation (2.2.1). This matching condition is dependent on d as well as the value of λ. It may be shown that the following condition,

$$D(\lambda) = e^{-\int_a^d \mathrm{tr}A(s,\lambda)ds}|\mathbf{N}(d,\lambda)| = 0, \tag{2.2.13}$$

is independent of the value of d. This may be proved using the matrix property

$$\frac{d(\det A)}{dx} = \mathrm{tr}(\mathrm{adj}(A)\frac{dA}{dx}) \tag{2.2.14}$$

for any square matrix A, see for instance Chadwick (1999).

2.2.2 Compound matrix method

Compound matrix method can be used to solve numerically difficult boundary-value problems involving linear ordinary differential-equation systems. The elements of the compound matrix are the minors of the solution matrix. The compound matrix method was used to investigate the linear stability/bifurcation analysis of fluid flows (Afendikov

& Bridges 2001), solitary waves (Pego & Weinstein 1992), and pre-stressed elastic bodies (Fu and Pour 2002). Ng and Reid (1985), Bridges (1999) used this method for the numerical solution of linear two-point boundary value and eigenvalue problems involving stiff differential operators with separated boundary conditions.

In the previous determinant based method, numerical difficulties may arise for some eigenvalue problems due to the presence of exponentially growing solutions. We therefore introduce the compound matrix method to overcome this difficulty. We use the two sets of linearly independent solutions, $(\mathbf{y}^{(1)}, \mathbf{y}^{(2)}, ...\mathbf{y}^{(m)})$ and $(\mathbf{y}^{(m+1)}, \mathbf{y}^{(m+2)}, ...\mathbf{y}^{(n)})$, as defined in the previous section. The matrix $M^{-}(Z, \lambda)$ defined in (2.2.5) has $\binom{n}{m}$ 2 by 2 minors, which we denote by $\phi_1, \phi_2, \ldots$. When $m = 2$ and $n = 4$ we have

$$\phi_1 = \begin{vmatrix} y_1^{(1)} & y_1^{(2)} \\ y_2^{(1)} & y_2^{(2)} \end{vmatrix} \equiv (1,2), \qquad \phi_2 = \begin{vmatrix} y_1^{(1)} & y_1^{(2)} \\ y_3^{(1)} & y_3^{(2)} \end{vmatrix} \equiv (1,3), \tag{2.2.15}$$

we may define the other minors in the same way by $\phi_3 = (1,4)$, $\phi_4 = (2,3)$, $\phi_5 = (2,4)$, $\phi_6 = (3,4)$. We can find the first-order differential equations satisfied by these ϕ's by differentiating inside the determinant as,

$$\phi_1' = \begin{vmatrix} y_1^{(1)\prime} & y_1^{(2)\prime} \\ y_2^{(1)} & y_2^{(2)} \end{vmatrix} + \begin{vmatrix} y_1^{(1)} & y_1^{(2)} \\ y_2^{(1)\prime} & y_2^{(2)\prime} \end{vmatrix}$$

$$= \begin{vmatrix} \sum_{i=1}^{4} A_{1i} y_i^{(1)} & \sum_{i=1}^{4} A_{1i} y_i^{(2)} \\ y_2^{(1)} & y_2^{(2)} \end{vmatrix} + \begin{vmatrix} y_1^{(1)} & y_1^{(2)} \\ \sum_{i=1}^{4} A_{2i} y_i^{(1)} & \sum_{i=1}^{4} A_{2i} y_i^{(2)} \end{vmatrix}$$

$$= A_{11}\phi_1 - A_{13}\phi_4 - A_{14}\phi_5 + A_{22}\phi_1 + A_{23}\phi_2 + A_{24}\phi_3, \tag{2.2.16}$$

which therefore may be written as a matrix equation,

$$\phi' = \boldsymbol{Q}(Z;\lambda)\phi, \quad a \leq Z \leq b, \tag{2.2.17}$$

where the $\binom{n}{m}$ by $\binom{n}{m}$ matrix Q is given by, in the $m = 2$ and $n = 4$ case,

$$\boldsymbol{Q} = \begin{bmatrix} A_{11}+A_{22} & A_{23} & A_{24} & -A_{13} & -A_{14} & 0 \\ A_{32} & A_{11}+A_{33} & A_{34} & A_{12} & 0 & -A_{14} \\ A_{42} & A_{43} & A_{11}+A_{44} & 0 & A_{12} & A_{13} \\ -A_{31} & A_{21} & 0 & A_{22}+A_{33} & A_{34} & -A_{24} \\ -A_{41} & 0 & A_{21} & A_{43} & A_{22}+A_{44} & A_{23} \\ 0 & -A_{41} & A_{31} & -A_{42} & A_{32} & A_{33}+A_{44} \end{bmatrix}. \tag{2.2.18}$$

The boundary conditions for $\phi' s$ are as follows. For instance, if two independent vectors that satisfy the boundary condition $x = a$ are given by $\boldsymbol{y}_0^{(1)} = (1,0,0,0)^T$ and $\boldsymbol{y}_0^{(2)} = (0,0,1,0)^T$, and ϕ_i are the minors of the corresponding matrix $\boldsymbol{M}^-(a,\lambda)$, then

$$\boldsymbol{M}^-(a,\lambda) = \begin{bmatrix} 1 & 0 \\ 0 & 0 \\ 0 & 1 \\ 0 & 0 \end{bmatrix}, \quad \phi_1(a) = \begin{vmatrix} 1 & 0 \\ 0 & 0 \end{vmatrix} = 0, \quad \phi_2(a) = \begin{vmatrix} 1 & 0 \\ 0 & 1 \end{vmatrix} = 1. \tag{2.2.19}$$

We also have $\phi_3(a) = 0$, $\phi_4(a) = 0$, $\phi_5(a) = 0$, $\phi_6(a) = 0$. It then follows that

$$\phi^-(a) = (0,1,0,0,0,0)^T. \tag{2.2.20}$$

Similarly, $\phi^+(b)$ is formed from the minors of $\boldsymbol{M}^+(b,\lambda) = [\boldsymbol{y}^{(m+1)}, \boldsymbol{y}^{(m+2)}, ...\boldsymbol{y}^n]$.

With these boundary conditions $\phi^-(a)$ and $\phi^+(a)$, we may shoot from $Z = a$ and $Z = b$

to match at $Z = d$. When $m = 2,\ n = 4$, the matching condition $|\mathbf{N}(Z,\lambda)|$ may be expanded using the Laplace expansion of the first two columns as,

$$|N(Z,\lambda)| = |[\boldsymbol{y}^{(1)}(Z), \boldsymbol{y}^{(2)}(Z), \boldsymbol{y}^{(3)}(Z), \boldsymbol{y}^{(4)}(Z)]| = \begin{vmatrix} y_1^{(1)} & y_1^{(2)} & y_1^{(3)} & y_1^{(4)} \\ y_2^{(1)} & y_2^{(2)} & y_2^{(3)} & y_2^{(4)} \\ y_3^{(1)} & y_3^{(2)} & y_3^{(3)} & y_3^{(4)} \\ y_4^{(1)} & y_4^{(2)} & y_4^{(3)} & y_4^{(4)} \end{vmatrix}$$

$$= \begin{vmatrix} y_1^{(1)} & y_1^{(2)} \\ y_2^{(1)} & y_2^{(2)} \end{vmatrix} (-1)^{1+2+3+4} \begin{vmatrix} y_3^{(3)} & y_3^{(4)} \\ y_4^{(3)} & y_4^{(4)} \end{vmatrix} + \begin{vmatrix} y_1^{(1)} & y_1^{(2)} \\ y_3^{(1)} & y_3^{(2)} \end{vmatrix} (-1)^{1+2+2+4} \begin{vmatrix} y_2^{(3)} & y_2^{(4)} \\ y_4^{(3)} & y_4^{(4)} \end{vmatrix}$$

$$+ \begin{vmatrix} y_1^{(1)} & y_1^{(2)} \\ y_4^{(1)} & y_4^{(2)} \end{vmatrix} (-1)^{1+2+2+3} \begin{vmatrix} y_2^{(3)} & y_2^{(4)} \\ y_3^{(3)} & y_3^{(4)} \end{vmatrix} + \begin{vmatrix} y_2^{(1)} & y_2^{(2)} \\ y_3^{(1)} & y_3^{(2)} \end{vmatrix} (-1)^{1+2+1+4} \begin{vmatrix} y_1^{(3)} & y_1^{(4)} \\ y_4^{(3)} & y_4^{(4)} \end{vmatrix}$$

$$+ \begin{vmatrix} y_2^{(1)} & y_2^{(2)} \\ y_4^{(1)} & y_4^{(2)} \end{vmatrix} (-1)^{1+2+1+3} \begin{vmatrix} y_1^{(3)} & y_1^{(4)} \\ y_3^{(3)} & y_3^{(4)} \end{vmatrix} + \begin{vmatrix} y_3^{(1)} & y_3^{(2)} \\ y_4^{(1)} & y_4^{(2)} \end{vmatrix} (-1)^{1+2+1+2} \begin{vmatrix} y_1^{(3)} & y_1^{(4)} \\ y_2^{(3)} & y_2^{(4)} \end{vmatrix}, \tag{2.2.21}$$

which may then be written as,

$$|N(d,\lambda)| = \phi_1^- \phi_6^+ - \phi_2^- \phi_5^+ + \phi_3^- \phi_4^+ + \phi_4^- \phi_3^+ - \phi_5^- \phi_2^+ + \phi_6^- \phi_1^+. \tag{2.2.22}$$

We iterate on λ so that the matching condition $D(\lambda) = 0$ is satisfied.

2.3 Conservation Laws

2.3.1 Noether's theorem

Noether's theorem states that when the equilibrium equations are derivable from a variational principle, a general and systematic procedure for the establishment of conservation laws can be developed from a direct study of the variational integral. A well-known conservation law is the conservation of energy. It applies to Lagrangians and Lagrangian densities that depend on an arbitrary number of fields with arbitrary numbers of derivatives (Noether 1971).

In the case of N independent variables and M dependent variables we apply the variational procedure to an integral of the form

$$\mathcal{L}[\boldsymbol{u}] = \int_{\Omega_0} L(x_i, u_\alpha, u_{\alpha,i}) dv, \tag{2.3.1}$$

where Ω_0 is an arbitrary N-dimensional volume in the space of the variables $x_i, i = 1, ...N$ and the Lagrangian L is a function depending on a finite number of differential variables. $L(u)$ is refereed to as the variational integral of the system. The partial derivatives of the dependent variables with respect to the independent variables will be indicated by the index notation $u_{\alpha,i} = \frac{\partial u_\alpha}{\partial x_i}$, $u_{\alpha,ij} = \frac{\partial^2 u_\alpha}{\partial x_i \partial x_j}$.

Taking the first variation of (2.3.1), we obtain

$$\delta L = \int_{\Omega_0} \left(\frac{\partial L}{\partial u_\alpha} \dot{u}_\alpha + \frac{\partial L}{\partial u_{\alpha,i}} \dot{u}_{\alpha,i} \right) dv. \tag{2.3.2}$$

Since the first variation must vanish for arbitrary variations, the corresponding Euler-Lagrange equations have the form

$$\frac{\partial L}{\partial u_\alpha} - \frac{\partial}{\partial x_i} \left(\frac{\partial L}{\partial u_{\alpha,i}} \right) = 0, \tag{2.3.3}$$

which can be used to derive the equilibrium equations (3.1.9) and (3.1.10). In the above definition, L is a function of the independent variables, dependent variables and their first partial derivatives, but contains no derivatives of the dependent variables higher than the first. However, when the bending stiffness is taken into account which appears in our problem of shell theory in Chapter 4 where we assumed that bending stiffness depends on shell curvature through the tube radius and its first and second order derivatives, the Lagrangian, L contains first order derivatives as well as second order derivatives of the dependent variables. Therefore, the energy functional takes the form

$$\mathcal{L}[\boldsymbol{u}] = \int_{\Omega_0} L(x_i, u_\alpha, u_{\alpha,i}, u_{\alpha,ij}) dv,$$

and so

$$\delta L = \int_{\Omega_0} \left(\frac{\partial L}{\partial u_\alpha} \dot{u}_\alpha + \frac{\partial L}{\partial u_{\alpha,i}} \dot{u}_{\alpha,i} + \frac{\partial L}{\partial u_{\alpha,ij}} \dot{u}_{\alpha,ij} \right) dv, \tag{2.3.4}$$

$$\begin{aligned} &= \int_{\Omega_0} (\frac{\partial L}{\partial u_\alpha} \dot{u}_\alpha + \frac{\partial}{\partial x_i} \left(\frac{\partial L}{\partial u_{\alpha,i}} \dot{u}_\alpha \right) - \frac{\partial}{\partial x_i} \left(\frac{\partial L}{\partial u_{\alpha,i}} \right) \dot{u}_\alpha + \\ &\frac{\partial}{\partial x_j} \left(\frac{\partial}{\partial x_i} \left(\frac{\partial L}{\partial u_{\alpha,ij}} \dot{u}_\alpha \right) \right) - \frac{\partial}{\partial x_j} \left(\frac{\partial L}{\partial u_{\alpha,ij}} \right) \dot{u}_{\alpha,i} - \frac{\partial^2}{\partial x_i \partial x_j} \left(\frac{\partial L}{\partial u_{\alpha,ij}} \right) \dot{u}_\alpha \\ &- \frac{\partial}{\partial x_i} \left(\frac{\partial L}{\partial u_{\alpha,ij}} \right) \dot{u}_{\alpha,j}) dv, \end{aligned} \tag{2.3.5}$$

Thus, in this case the Euler-Lagrangian equations become

$$\frac{\partial L}{\partial u_\alpha} - \frac{\partial}{\partial x_i} \left(\frac{\partial L}{\partial u_{\alpha,i}} \right) - \frac{\partial^2}{\partial x_i \partial x_j} \left(\frac{\partial L}{\partial u_{\alpha,ij}} \right) = 0. \tag{2.3.6}$$

which can be used to derive the equilibrium equations (4.2.26) and (4.2.27).

2.3.2 Conservation laws

The functional (2.3.1) is said to be invariant with respect to the transformation

$$x_i' = x_i'(\mathbf{x}, \mathbf{u}, \epsilon) = x_i + \epsilon\zeta_i(\mathbf{x}, \mathbf{u}) + O(\epsilon^2),$$

$$u_\alpha' = u_\alpha'(\mathbf{x}, \mathbf{u}, \epsilon) = u_\alpha + \epsilon\phi_\alpha(\mathbf{x}, \mathbf{u}) + O(\epsilon^2), \tag{2.3.7}$$

if $\forall\Omega \subset \Omega_0$,

$$\int_{\Omega'} L(x_i', u_\alpha', \frac{\partial u_\alpha'}{\partial x_i'})dx_1'dx_2'dx_3' = \int_\Omega L(x_i, u_\alpha, \frac{\partial u_\alpha}{\partial x_i})dx_1dx_2dx_3, \tag{2.3.8}$$

where Ω' is the image of Ω under the transformation (2.3.7). Noether's theorem says that a conservation law can be derived from each invariance condition. To derive the conservation law, we first have

$$\frac{\partial x_j}{\partial x_i'} = \delta_{ji} - \epsilon D_i\zeta_j + O(\epsilon^2), \quad \frac{\partial x_j'}{\partial x_i} = \delta_{ji} + \epsilon D_i\zeta_j + O(\epsilon^2),$$

$$\frac{\partial u_\alpha'}{\partial x_i'} = \frac{\partial u_\alpha'}{\partial x_i} - \epsilon\frac{\partial u_\alpha}{\partial x_j}D_i\zeta_j + O(\epsilon^2), \tag{2.3.9}$$

where the total spatial derivative D_i is defined by

$$D_i = \frac{\partial}{\partial x_i} + \frac{\partial u_\alpha}{\partial x_i}\frac{\partial}{\partial u_\alpha}. \tag{2.3.10}$$

We have,

$$dx_1'dx_2'dx_3' = \left| \frac{\partial(x_1', x_2', x_3')}{\partial(x_1, x_2, x_3)} \right| dx_1dx_2dx_3 = \left| \left[\frac{\partial x_i'}{\partial(x_j)} \right] \right| dx_1dx_2dx_3, \tag{2.3.11}$$

$$= \det[\delta_{ij} + \epsilon D_j\zeta_i + O(\epsilon^2)]dx_1dx_2dx_3 = (1 + \mathrm{tr}(\epsilon D_j\zeta_i) + O(\epsilon^2))dx_1dx_2dx_3$$

$$= (1 + \epsilon D_i\zeta_i + O(\epsilon^2))dx_1dx_2dx_3. \tag{2.3.12}$$

Substituting these expressions into (2.3.8) then gives

$$\delta\int_\Omega L(x_i, u_\alpha, u_{\alpha,i})dv + \epsilon\int_\Omega (LD_i\zeta_i + \frac{\partial L}{\partial x_i}\zeta_i - \frac{\partial L}{\partial u_{\alpha,i}}u_{\alpha,j}D_i\zeta_j)dv = O(\epsilon^2), \tag{2.3.13}$$

where

$$\delta \int_\Omega L(x_i, u_\alpha, u_{\alpha,i}) dv = \int_\Omega \left(\; L(x_i, u'_\alpha, \tfrac{\partial u'_\alpha}{\partial x_i}) - L(x_i, u_\alpha, \tfrac{\partial u_\alpha}{\partial x_i}) \; \right) dv. \tag{2.3.14}$$

Making use of (2.3.2) and (2.3.3) and the fact that $\dot{u}_\alpha = \epsilon \phi_\alpha$, we obtain

$$\begin{aligned} \delta \int_\Omega L(x_i, u_\alpha, u_{\alpha,i}) dv &= \int_\Omega \left[\frac{\partial L}{\partial u_\alpha} \dot{u}_\alpha + \frac{\partial}{\partial x_i} \left(\; \tfrac{\partial L}{\partial u_{\alpha,i}} \dot{u}_\alpha \; \right) \right] dv, \\ &= \epsilon \int_\Omega \left[\frac{\partial}{\partial x_i} \left(\; \tfrac{\partial L}{\partial u_{\alpha,i}} \dot{\phi}_\alpha \; \right) \right] dv + O(\epsilon^2). \end{aligned} \tag{2.3.15}$$

For the second term in (2.3.13), we have

$$\begin{aligned} LD_i\zeta_i + \frac{\partial L}{\partial x_i}\zeta_i - \frac{\partial L}{\partial u_{\alpha,i}} u_{\alpha,j} D_i \zeta_j &= LD_i\zeta_i + \frac{\partial L}{\partial x_i}\zeta_i - \frac{\partial L}{\partial u_{\alpha,i}} [D_i(u_{\alpha,j}\zeta_j) - u_{\alpha,ij}\zeta_j], \\ &= LD_i\zeta_i + \zeta_i D_i L - D_i(\frac{\partial L}{\partial u_{\alpha,i}} u_{\alpha,j}\zeta_j) = D_i(\zeta_i L - \frac{\partial L}{\partial u_{\alpha,i}} u_{\alpha,j}\zeta_j). \end{aligned} \tag{2.3.16}$$

On substituting (2.3.15) and (2.3.16) into (2.3.13) and equating the coefficients of ϵ to zero, we obtain

$$\int_\Omega D_i P_i dv = \int_\Omega \text{div}\mathbf{P} dv = 0, \tag{2.3.17}$$

where

$$P_i = \zeta_i L + (\phi_\alpha - u_{\alpha,j}\zeta_j) \frac{\partial L}{\partial u_{\alpha,i}}. \tag{2.3.18}$$

Since (2.3.17) is true for arbitrary Ω, it follows that

$$\text{div}\mathbf{P} = 0. \tag{2.3.19}$$

Using the divergence theorem, (2.3.17) becomes

$$\int_{\partial\Omega} \mathbf{P} \cdot \mathbf{n} ds = 0, \tag{2.3.20}$$

which says that the flux of a quantity $\mathbf{P}$ through the surface of Ω is zero and hence the quantity of $\mathbf{P}$ inside Ω must be conserved. This is why an equation of the form (2.3.19) is usually referred to a conservation law. For the $1D$ case, (2.3.19) reduces to

$$\frac{dP}{dZ} = 0, \quad \Rightarrow \quad P = \text{constant}. \tag{2.3.21}$$

2.3.3 Extension to the case when second-order derivatives are involved

When bending stiffness is taken into account, the energy functional has the form

$$\mathcal{L}[\boldsymbol{u}] = \int_{\Omega_0} L(x_i, u_\alpha, u_{\alpha,i}, u_{\alpha,ij}) dv, \tag{2.3.22}$$

and the associated Euler Lagrangian equations are given by

$$\frac{\partial L}{\partial u_\alpha} - \frac{\partial}{\partial x_i}\left(\frac{\partial}{\partial u_{\alpha,i}}\right) - \frac{\partial^2}{\partial x_i \partial x_j}\left(\frac{\partial L}{\partial u_{\alpha,ij}}\right) = 0. \tag{2.3.23}$$

The functional (2.3.22) is said to be invariant with respect to the transformation (2.3.7) if $\forall \Omega \subset \Omega_0$,

$$\int_{\Omega'} L(x'_i, u'_\alpha, \frac{\partial u'_\alpha}{\partial x'_i}, \frac{\partial^2 u'_\alpha}{\partial x'_i \partial x'_j}) dx'_1 dx'_2 dx'_3 = \int_{\Omega} L(x_i, u_\alpha, \frac{\partial u_\alpha}{\partial x_i}, \frac{\partial^2 u_\alpha}{\partial x_i \partial x_j}) dx_1 dx_2 dx_3, \tag{2.3.24}$$

where Ω' is the image of Ω under the transformation (2.3.7). Noether's theorem says that a conservation law can be derived from this invariance condition. To derive the conservation law, we first have

$$\frac{\partial}{\partial x'_i} = \frac{\partial}{\partial x_j}\frac{\partial x_j}{\partial x'_i} = \frac{\partial}{\partial x_i} - \epsilon D_i \zeta_k \frac{\partial}{\partial x_k}, \tag{2.3.25}$$

and

$$\frac{\partial^2}{\partial x'_i \partial x'_j} = \frac{\partial^2}{\partial x_i \partial x_j} - \epsilon \left(D_i D_j \zeta_m \frac{\partial}{\partial x_m} + D_j \zeta_m \frac{\partial^2}{\partial x_i \partial x_m} + D_j \zeta_k \frac{\partial^2}{\partial x_i \partial x_j} \right) + O(\epsilon^2). \tag{2.3.26}$$

Thus, (2.3.25) and (2.3.26) become

$$\frac{\partial u'_\alpha}{\partial x'_i} = \frac{\partial u'_\alpha}{\partial x_i} - \epsilon D_i \zeta_k \frac{\partial u'_\alpha}{\partial x_k}, \tag{2.3.27}$$

$$\frac{\partial^2 u_\alpha}{\partial x'_i \partial x'_j} = \frac{\partial^2 u'_\alpha}{\partial x_i \partial x_j} - \epsilon \left(D_i D_j \zeta_m \frac{\partial u_\alpha}{\partial x_m} + D_j \zeta_m \frac{\partial^2 u_\alpha}{\partial x_i \partial x_m} + D_j \zeta_k \frac{\partial^2 u_\alpha}{\partial x_i \partial x_j} \right) + O(\epsilon^2). \tag{2.3.28}$$

Substituting these expressions into (2.3.24) then gives

$$\delta \int_\Omega L(x_i, u_\alpha, u_{\alpha,i}, u_{\alpha,ij})dv + \epsilon \int_\Omega (LD_i\zeta_i + \frac{\partial L}{\partial x_i}\zeta_i - \frac{\partial L}{\partial u_{\alpha,i}}u_{\alpha,j}D_i\zeta_j)dv -$$

$$\epsilon \int_\Omega \frac{\partial L}{\partial u_{\alpha,ij}}(D_iD_j\zeta_m u_{\alpha,m} + 2D_j\zeta_m u_{\alpha,im})dv = O(\epsilon^2), \tag{2.3.29}$$

where

$$\delta \int_\Omega L(x_i, u_\alpha, u_{\alpha,i})dv = \int_\Omega [L(x_i, u'_\alpha, \frac{\partial u'}{\partial x_i}, \frac{\partial u'}{\partial x_i \partial x_j})$$

$$-L(x_i, u_\alpha, \frac{\partial u_\alpha}{\partial x_i \partial x_j})]dv, \tag{2.3.30}$$

Making use of (2.3.5), (2.3.23) and the fact that $\dot{u}_\alpha = \epsilon\phi_\alpha$, we obtain

$$\delta \int_\Omega L(x_i, u_\alpha, u_{\alpha,i})dv =$$

$$\epsilon \int_\Omega \frac{\partial}{\partial x_i}\left[\frac{\partial L}{\partial u_{\alpha,i}}\phi_\alpha + \frac{\partial L}{\partial u_{\alpha,ij}}D_j\phi_\alpha - \frac{\partial}{\partial x_j}\left(\frac{\partial L}{\partial u_{\alpha,ij}}\right)\phi_\alpha\right]dv + O(\epsilon^2). \tag{2.3.31}$$

For the second term in (2.3.29), we have

$$LD_i\zeta_i + \frac{\partial L}{\partial x_i}\zeta_i - \frac{\partial L}{\partial u_{\alpha,i}}u_{\alpha,j}D_i\zeta_j = LD_i\zeta_i + \frac{\partial L}{\partial x_i}\zeta_i$$

$$-\frac{\partial L}{\partial u_{\alpha,i}}u_{\alpha,j}[D_i(u_{\alpha,j}\zeta_j) - u_{\alpha,ij}\zeta_j]$$

$$= LD_i\zeta_i + \frac{\partial L}{\partial x_i}\zeta_i - D_i(\frac{\partial L}{\partial u_{\alpha,i}}u_{\alpha,j}\zeta_j) + u_{\alpha,j}\zeta_j D_j(\frac{\partial L}{\partial u_{\alpha,i}}) + \frac{\partial L}{\partial u_{\alpha,i}}u_{\alpha,ij}\zeta_j,$$

$$= LD_i\zeta_i + \frac{\partial L}{\partial x_i}\zeta_i - D_i(\frac{\partial L}{\partial u_{\alpha,i}}u_{\alpha,j}\zeta_j) + u_{\alpha,j}\zeta_j\frac{\partial L}{\partial u_\alpha} + u_{\alpha,j}\zeta_j D_kD_i$$

$$(\frac{\partial L}{\partial u_{\alpha,ik}}) + \frac{\partial L}{\partial u_{\alpha,i}}u_{\alpha,ij}\zeta_j,$$

$$= LD_i\zeta_i + \zeta_i D_iL - \zeta_i u_{\alpha,kli}\frac{\partial L}{\partial u_{\alpha,kl}} - D_i(\frac{\partial L}{\partial u_{\alpha,i}}u_{\alpha,j}\zeta_j) + u_{\alpha,j}\zeta_j D_kD_i(\frac{\partial L}{\partial u_{\alpha,ik}}). \tag{2.3.32}$$

For the third term in (2.3.29), we have

$$\frac{\partial L}{\partial u_{\alpha,ij}}D_j\zeta_m u_{\alpha,im} = D_j\left(\frac{\partial L}{\partial u_{\alpha,ij}}\zeta_m u_{\alpha,im}\right) - D_j\left(\frac{\partial L}{\partial u_{\alpha,ij}}\right)u_{\alpha,im}\zeta_m - \frac{\partial L}{\partial u_{\alpha,ij}}u_{\alpha,ijm}\zeta_m,$$

and

$$\frac{\partial L}{\partial u_{\alpha,ij}}u_{\alpha,m}D_iD_j\zeta_m = D_i\left(\frac{\partial L}{\partial u_{\alpha,ij}}u_{\alpha,m}D_j\zeta_m\right) - D_j\zeta_m D_i\left(\frac{\partial L}{\partial u_{\alpha,ij}}u_{\alpha,m}\right),$$

$$= D_i\left(\frac{\partial L}{\partial u_{\alpha,ij}}u_{\alpha,m}D_j\zeta_m\right) - D_j\left[\zeta_m D_i\left(\frac{\partial L}{\partial u_{\alpha,ij}}u_{\alpha,m}\right)\right]$$

$$+\zeta_m D_iD_j\left(\frac{\partial L}{\partial u_{\alpha,ij}}u_{\alpha,m}\right),$$

$$= D_i\left[\frac{\partial L}{\partial u_{\alpha,ij}}u_{\alpha,m}D_j\zeta_m - \zeta_m D_j\left(\frac{\partial L}{\partial u_{\alpha,ij}}u_{\alpha,m}\right)\right]$$

$$+\zeta_m\left[D_iD_j\left(\frac{\partial L}{\partial u_{\alpha,ij}}\right)u_{\alpha,m} + 2D_i\left(\frac{\partial L}{\partial u_{\alpha,ij}}\right)u_{\alpha,mj} + \frac{\partial L}{\partial u_{\alpha,ij}}u_{\alpha,mij}\right]. \tag{2.3.33}$$

On substituting these expressions back into (2.3.29) and simplifying, we obtain

$$\int_\Omega D_iQ_i dv = 0, \tag{2.3.34}$$

and hence

$$D_iQ_i = 0, \tag{2.3.35}$$

where

$$Q_i = \zeta_i L - \zeta_i u_{\alpha,j}\frac{\partial L}{\partial u_{\alpha,i}} + \phi_\alpha\left[\frac{\partial L}{\partial u_{\alpha,i}} - D_j\left(\frac{\partial L}{\partial u_{\alpha,ij}}\right)\right]$$

$$+\frac{\partial L}{\partial u_{\alpha,ij}}D_j\phi_\alpha - \zeta_m u_{\alpha,mj}\frac{\partial L}{\partial u_{\alpha,ij}} - \frac{\partial L}{\partial u_{\alpha,ij}}u_{\alpha,m}D_j\zeta_m + \zeta_m u_{\alpha,mj}D_j\left(\frac{\partial L}{\partial u_{\alpha,ij}}\right). \tag{2.3.36}$$

2.3.4 Application to inflation of a membrane tube

The equilibrium equations for an inflated membrane tube can be obtained by minimising the energy functional

$$\int_{-L}^{L} W(\lambda_1,\lambda_2)2\pi RHdZ - P\int_{-L}^{L}\pi r^2 dz = \int_{-L}^{L}(2\pi RHW(\lambda_1,\lambda_2) - P\pi r^2 z')dZ, \tag{2.3.37}$$

where prime denotes the differentiation with respect to Z. This functional is in the form (2.3.1) with

$$x_1 = Z,\ u_1 = r(Z),\ u_2 = z(Z),\ L(x_i, u_\alpha, u_{\alpha,i}) = 2RHW(\lambda_1, \lambda_2) - Pr^2 z'. \quad (2.3.38)$$

We have

$$\frac{\partial L}{\partial r'} = 2RHW_2(\lambda_1, \lambda_2)\frac{r'}{\lambda_2}, \quad \frac{\partial L}{\partial z'} = 2RHW_2(\lambda_1, \lambda_2)\frac{z'}{\lambda_2} - Pr^2. \quad (2.3.39)$$

The energy functional is clearly invariant with respect to the translations in z and Z. Translations in Z correspond to (2.3.7) with

$$\zeta_1 = 1, \quad \phi_\alpha = 0, \quad (2.3.40)$$

and (2.3.18) gives

$$L - \frac{\partial L}{\partial r'}r' - \frac{\partial L}{\partial z'}z' = \text{constant}. \quad (2.3.41)$$

With the use of (2.3.39), (2.3.41) becomes

$$2RHW(\lambda_1, \lambda_2) - 2RHW_2(\lambda_1, \lambda_2)\lambda_2 = \text{constant}, \quad (2.3.42)$$

which is Fu et al's (2008) equation (2.7). Translations in z correspond to (2.3.7) with

$$\zeta_1 = 0, \quad \phi_1 = 0, \quad \phi_2 = 1, \quad (2.3.43)$$

and (2.3.18) then gives

$$\frac{\partial L}{\partial z'} = \text{constant}. \quad (2.3.44)$$

With the use of (2.3.39), this becomes

$$2RHW_2(\lambda_1, \lambda_2)\frac{z'}{\lambda_2} - P\pi r^2 = \text{constant}, \quad (2.3.45)$$

which is Fu et al's (2008) equation (2.5).

2.3.5 Application to inflation of a thin-walled tube with bending stiffness

When bending stiffness is taken into account, the energy functional will have the form

$$L[\boldsymbol{u}] = \int_{-L}^{L} L(\boldsymbol{u}, \boldsymbol{u}', \boldsymbol{u}'')dZ = \int_{-L}^{L} L(r, r', r'', z', z'')dZ. \tag{2.3.46}$$

The energy functional is invariant with respect to the translations in z and Z. Translations in Z correspond to (2.3.7) with

$$\zeta_1 = 1, \quad \phi_\alpha = 0, \tag{2.3.47}$$

and (2.3.35) then gives

$$L - \frac{\partial L}{\partial r'}r' - \frac{\partial L}{\partial z'}z' - \frac{\partial L}{\partial r''}r'' - \frac{\partial L}{\partial z''}z'' + r'(\frac{\partial L}{\partial r''})' + z'(\frac{\partial L}{\partial z''})' = \text{constant}. \tag{2.3.48}$$

Translations in Z correspond to (2.3.7) with

$$\zeta_1 = 0, \quad \phi_1 = 0, \quad \phi_2 = 1, \tag{2.3.49}$$

and (2.3.35) then gives

$$\frac{\partial L}{\partial z'} - (\frac{\partial L}{\partial z''})' = \text{constant}. \tag{2.3.50}$$

2.4 Finite Difference Method

In many situations, finding an analytic solution to a ordinary differential equation or a system of such equations is impossible. Thus, the development of accurate numerical

methods that utilize computer algorithms are used to find approximation solutions. One of the basic numerical solution schemes for ordinary differential equations is the Finite Difference Method, obtained by replacing the derivatives in the equation by the appropriate numerical differentiation formulae. One advantage of the Finite Difference Method is that Taylor series expansion can be easily applied to analyse local truncation errors. But there is an important limitation in applying this method, which is the requirement of a structured grid. Therefore, the method cannot easily be applied in complex domains. For a finite difference scheme to be convergent, the calculated numerical solution of the equation must approach the exact solution at any point in space, when the cell length h tends towards zero. To improve the order of accuracy of finite difference approximations we need more sample points and higher precision. For a detailed description of Finite difference method, one can refer to standard texts like Forsythe and Wasow (1964), Hildebrand (1974), Mitchell and Griffiths (1980).

For the sake of simplicity, we shall consider the one-dimensional case only. Suppose the function u is C^2 continuous in the neighbourhood of x. For any $h > 0$ we have

$$u(x+h) = u(x) + hu'(x) + \frac{h^2}{2}u''(x) + \frac{h^3}{2}u'''(x) + O(h^4),$$
$$u(x-h) = u(x) - hu'(x) + \frac{h^2}{2}u''(x) - \frac{h^3}{2}u'''(x) + O(h^4), \tag{2.4.1}$$

where the term $O(h^4)$ indicates the order of error of the approximation. The second and third order terms in equation (2.4.1) are neglected for the purpose of this derivation. The second order approximation of $u'(x)$ can be written as

$$u'(x) = \frac{u(x+h) - u(x-h)}{2h} + O(h^2), \tag{2.4.2}$$

where the truncation error, $O(h^2)$ tends to zero, as $h \to 0$. In other words, h should be sufficiently small to get a good approximation. As an example, we consider solving a

non-linear system of first order ordinary differential equations given by

$$\boldsymbol{u}'(x) = f(\boldsymbol{u}(x)), \quad a \leq x \leq b, \tag{2.4.3}$$

with boundary conditions $\boldsymbol{u}(a) = \boldsymbol{u}_1,\ \boldsymbol{u}(b) = \boldsymbol{u}_{n+1}$, where $\boldsymbol{u}(x) = (u_1(x), u_2(x), ..., u_m(x))$ represents a vector of unknowns. The solution of the equation (2.4.3) on a $1D$ domain with n cells are shown in Figure (2.4.1). The domain length is $(b-a)$, with $n-1$ internal nodes and two boundary nodes. Since the grid spacing is equal, the length of each cell is $h = \frac{b-a}{n}$. Typically, the spacing is aimed at becoming very small as the number of grid points will become very large. The first order accurate central differencing formula is used to approximate the equations (2.4.3).

The discretisation equation can be written as

$$\frac{\boldsymbol{u}_{i+1} - \boldsymbol{u}_{i-1}}{2h} = f(\boldsymbol{u}_i), \tag{2.4.4}$$

with a leading error of $O(h)$. The index i refers to any node in the domain, $i-1$ refers

Figure 2.4.1: $1D$ uniform mesh with n cells.

to the left side node of cell i and $i+1$ refers to the right side node of cell i. Since

$\boldsymbol{u}_1$ and $\boldsymbol{u}_{n+1}$ are boundary nodes, their values are already known. After applying the discretisation equation (2.4.4) at every internal node, $m(n-1)$ coupled linear algebraic equations with $m(n-1)$ unknowns can be formed. The resulting system of $m(n-1)$ algebraic equations can be solved with the aid of Mathematica.

3 Localized Bulging in an Inflated Membrane Tube without Bending Stiffness

3.1 Introduction

In this chapter we consider the deformation of a cylindrical, hyperelastic, isotropic, incompressible membrane subject to an internal pressure. We consider deformations which are axially symmetric with respect to the axis of the membrane. This study has been recently described numerically and analytically by Fu and co-workers. This section provides a review of these recent research in the area of thin-walled tubes without bending stiffness. In particular, the weakly non-linear analysis and the Finite Difference Method are used to derive the bifurcation condition and to determine the localized bulging solutions respectively. We shall use these techniques in Chapter 4 in order to investigate the effect of bending stiffness in the inflation of thin-walled cylindrical tubes.

3.1.1 Governing equations

We use cylindrical polar coordinates throughout this study, and so the undeformed configuration is described by coordinates $(R,\ \Theta,\ Z)$, where $0 \leq \Theta \leq 2\pi,\ -\infty \leq Z \leq$

∞. The position vector $\boldsymbol{X}$ is given by

$$\boldsymbol{X} = R\boldsymbol{e}_R(\Theta) + Z\boldsymbol{e}_Z. \tag{3.1.1}$$

The undeformed tube is subjected to a uniform internal pressure, which drives the deformation. The axisymmetric deformed configuration expressed using cylindrical polar coordinates $(r,\ \theta,\ z)$ is given by $r = r(Z),\quad \theta = \Theta,\quad z = z(Z)$. The deformed position vector $\boldsymbol{x}$ is given by

$$\boldsymbol{x} = r\boldsymbol{e}_r(\theta) + z\boldsymbol{e}_z, \tag{3.1.2}$$

where Z and z are the axial coordinates of a representative material particle before and after inflation respectively, r is the mid-plane radius after the inflation, and h and H are the wall thickness in the deformed and reference configurations, respectively. To characterise the deformation we use three principal stretches, $\lambda_1, \lambda_2, \lambda_3$ in the latitudinal, the meridional and the normal directions respectively. We have

$$\lambda_1 = \frac{r}{R},\quad \lambda_2 = \sqrt{r'^2 + z'^2},\quad \lambda_3 = \frac{h}{H}, \tag{3.1.3}$$

where primes indicate differentiation with respect to Z. The principal Cauchy stresses $\sigma_1, \sigma_2, \sigma_3$ in the deformed configuration for an incompressible material are given by

$$\sigma_i = \lambda_i W_i - p,\quad i = 1, 2, 3, \tag{3.1.4}$$

where $W = W(\lambda_1, \lambda_2, \lambda_3)$ is the strain-energy function, $W_i = \partial W/\partial\lambda_i$ and p is the Lagrangian multiplier associated with the constraint of incompressibility $J = \det\boldsymbol{F} = \lambda_1\lambda_2\lambda_3 = 1$. We now regard W as a function of two independent stretches, λ_1 and λ_2 and introduce the new notation

$$w(\lambda_1, \lambda_2) = W(\lambda_1, \lambda_2, \lambda_1^{-1}\lambda_2^{-1}). \tag{3.1.5}$$

It then follows that

$$\sigma_1 - \sigma_3 = \lambda_1 W_1 - \lambda_3 W_3 = \lambda_1 w_1, \quad \sigma_2 - \sigma_3 = \lambda_2 W_2 - \lambda_3 W_3 = \lambda_2 w_2, \tag{3.1.6}$$

where $w_i = \partial w / \partial \lambda_i$. Using the membrane assumption of no stress in the thickness direction, $\sigma_3 = 0$, equation (3.1.6) becomes

$$\sigma_i = \lambda_i w_i, \quad i = 1, 2, \ \text{(no summation on i)}. \tag{3.1.7}$$

3.1.2 Euler-Lagrangian equations

We now derive equilibrium equations for the membrane surface, using Euler-Lagrangian equations associated with the variational problem as described in Chapter 2. We write (2.3.3) in terms of $\boldsymbol{u} = (r, z)$ as

$$\frac{\partial L}{\partial r} - \left(\frac{\partial L}{\partial r'}\right)' = 0, \quad \left(\frac{\partial L}{\partial z'}\right)' = 0, \tag{3.1.8}$$

where

$$L[\mathbf{u}, \mathbf{u}', \mathbf{u}''] = w(\lambda_1, \lambda_2) - \frac{P}{2RH} r^2 z',$$

$$\frac{\partial L}{\partial r} = w_1 \frac{1}{R} - \frac{P}{RH} r z', \quad \frac{\partial L}{\partial r'} = w_2 \frac{r'}{\lambda_2}, \quad \frac{\partial L}{\partial z'} = w_2 \frac{z'}{\lambda_2} - \frac{P r^2}{2RH}.$$

By setting the first variation to zero, we obtain the equilibrium equations in the form

$$w_1 \frac{1}{R} - \frac{P}{RH} r z' - \left(w_2 \frac{r'}{\lambda_2}\right)' = 0, \tag{3.1.9}$$

$$w_2 \frac{z'}{\lambda_2} - \frac{P}{2RH} r^2 = C_1, \tag{3.1.10}$$

where C_1 is a constant and a prime denotes differentiation with respect to Z.

Using Noether's Theorem, we have

$$L - \frac{\partial L}{\partial r'} \, r' - \frac{\partial L}{\partial z'} \, z' = \text{constant}, \tag{3.1.11}$$

which gives

$$w - \lambda_2 w_2 = C_2, \tag{3.1.12}$$

where C_2 is a constant. Equations (3.1.10) and (3.1.12) are equivalent to equations (2.5) and (2.7) of Fu et al.(2008) respectively, which are derived by considering equilibrium of an infinitesimal volume element in the z and r directions respectively. In this work we are interested in localized bulging solutions in which the tube has a constant radius r_∞ and constant axial stretch z_∞ far away from the localized bulge. It should be noted that r_∞ and z_∞ are defined when both R and H are constant, therefore in the subsequent asymptotic analysis r_∞ and z_∞ are dimensionless. We can find constants C_1 and C_2 by evaluating (3.1.10) and (3.1.12) in the limit $Z \to \infty$, as

$$C_1 = w_2^{(\infty)} - \frac{P r_\infty^2}{2}, \quad C_2 = w^{(\infty)} - z_\infty w_2^{(\infty)}. \tag{3.1.13}$$

where here and hereafter the superscript (∞) signifies evaluation at $\lambda_1 \to r_\infty$, $\lambda_2 \to z_\infty$. For uniform inflation, we have $r =$ constant, and so the equilibrium equation (3.1.9) becomes

$$P\lambda_1\lambda_2 = w_1, \tag{3.1.14}$$

which gives the pressure P in terms of r_∞ and z_∞ as

$$P = \frac{w_1^{(\infty)}}{r_\infty z_\infty}. \tag{3.1.15}$$

Figure 3.1.1 shows the connection between P and r_∞ when z_∞ is fixed at 1.1 for Ogden strain-energy function. It shows that the uniform inflation starts from the origin where $r_\infty = 1$ and $z_\infty = 1$. In Figure 3.1.2 we have shown that pressure is a monotonic increasing function with respect to r_∞ for the Gent strain energy function

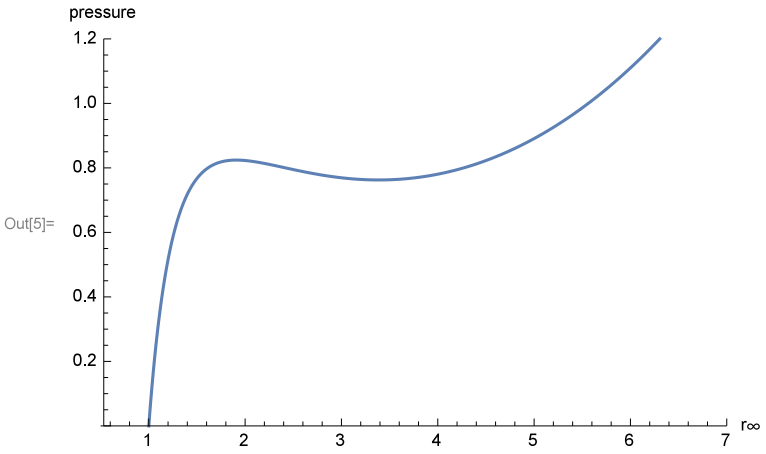

Figure 3.1.1: Pressure as a function of r_∞ for the Ogden strain-energy function when $z_\infty = 1.1$.

with $J_m = 30$. Evaluating (3.1.10) and (3.1.12) with the use of (3.1.13) at $Z = 0$, we obtain

$$w_2(r_0, z_0') - \frac{w_1^{(\infty)}}{2r_\infty z_\infty}(r_0^2 - r_\infty^2) - w_2^{(\infty)} = 0, \tag{3.1.16}$$

$$w(r_0, z_0') - z_0' w_2(r_0, z_0') - w^{(\infty)} + z_\infty w_2^{(\infty)} = 0, \tag{3.1.17}$$

where $r_0 = r(0), z_0' = z'(0)$. Equations (3.1.16) and (3.1.17) are two coupled non-linear equations for r_0 and z_0'. Theses two equations can be solved to find r_0 and z_0' as functions of r_∞ and they always admit the trivial solution $r_0 = r_\infty$ and $z_0' = z_\infty$ as a solution. Therefore the non-trivial solutions may bifurcate from this trivial solution when (3.1.16) and (3.1.17) have a solution other than $r_0 = r_\infty$ and $z_0' = z_\infty$. Using this fact, Fu et al. (2008) derived the bifurcation condition as $\omega(r_\infty) = 0$, where

$$\omega(r_\infty) = \frac{r_\infty(w_1^{(\infty)} - z_\infty w_{12}^{(\infty)})^2 + z_\infty^2 w_{22}^{(\infty)}(w_1^{(\infty)} - r_\infty w_{11}^{(\infty)})}{r_\infty z_\infty^2 w_{22}^{(\infty)}}, \tag{3.1.18}$$

where $w_{ij} = \partial^2 w/(\partial\lambda_i \partial\lambda_j)$ for $i, j = 1, 2$. The pressure (3.1.15) for the Ogden material

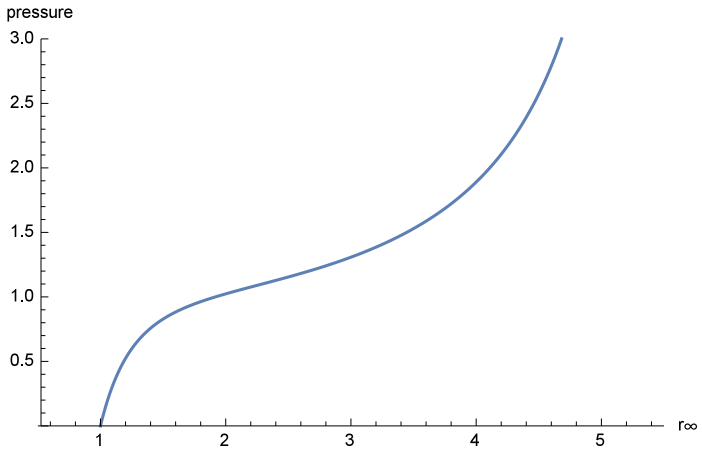

Figure 3.1.2: Pressure as a function of r_∞ for the Gent strain-energy function with $J_m = 30$ when $z_\infty = 1.1$.

is plotted in Figure 3.1.3 for different axial stretches. Figure 3.1.4 shows that the bifurcation condition $\omega(\lambda_1, \lambda_2) = 0$ and zero fixed axial force $F = 0$ have two intersection points for the Gent model with $J_m = 30$. These two bifurcation points correspond to the pressure maximum and pressure minimum in uniform inflation.

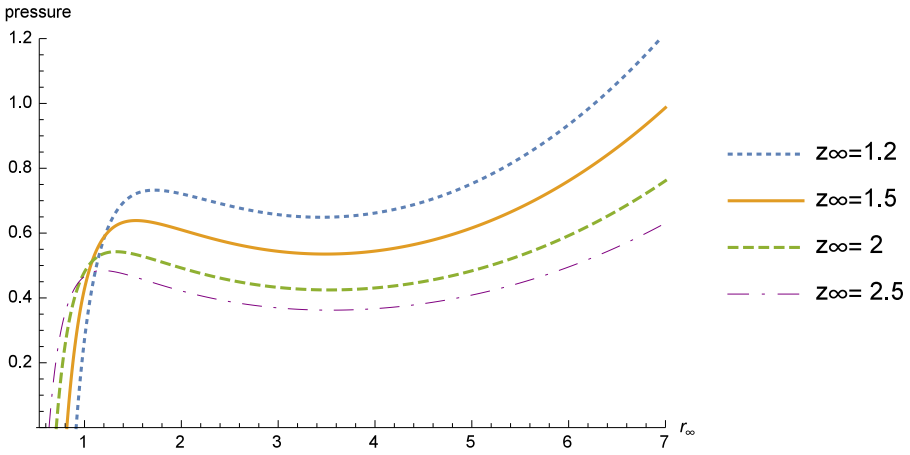

Figure 3.1.3: Pressure as a function of r_∞ for the Ogden strain-energy function with different z_∞ values when $z_\infty = 1.2, 1.5, 2, 2.5$.

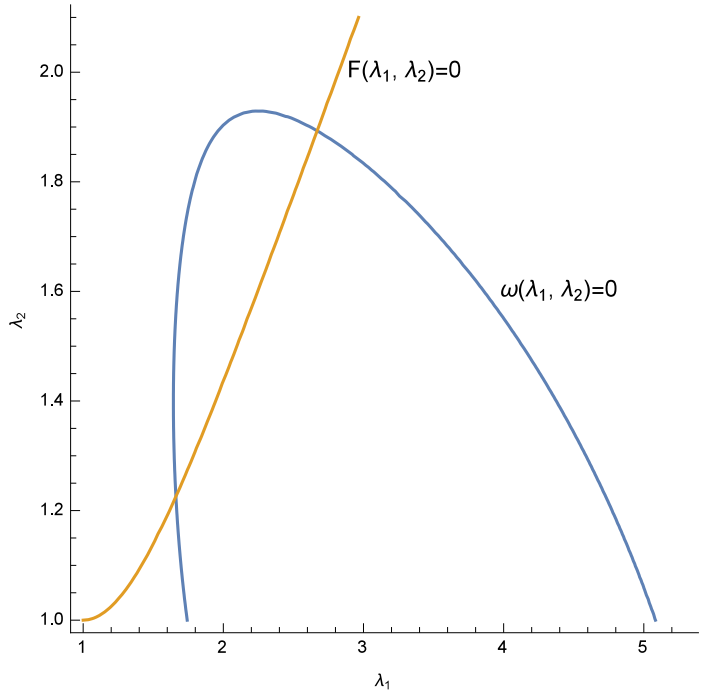

Figure 3.1.4: Plot of the bifurcation condition $\omega(\lambda_1, \lambda_2) = 0$ and zero fixed axial force condition $F = 0$ for the Gent model with $J_m = 30$.

3.1.3 Weakly non-linear analysis

We now demonstrate that a weakly non-linear analysis can be used to derive the same bifurcation condition as in (3.1.18). The variables $\lambda_1, \lambda_2, \phi$ defined in the previous section are expanded in terms of a small parameter ϵ which measures the departure of λ_1 and λ_2 from its critical values r_∞ and z_∞. Guided by the scalings in Fu et al. (2008), we define a far distance variable $s = \sqrt{\epsilon}z$, and the variables are expanded as

$$\begin{aligned} \lambda_1 &= r_\infty + \epsilon y_1(s) + \epsilon^2 y_2(s) + \epsilon^3 y_3(s), \\ \lambda_2 &= z_\infty + \epsilon z_1(s) + \epsilon^2 z_2(s) + \epsilon^3 z_3(s), \\ \phi &= \epsilon^{3/2}(\alpha_1(s) + \epsilon\alpha_2(s) + \epsilon^2\alpha_4(s)), \end{aligned} \tag{3.1.19}$$

where r_∞ , z_∞ are known and the remaining terms are unknowns which can be determined at successive orders of approximations.

To describe this method, we may rewrite the system of differential equations (5.1) as (Fu et al. 2008)

$$\begin{aligned} \lambda_1' &= \lambda_2 \sin\phi, \\ \lambda_2' &= \frac{w_1 - \lambda_2 w_{12}}{w_{22}} \sin\phi, \\ \phi' &= \frac{w_1}{w_2}\cos\phi - \frac{w_1^{(\infty)}}{r_\infty z_\infty w_2}\lambda_1\lambda_2. \end{aligned} \tag{3.1.20}$$

We now substitute the asymptotic expressions (3.1.19) into the governing equations (3.1.20) and expand the latter as power series in ϵ. At $O(1)$, we obtain the equations for the uniform state r_∞ and z_∞. Equating the coefficients of ϵ in the resulting equation of $(3.1.20)_3$, we can write $z_1(s)$ in terms of $y_1(s)$ as

$$z_1(s) = -z_\infty \frac{(w_1^{(\infty)} - r_\infty w_{11}^{(\infty)})}{r_\infty(w_1^{(\infty)} - z_\infty w_{12}^{(\infty)})} y_1(s). \tag{3.1.21}$$

Similarly we can also write $\alpha_1(s)$ in terms of $y_1(s)$. At $O(\epsilon^{3/2})$ the problem is in linear form. By equating the coefficients of $\epsilon^{3/2}$ in the resulting equations of $(3.1.20)_1$ and $(3.1.20)_2$, we obtain a matrix equation for $y_1'(s)$ and $\alpha_1(s)$ in the form

$$B\begin{pmatrix} y_1'(s) \\ \\ \alpha_1(s) \end{pmatrix} = \begin{pmatrix} 0 \\ \\ 0 \end{pmatrix}, \tag{3.1.22}$$

where

$$B = \begin{pmatrix} 1 & -z_\infty \\ \dfrac{-z_\infty(w_1 - r_\infty w_{11})}{r_\infty(w_1 - z_\infty w_{12})} & \dfrac{-w_1 + z_\infty w_{12}}{w_{22}} \end{pmatrix}. \tag{3.1.23}$$

In order for a non-trivial set of $y_1'(s)$ and $\alpha_1(s)$ to exist, we require the determinant of the matrix B to vanish, which gives the following expression.

$$\det(B) = \frac{-r_\infty(w_1^{(\infty)} - z_\infty w_{12}^{(\infty)})^2 + z_\infty^2 w_{22}^{(\infty)}(-w_1^{(\infty)} + r_\infty w_{11}^{(\infty)})}{r_\infty w_{22}^{(\infty)}(w_1^{(\infty)} - z_\infty w_{12}^{(\infty)})} = 0. \tag{3.1.24}$$

This expression when equal to zero is the bifurcation condition which is identical to that given in (3.1.18). It is important to note that the condition (3.1.24) describes the bifurcation mode having zero wave number (Haughton & Ogden 1979b). Figure 3.1.5 shows the bifurcation diagram for different strain-energy functions with unit axial stretch. It shows that Gent materials with $J_m = 30$ and $J_m = 97.2$ have two bifurcation values, while, Varga and Ogden materials each have only one bifurcation point. Figure 3.1.6 shows that Ogden material has two bifurcation points for the case of no axial force. For the case of fixed axial stretch with $z_\infty < 3.1$, the bifurcation behaviour of the Ogden material stays the same, that is it has only one bifurcation point, but there exist three bifurcation points when $z_\infty = 3.2$. On the same figure where z_∞ is fixed at 3.2, we have also used the dashed line to indicate these three bifurcation points at $r_\infty = 1.0358, 4.7987$ and 6.035.

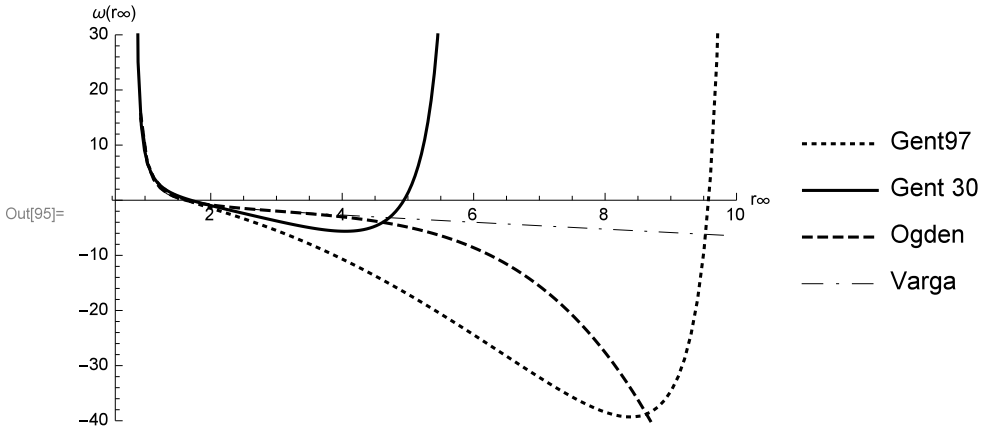

Figure 3.1.5: Function $\omega(r_\infty)$ for the Gent material with $J_m = 30$ and $J_m = 97.2$, Ogden and Varga strain-energy functions with unit axial stretch.

Bifurcation diagram for Gent material with $J_m = 97$ when the axial force is zero is shown in Figure 3.1.7, which looks very similar to the one shown in Figure 3.1.6 for the Ogden strain-energy function with zero axial force including two bifurcation points, the first of which is subcritical and the second is supercritical. Therefore bulging and necking solutions may both exist. However, in the case of fixed axial stretch, the kink solution can exist despite a second bifurcation point not existing.

Equating the coefficients of $O(\epsilon^{5/2})$ in the power series of ϵ obtained from the resulting equation of (3.1.20), we find that $y_2(s)$ and $\alpha_2(s)$ satisfy the inhomogeneous system

$$B \begin{pmatrix} y_2'(s) \\ \\ \phi_2(s) \end{pmatrix} = \begin{pmatrix} k_1(s) \\ \\ k_2(s) \end{pmatrix}, \tag{3.1.25}$$

where $k_1(s), k_2(s)$ contain $y_1(s), z_1(s), \alpha_1(s)$ and their derivatives with respect to s and

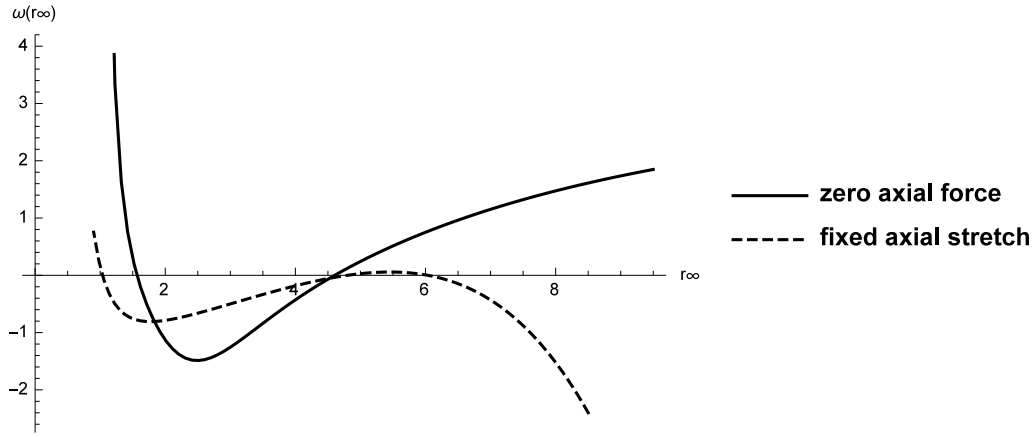

Figure 3.1.6: Function $\omega(r_\infty)$ for the Ogden strain-energy function. Solid line zero axial force, Dashed line fixed axial stretch with $z_\infty = 3.2$.

are given by

$$k_1(s) = z_1(s)\alpha_1(s), \tag{3.1.26}$$

$$\begin{aligned} k_2(s) \;=\; & -r_{cr}^2 z_\infty \alpha_1''(s) w_2^2 w_{22}^2 + r_{cr}(y_1(s)(r_{cr}\alpha_1(s)w_2(w_1 - z_\infty w_{12})(w_1 w_{122} \\ & -z_\infty w_{12} w_{122} + w_{22}(-w_{11} + z_\infty w_{112})) + z_1'(s) w_{22}^2 (r_{cr} w_{12}(w_1 - z_\infty w_{12}) \\ & +z_\infty w_{22}(w_1 - r_{cr} w_{11}) + w_2(-w_1 + r_{cr} z_\infty w_{112}))) + r_{cr}(z_1(s)(z_1'(s) w_{22}^2 \\ & (2w_{22}(w_1 - z_\infty w_{12}) + z_\infty w_2 w_{122}) + \alpha_1(s) w_2(w_1 - z_\infty w_{12})(w_{222}(w_1 \\ & -z_\infty w_{12}) + z_\infty w_{22} w_{122})) + (z_1'(s) w_{22}^2 (w_1 w_{12} - z_\infty w_{12}^2 + w_2(-w_{11} \\ & +z_\infty w_{112})) + \alpha_1(s) w_2(w_1 - z_\infty w_{12})(w_1 w_{122} - z_\infty w_{12} w_{122} + w_{22}(-w_{22} \\ & +z_\infty w_{112}))))) + y_1'(s) w_{22}^2 (r_{cr}(z_\infty(r_1 + 2y_1(s)) w_{12}(w_1 - r_{cr} w_{11}) + z_1(s) \\ & (r_{cr} w_{12}(w_1 - z_\infty w_{12}) + z_\infty w_{22}(w_1 - r_{cr} w_{11}))) + w_2((r_1 z_\infty - r_{cr} z_1(s)) w_1 \\ & +r_{cr} z_\infty(-r_1 w_{11} + r_{cr}(z_1(s) w_{112} + (r_1 + y_1(s)) w_{11}))))) / \\ & (r_{cr}^2 w_2 w_{22}^2 (w_1 - z_\infty w_{12}). \end{aligned}$$

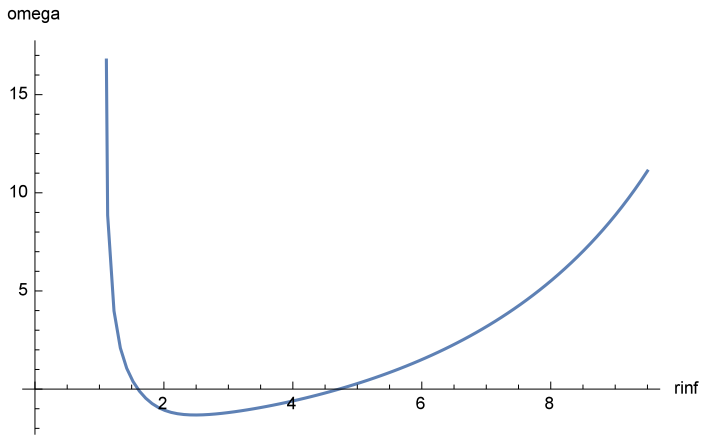

Figure 3.1.7: Function $\omega(r_\infty)$ for the Gent tube with $J_m = 97$ with zero axial force.

Clearly, B is a singular matrix since $\det B = 0$. We now impose a solvability condition in order to find a solution to (3.1.25). We do this by taking the dot product of (3.1.25) with the left eigenvector $\boldsymbol{a}$ of B. By the definition of left eigenvector

$$\boldsymbol{a} \cdot B\boldsymbol{b}^{(1)} = \boldsymbol{b}^{(1)} \cdot B^T\boldsymbol{a} = 0. \tag{3.1.27}$$

We thus have $\boldsymbol{a} \cdot [k_1, k_2]^T = 0$, which then yields

$$y'^2 = \omega(r_\infty)y^2 + \gamma(r_\infty)y^3 + O(y^4), \tag{3.1.28}$$

where the function $\omega(r_\infty)$ is given by (3.1.18) and the expression for $\gamma(r_\infty)$ is given by

$$\begin{aligned}\gamma(r_\infty) &= -((r_\infty(w_1^{(\infty)} - z_\infty w_{12}^{(\infty)})^3(r_\infty(-w_1^{(\infty)} + z_\infty w_{12}^{(\infty)})w_{122}^{(\infty)} + z_\infty w_{222}^{(\infty)} \\ &\quad (w_1^{(\infty)} - r_\infty w_{11}^{(\infty)})) + r_\infty w_{22}^{(\infty)}(w_1^{(\infty)} - z_\infty w_{12}^{(\infty)})^2(w_1^{(\infty)}(z_\infty^2 w_{122}^{(\infty)} + r_\infty(w_{11}^{(\infty)} \\ &\quad -z_\infty w_{112}^{(\infty)})) + r_\infty z_\infty(-z_\infty w_{122}^{(\infty)} w_{11}^{(\infty)} + w_{12}^{(\infty)}(-w_{11}^{(\infty)} + z_\infty w_{112}^{(\infty)}))) \\ &\quad -z_\infty^2(w_{22}^{(\infty)})^2(3(w_1^{(\infty)})^3 + r_\infty^2 z_\infty(z_\infty w_{122}^{(\infty)}(w_{11}^{(\infty)})^2 - w_{12}^{(\infty)} w_{11}^{(\infty)}(w_{11}^{(\infty)} \\ &\quad +2z_\infty w_{112}^{(\infty)}) + z_\infty(w_{12}^{(\infty)})^2 w_{112}^{(\infty)}) + r_\infty w_1^{(\infty)}(w_{11}^{(\infty)}(-2z_\infty^2 w_{122}^{(\infty)} + r_\infty(w_{11}^{(\infty)} \\ &\quad +2z_\infty w_{112}^{(\infty)})) + 2z_\infty w_{12}^{(\infty)}(2w_{11}^{(\infty)} + z_\infty w_{112}^{(\infty)} - r_\infty w_{111}^{(\infty)})) + (w_1^{(\infty)})^2 \\ &\quad (-3z_\infty w_{12}^{(\infty)} + z_\infty^2 w_{122}^{(\infty)} + r_\infty(-4w_{12}^{(\infty)} - 2z_\infty w_{112}^{(\infty)} + r_\infty w_{111}^{(\infty)})))) \\ &\quad /(3r_\infty^2 z_\infty w_2^{(\infty)}(w_{22}^{(\infty)})^2(w_1^{(\infty)} - z_\infty w_{12}^{(\infty)})^2)).\end{aligned}$$

In the near critical post bifurcation analysis, $r_\infty = r_{cr} + \epsilon r_1$, $y = y_1 + O(\epsilon^2)$, where ϵ is a small positive constant and r_1 is an $O(1)$ constant. Then at leading order (3.1.29) gives

$$\frac{d^2 y_1(s)}{ds^2} = \omega'(r_{cr})(r_\infty - r_{cr})y_1(s) + \frac{3}{2}\gamma(r_{cr})y_1(s)^2, \quad s = \sqrt{\epsilon}Z, \tag{3.1.29}$$

which has a localized solution given by

$$y_1(s) = -\frac{\omega'(r_{cr})(r_\infty - r_{cr})}{\gamma(r_{cr})}\,\mathrm{sech}^2\frac{\sqrt{\omega'(r_{cr})(r_\infty - r_{cr})}Z}{2}, \tag{3.1.30}$$

where $\omega'(r_{cr}) = d\omega(r_{cr})/dr_{cr}$. We note that at the first critical point, both $\omega'(r_{cr})$ and $\gamma(r_{cr})$ are negative for any strain-energy function. Therefore (3.1.32) represents a localized bulging solution provided that $\omega'(r_{cr})(r_\infty - r_{cr}) > 0$. Of course, this is only a leading-order approximation. The exact localized bulging solution can be determined by integrating the system (3.1.20) from $Z = 0$ towards ∞ subject to the initial conditions

$$\lambda_1(0) = r_0, \quad \lambda_2(0) = z_0', \quad \phi(0) = 0, \tag{3.1.31}$$

where r_0 and z_0' are determined by solving (3.1.16) and (3.1.17). This is discussed in the next section.

3.2 Fully Non-Linear Solution

We define two methods that may be used to find the fully non-linear localized bulging solutions, namely the shooting method and the Finite Difference Method.

3.2.1 Numerical solutions - shooting method

The basic idea for a shooting method is to convert the solution of a two-point boundary value problem into that of an initial value problem. We need to begin the solution at one end of the boundary value problem, and shoot to the other end with an initial value solver until the boundary condition at the other end converges to its correct value. See, e.g., Ascher et al. (1988) for a discussion of shooting method for systems of ordinary differential equations. The localized bulging solution must tend to the uniform state in the limit $Z \to \infty$, and thus satisfy the terminal conditions

$$\lambda_1 \to r_\infty,\ \lambda_2 \to z_\infty,\ \phi \to 0 \ \text{ as } \ Z \to \infty. \tag{3.2.1}$$

In this limit, $(\lambda_1 - r_\infty)$ is small and so (3.1.29) can be applied. We thus impose the decay condition

$$\lambda_1'(L) + \sqrt{\omega(r_\infty)}(\lambda_1(L) - r_\infty) = 0, \tag{3.2.2}$$

where L is a sufficiently large positive constant. We now assume that we have only one integral that we can use. So we have one equation with two unknowns. In doing so we can find a similar argument for determining r_0 and z_0' when the tube is modelled with or without bending stiffness. The localized bulging solution can be determined by integrating the system (3.1.20) from $Z = 0$ towards ∞ subject to the initial conditions

$$\lambda_1(0) = r_0, \quad \lambda_2(0) = z_0', \quad \phi(0) = 0, \tag{3.2.3}$$

where r_0 is to be guessed in our shooting procedure and z_0' is determined from one of the two integrals in (3.1.16) or (3.1.17). Then for each specified r_∞, we adjust r_0 in order to satisfy the decay condition (3.2.2). Figure 3.2.1 shows the profile of the bulge for the Gent tube with $J_m = 30$ near the bifurcation point. Axial stretch at infinity is fixed to 1.1. Critical value is found at $r_\infty = 1.69807$. In this case shooting method can

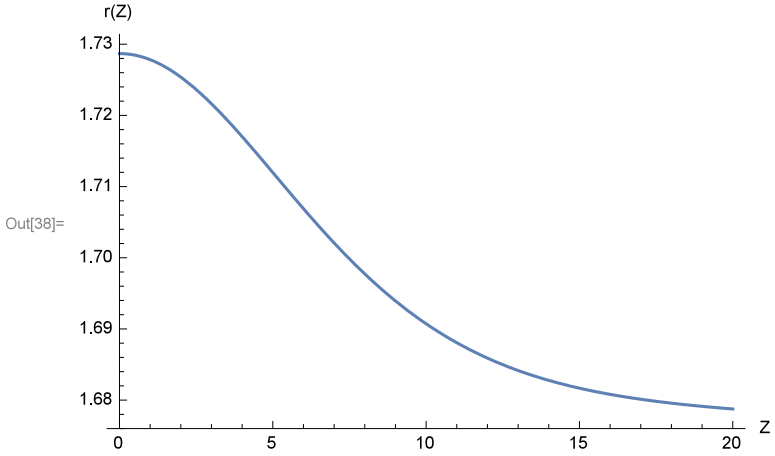

Figure 3.2.1: Profile of the bulge for the Gent tube with $J_m = 30$ when the axial stretch is fixed to be 1.1.

be applied by guessing a value for r_0 using the weakly non-linear results obtained in the

previous section. Then solve the equilibrium equation with the guess value of r_0. Once a solution is found, decrease r_∞ in small steps using the solution from the previous step as the initial guess for the current step. This method is applied in Chapter 4.5.1.

Horgan and Saccomandi (2003) use the Gent strain-energy function to model arteries, giving values of J_m in the range between 0.422 and 3.93 for healthy human arteries, corresponding to a maximum stretch ratio between 1.4 and 1.8. These values of J_m are less than the value of J_m for $z_\infty = 1.5$, implying there are no bifurcation points for values of J_m appropriate to healthy arterial walls. Similarly, for the Fung strain-energy function with $z_\infty = 1.5$, bifurcation points are only found for $\Gamma < 0.075$. Above this value of Γ no bifurcation points exist, showing that no aneurysm/bulging for healthy artery wall.

3.2.2 Finite Difference Method

We now use Finite Difference Method to solve the system of ordinary differential equations (3.1.20), in order to determine the localized bulging solutions. To start this method, the differential equations are replaced by the corresponding finite first order central differencing equations as in (2.4.4). The domain length is taken as L, with n cells in the domain and $n-1$ internal nodes and two boundary nodes. Since we have equal grid spacing, the length of each cell is taken as L/N. First order central differencing formulae are used to approximate the equations (3.1.20). The left boundary value of ϕ, given by

$$\phi(0) = 0, \tag{3.2.4}$$

is known. However, it can be seen that all of the other left and right boundary values are unknown. λ_1, λ_2 and ϕ at the node i, $(i = 1, 2, ..., n + 1)$ are represented as $\lambda_1^{(i)}$, $\lambda_2^{(i)}$ and $\phi^{(i)}$ respectively. For the implementation of Finite Difference Method, 1D grid discretization of the domain with n cells is presented in figure 3.2.2. Finite

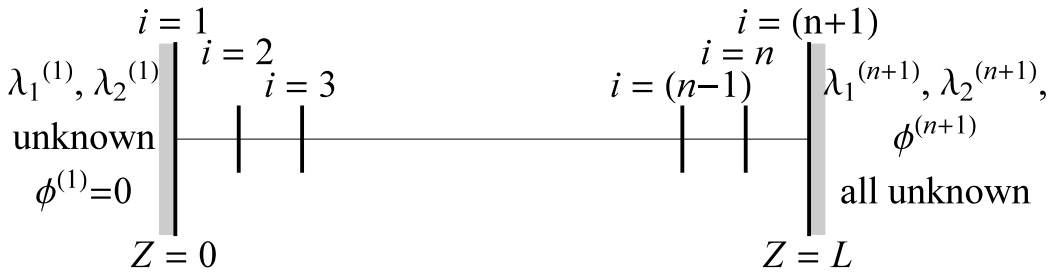

Figure 3.2.2: Finite difference discretization

difference approximations of the governing equations (3.1.20) at the second node in the domain are in the form

$$\frac{\lambda_1^{(3)} - \lambda_1^{(1)}}{2h} = \lambda_2^{(2)} \sin\phi^{(2)}, \tag{3.2.5}$$

$$\frac{\lambda_2^{(3)} - \lambda_2^{(1)}}{2h} = \frac{w_1(\lambda_1^{(2)}, \lambda_2^{(2)}) - \lambda_2^{(2)} w_{12}(\lambda_1^{(2)}, \lambda_2^{(2)})}{w_{22}(\lambda_1^{(2)}, \lambda_2^{(2)})} \sin\phi^{(2)}, \tag{3.2.6}$$

$$\frac{\phi^{(3)} - \phi^{(1)}}{2h} = \frac{w_1(\lambda_1^{(2)}, \lambda_2^{(2)})}{w_2(\lambda_1^{(2)}, \lambda_2^{(2)})} \cos\phi^{(2)} - \frac{w_1{}^{(\infty)}}{r_\infty z_\infty w_2(\lambda_1^{(2)}, \lambda_2^{(2)})} \lambda_1^{(2)} \lambda_2^{(2)}. \tag{3.2.7}$$

We have neglected the discretization error, keeping in mind that the discretization is first order accurate in h. Similarly, we can write the other set of finite difference approximations corresponding to the rest of the internal nodes in the domain. It can be shown that due to symmetric property of ϕ, we have

$$-\phi^{(0)} = \phi^{(2)}. \tag{3.2.8}$$

Thus applying the Finite Difference Method to $(3.1.20)_3$ at the first node we get

$$\frac{\phi^{(2)}}{h} = -\frac{{w_1}^{(\infty)}}{r_\infty z_\infty w_2(\lambda_1^{(1)}, \lambda_2^{(1)})}\lambda_1^{(1)}\lambda_2^{(1)}. \tag{3.2.9}$$

Now, combining (3.2.9) with the set of finite difference equations at each internal node, we have a system of $3n-2$ equations. Since the left boundary value of ϕ is known, it can be shown that there exists $3n+2$ unknowns corresponding to $3(n-1)$ internal nodes, two left boundary nodes and three right boundary nodes. To solve this system of equations four more conditions are required. We therefore use two integrals (3.1.16) and (3.1.17) along with the two decaying conditions derived in the next section.

3.2.3 Decaying condition

In the limit $Z \to \infty$, we look for an asymptotic solution of the form

$$\begin{aligned} \lambda_1 &= r_\infty + \epsilon y_1(Z) + ..., \\ \lambda_2 &= z_\infty + \epsilon z_1(Z) + ..., \\ \phi &= \epsilon\phi(Z) + ... \end{aligned} \tag{3.2.10}$$

Substitute (3.2.10) into (3.1.20) and expand asymptotically in terms of ϵ. Equating the coefficients of ϵ, the system of non-linear differential equations (3.1.20) can be written as a matrix equation

$$\boldsymbol{u}' = M(r_\infty)\boldsymbol{u}, \tag{3.2.11}$$

where $\boldsymbol{u} = (y_1, z_1, \phi)^T$ and

$$M(r_\infty) = \begin{pmatrix} 0 & 0 & z_\infty \\ 0 & 0 & \frac{w_1^{(\infty)} - z_\infty w_{12}^{(\infty)}}{w_{22}^{(\infty)}} \\ \frac{-z_\infty w_1^{(\infty)} + r_\infty z_\infty w_{11}^{(\infty)}}{r_\infty z_\infty w_2^{(\infty)}} & \frac{-r_\infty w_1^{(\infty)} + r_\infty z_\infty w_{12}^{(\infty)}}{r_\infty z_\infty w_2^{(\infty)}} & 0 \end{pmatrix}. \tag{3.2.12}$$

We now look for a solution of the form $\boldsymbol{u} = e^{mZ}\boldsymbol{a}$, and obtain $(M(r_\infty) - mI)\boldsymbol{a} = \boldsymbol{0}$. We note that 0 is always an eigenvalue due to the translational invariance in Z. Thus, the eigenvalues of $M(r_\infty)$ are given by 0, $\pm\sigma$ with $\sigma > 0$, where

$$\sigma = (-(w_1^{(\infty)})^2\lambda_1 + 2w_1^{(\infty)}w_{12}^{(\infty)}\lambda_1\lambda_2 - w_1^{(\infty)}w_{22}^{(\infty)}\lambda_2^2$$

$$-(w_{12}^{(\infty)})^2\lambda_1\lambda_2^2 + w_{11}^{(\infty)}w_{22}^{(\infty)}\lambda_1\lambda_2^2)^{1/2}/(w_2^{(\infty)}w_{22}^{(\infty)}\lambda_1\lambda_2). \tag{3.2.13}$$

The bifurcation condition $\omega(r_\infty) = 0$ is then reproduced by the fact that $\sigma = 0$. Thus, 0 becomes a triple eigenvalue when the bifurcation condition is satisfied. We denote the left eigenvector associated with the eigenvalue 0 by $(n_{11}, n_{12}, n_{13})^T$ and the left eigenvector associated with the eigenvalue $+\sigma$ by $(n_{21}, n_{22}, n_{23})^T$. These two vectors are given by

$$\begin{aligned} n_{11} &= 1, \qquad n_{21} = 1, \\ n_{12} &= \frac{z_\infty w_{22}^{(\infty)}(-w_1^{(\infty)} + z_\infty w_{12}^{(\infty)})}{\sigma^2 z_\infty w_2^{(\infty)} w_{22}^{(\infty)} + (w_1^{(\infty)} - z_\infty w_{12}^{(\infty)})^2}, \\ n_{22} &= \frac{-z_\infty w_{22}^{(\infty)}}{w_1^{(\infty)} - z_\infty w_{12}^{(\infty)}}, \\ n_{13} &= \frac{\sigma\ z_\infty^2 w_2^{(\infty)} w_{22}^{(\infty)}}{\sigma^2 z_\infty w_2^{(\infty)} w_{22}^{(\infty)} + (w_1^{(\infty)} - z_\infty w_{12}^{(\infty)})^2}, \quad n_{23} = 0. \end{aligned}$$

These two eigenvectors must necessarily be orthogonal to the right eigenvector associated with the eigenvalue $-\sigma$, and hence to the decaying solution. Thus, as $Z \to \infty$ the

decaying conditions may be written as

$$(\lambda_1^{(n+1)} - r_\infty) + (\lambda_2^{(n+1)} - z_\infty)n_{12} + \phi^{(n+1)}n_{13} = 0, \tag{3.2.14}$$

$$(\lambda_1^{(n+1)} - r_\infty) + (\lambda_2^{(n+1)} - z_\infty)n_{22} + \phi^{(n+1)}n_{23} = 0. \tag{3.2.15}$$

We now solve the system of $3n + 3$ equations. To do this, we use the set of $3n - 2$ finite difference equations derived in Section 3.2.2 along with the boundary condition $\phi(0) = 0$, two decaying conditions (3.2.15) and (3.2.16), and two coupled first-order non-linear differential equations,

$$w_2(r_0, z_0') - \frac{w_1^{(\infty)}}{2r_\infty z_\infty}(r_0^2 - r_\infty^2) - w_2^{(\infty)} = 0, \tag{3.2.16}$$

$$w(r_0, z_0') - z_0' w_2(r_0, z_0') - w^{(\infty)} + z_\infty w_2^{(\infty)} = 0. \tag{3.2.17}$$

3.2.4 Connection with the scaling and the eigenvectors in the weakly non-linear theory.

We denote by $(n_{31}, n_{32}, n_{33})^T$ the right eigenvector associated with the eigenvalue $-\sigma$ in (3.2.13). Then we may write

$$\begin{aligned} \sigma n_{31} + z_\infty n_{33} &= 0, \\ \sigma n_{32} + a_{23} n_{33} &= 0, \\ \sigma n_{33} + a_{31} n_{31} + a_{32} n_{32} &= 0, \end{aligned} \tag{3.2.18}$$

where

$$a_{23} = \frac{w_1^{(\infty)} - z_\infty w_{12}^{(\infty)}}{w_{22}^{(\infty)}}, \quad a_{31} = \frac{-z_\infty w_1^{(\infty)} + r_\infty z_\infty w_{11}^{(\infty)}}{r_\infty z_\infty w_2^{(\infty)}},$$

$$a_{32} = \frac{-r_\infty w_1^{(\infty)} + r_\infty z_\infty w_{12}^{(\infty)}}{r_\infty z_\infty w_2^{(\infty)}}.$$

Therefore it may be easily deduced that in the limit $\sigma \to 0$,

$$n_{32} = O(n_{31}), \quad \text{and} \quad n_{33} = O(\sigma\, n_{31}). \tag{3.2.19}$$

It follows that when $r_\infty = r_{cr} + \epsilon r_1$, $n_{31} = O(\epsilon)$, so that $\sigma = O(\epsilon^{1/2})$, and we have $n_{32} = O(\epsilon), n_{33} = O(\epsilon^{3/2})$. They are the scaling used in the asymptotic expansion (3.1.19).

3.2.5 Computer programming

We have written a Mathematica code to solve the system of $3n+2$ equations derived in Section 3.2.2 in order to solve the system of differential equations (3.1.20). We choose the domain length of the Z variable to be $[0, L]$, where L is the length of the tube. We first choose

r_∞ to be very close to the critical value of λ_1 in order to use the weakly non-linear solutions as the initial values to find the localized solution. Step size h was selected as $h = \frac{Z_{max} - Z_{min}}{n}$ where $z_{max} = 30,\ z_{min} = 0,$ and, $n = 640$ were used in our calculations. We have seen that as Z_{max} and n increase, the behaviour of the localized solution stay the same. Figure 3.2.3 shows a typical profile of localized bulging solution when r_∞ is close to the critical value, $r_{cr} = 1.69807$ for the Gent tube with $J_m = 30$ when z_∞ is fixed at 1.1. We now decrease r_∞ in small steps and the computation is repeated by taking the solutions of the previous step as the new initial values to find the profile of $r(Z)$, until the bulge begins to propagate down the tube as the turning point, marked as

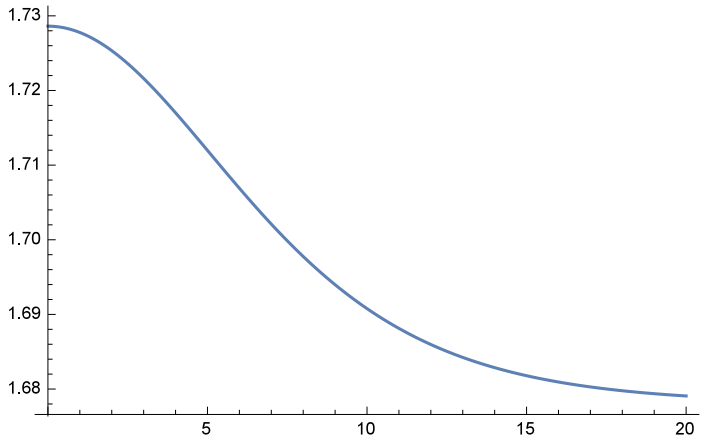

Figure 3.2.3: Profile of the bulge corresponding to $r_\infty = 1.67807$ for the Gent tube with $J_m = 30$ when z_∞ is fixed at 1.1.

T in Figure 3.2.5 is approached. Figure 3.2.4 shows the profile of $r(Z)$ as we approach the turning point T. In Figure 3.2.5 we show the existence of the two bifurcation points at 1.69807 and 4.93941 for the Gent strain-energy function with $J_m = 30$. The first bifurcation point corresponds to a bulging solution and the second to a necking solution since $\omega'(1.698070) = -3.54653 < 0$ and $\omega'(4.93941) = 19.6607 > 0$. As we vary r_∞ from the bifurcation point along the curve, the radius at the centre of the bulge will increase monotonically until we reach the turning point T, where the bulge flattens out at its centre, stop growing in its radius and then starts to propagate in both directions and becomes a kink solution. Figure 3.2.6 shows the profile of $r(Z)$ as r_∞ decreases for the Gent strain-energy function with $J_m = 30$. It shows how the bulge increases while r_∞ decreases. In Figure 3.2.7 we have shown the corresponding results when $z_\infty = 1.5$.

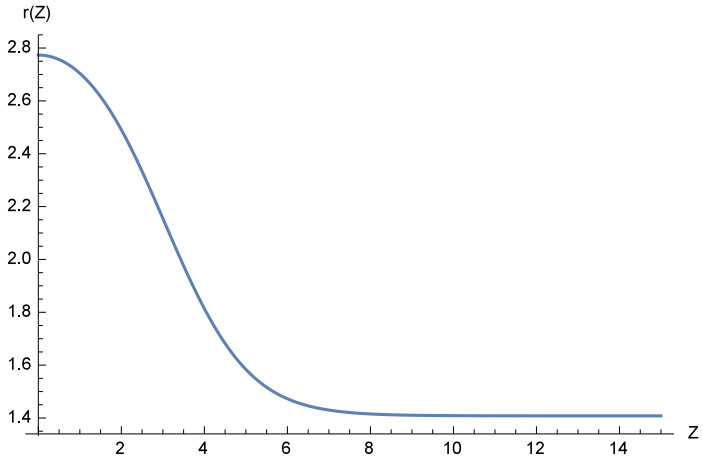

Figure 3.2.4: Profile of $r(Z)$ corresponding to $r_\infty = 1.40807$ for the Gent tube with $J_m = 30$ when z_∞ is fixed at 1.1.

3.3 Conclusion

Fu et al. (2008) derived the bifurcation condition $\omega(r_\infty) = 0$ for a membrane tube from the two simple equations (3.1.16) and (3.1.17), that determine the two principal stretches at the point where the radius is a maximum. In this Chapter we detailed how the bifurcation condition can also be derived by using two different methods, namely, weakly non-linear bifurcation analysis and solution of an eigenvalue problem. It can be seen that the solitary wave type bulged solution exists close to the first critical point with the properties $\omega'(r_{cr}) < 0$ and $\gamma(r_{cr}) < 0$ for any given strain-energy function. Calculation of localized solutions was done by the Finite Difference Method and the shooting method. Finally we compared the derivations in Fu et al. (2008) with our corresponding results, showing that our results derived here are identical with their results.

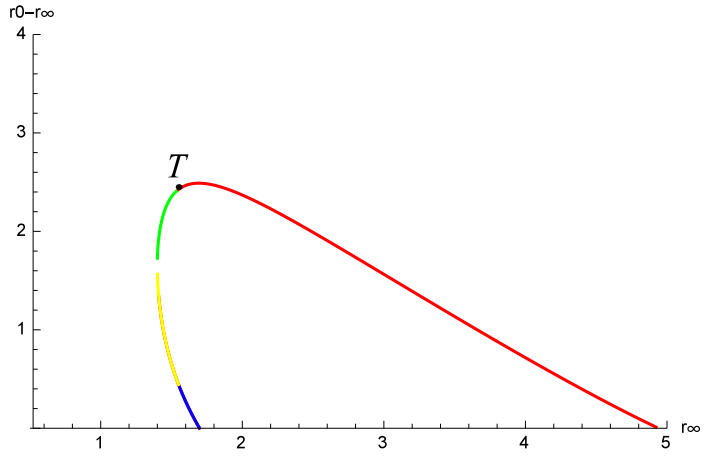

Figure 3.2.5: Dependence of $r_0 - r_\infty$ on r_∞ for the Gent tube with $J_m = 30$ when z_∞ is fixed at 1.1.

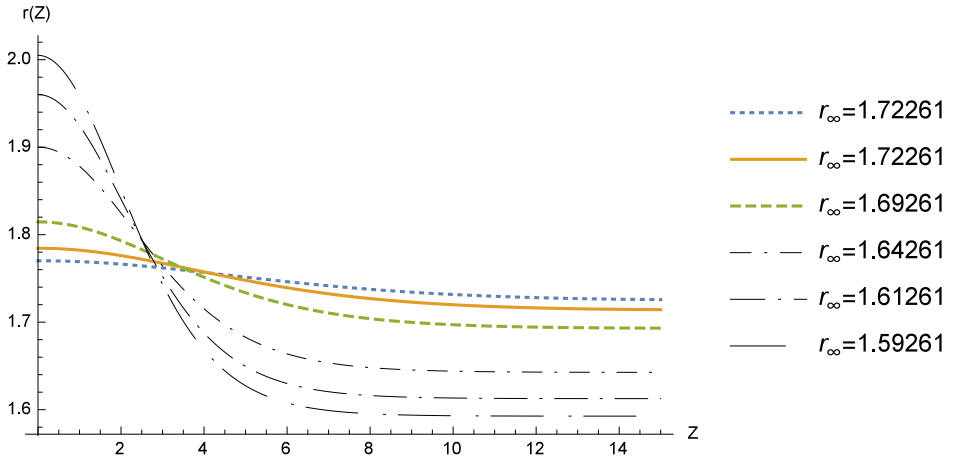

Figure 3.2.6: Profile of $r(Z)$ for the Gent tube with $J_m = 30$ when $z_\infty = 1.0$.

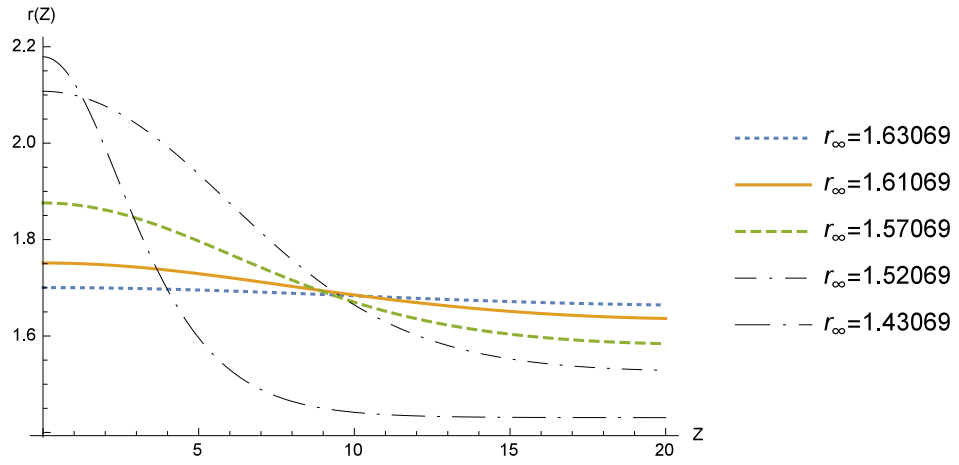

Figure 3.2.7: Profile of $r(Z)$ for the Gent tube with $J_m = 30$ when $z_\infty = 1.5$.

4 Effect of Bending Stiffness on Localized Bulging in a Pressurized Cylindrical Tube

4.1 Introduction

In this chapter we study localized bulging in inflated thin-walled elastic tubes with bending stiffness. A complete theory for the same problem with bending stiffness neglected has recently been developed by Fu and co-workers. We develop a parallel theory by incorporating bending stiffness in the constitutive modelling and use the theory to assess the effect of bending stiffness on the initiation of localized bulging in inflated thin-walled elastic tubes. In accordance with Chapter 3, we only consider deformations which are axisymmetric around the Z axis. This research is motivated by its possible application in the mathematical modelling of aneurysm initiation and development in human arteries.

4.2 Inflation of a Cylindrical Tube

4.2.1 Governing equations

The analysis considered here is for a thin-walled incompressible, hyperelastic, isotropic, cylindrical tube. We consider only axially symmetric deformations from the originally

axially symmetric configuration. Therefore, when the tube is inflated by an internal pressure, it is assumed that the inflated configuration maintains axial symmetry and the radius of the tube may be constant or vary along the axial direction. The analysis is based on two-dimensional incremental equilibrium equations, which are derived using Euler-Lagrangian equations and then solved for specific strain-energy functions. In future, we will try to move forward to the full three-dimensional problem. For prismatic deformations we refer to Haughton & Ogden (1979a). The tube is assumed to have uniform thickness H and uniform inner radius R before inflation. The axisymmetric deformations are represented in terms of cylindrical polar coordinates, by

$$r = r(Z),\ \theta = \Theta,\ z = z(Z), \tag{4.2.1}$$

where Z and z are the axial coordinates of a representative material particle before and after inflation respectively, and r is the radius of the middle plane after inflation. The principal directions of the deformation correspond to the lines of latitudinal and meridional directions, respectively. Hence, the principal stretches are given by

$$\lambda_1 = \frac{r}{R},\ \ \lambda_2 = \sqrt{r'^2 + z'^2}, \tag{4.2.2}$$

where the indices 1 and 2 are used for latitudinal and meridional directions respectively. A prime denotes differentiation with respect to Z. The position vectors of a representative material particle in the reference and deformed configurations are given by

$$\mathbf{Y} = R\mathbf{e}_r(\theta) + Z\mathbf{e}_z \ \text{ and } \ \mathbf{y} = r(Z)\mathbf{e}_r(\theta) + z(Z)\mathbf{e}_z, \tag{4.2.3}$$

respectively, where θ and Z parametrize the surface and we write $(\theta_1, \theta_2) = (\theta, Z)$. These coordinates induce tangent vectors $G_\alpha = Y_{,\alpha},\ g_\alpha = y_{,\alpha},\ \alpha \in 1, 2$ where $,\alpha$ represents differentiation with respect to θ_α. The tangent vectors in the reference

configuration are then given by

$$\mathbf{G}_1 = \frac{\partial \mathbf{Y}}{\partial \theta_1} = R\mathbf{e}_\theta, \;\; G_2 = \frac{\partial \mathbf{Y}}{\partial \theta_2} = \mathbf{e}_z. \tag{4.2.4}$$

The components of the metric tensors $(G_{\alpha\beta})$, $(G^{\alpha\beta})$ as well as the dual tangent vectors G^α, for the undeformed configuration are calculated using the following formula,

$$G_{\alpha\beta} = \mathbf{G}_\alpha \cdot \mathbf{G}_\beta, \;\; \mathbf{G}^\alpha \cdot \mathbf{G}_\beta = \delta_{\alpha\beta}, \;\; G^{\alpha\beta} = \mathbf{G}^\alpha \cdot \mathbf{G}^\beta, \tag{4.2.5}$$

where $\delta_{\alpha\beta}$ is the Kronecker Delta such that $\delta_{\alpha\beta} = 1$, when $\alpha = \beta$ and $\delta_{\alpha\beta} = 0$, when $\alpha \neq \beta$.

Then

$$\begin{gathered} G_{11} = R^2, \;\; G_{12} = G_{21} = 0, \;\; G_{22} = 1, \\ G^{11} = \frac{1}{R^2}, \;\; G^{12} = G^{21} = 0, \;\; G^{22} = 1, \\ \mathbf{G}^1 = \frac{1}{R}\,\mathbf{e}_\theta, \;\; \mathbf{G}^2 = \mathbf{e}_z, \\ G = \det(G_{\alpha\beta}) = R^2. \end{gathered} \tag{4.2.6}$$

The unit normal vector in the reference configuration is given by

$$\mathbf{N} = \frac{1}{\sqrt{G}}(\mathbf{G}_1 \times \mathbf{G}_2) = \frac{1}{R}(R\mathbf{e}_\theta \times \mathbf{e}_z) = \frac{1}{(R'^2 + Z'^2)^{1/2}}\mathbf{e}_r = \mathbf{e}_r. \tag{4.2.7}$$

The derivatives of the tangent vectors are given by

$$\mathbf{G}_{1,1} = -R\mathbf{e}_r, \;\; \mathbf{G}_{1,2} = \mathbf{G}_{2,1} = \mathbf{G}_{2,2} = 0. \tag{4.2.8}$$

Similarly, the tangent vectors in the deformed configuration are given by

$$\mathbf{g}_1 = \frac{\partial \mathbf{y}}{\partial \theta_1} = r\mathbf{e}_\theta, \;\; g_2 = \frac{\partial \mathbf{y}}{\partial \theta_2} = r'\mathbf{e}_r + z'\mathbf{e}_z. \tag{4.2.9}$$

The components of the metric tensors ($g_{\alpha\beta}$), ($g^{\alpha\beta}$) as well as the dual tangent vectors g^{α}, for the deformed configuration is calculated using the following formula,

$$g_{\alpha\beta} = \mathbf{g}_{\alpha} \cdot \mathbf{g}_{\beta}, \;\; \mathbf{g}^{\alpha} \cdot \mathbf{g}_{\beta} = \delta_{\alpha\beta}, \;\; g^{\alpha\beta} = \mathbf{g}^{\alpha} \cdot \mathbf{g}^{\beta}. \tag{4.2.10}$$

Then

$$\begin{gathered} g_{11} = r^2, \;\; g_{12} = g_{21} = 0, \;\; g_{22} = r'^2 + z'^2, \\ g^{11} = \frac{1}{r^2}, \;\; g^{12} = g^{21} = 0, \;\; g^{22} = \frac{1}{r'^2 + z'^2}, \\ \mathbf{g}^1 = \frac{1}{R}\,\mathbf{e}_{\theta}, \;\; \mathbf{g}^2 = \frac{r'\mathbf{e}_r + z'\mathbf{e}_z}{r'^2 + z'^2}, \\ g = \det(\mathrm{g}_{\alpha\beta}) = r^2(r'^2 + z'^2). \end{gathered} \tag{4.2.11}$$

The derivatives of the tangent vectors are given by

$$\mathbf{g}_{1,1} = -r\mathbf{e}_r, \;\; \mathbf{g}_{1,2} = r'\mathbf{e}_{\theta}, \;\; \mathbf{g}_{2,1} = 0, \;\; \mathbf{g}_{2,2} = r''\mathbf{e}_r + z''\mathbf{e}_z. \tag{4.2.12}$$

In the deformed configuration, the contra-variant components of the stress and moment tensors ($\sigma^{\alpha\beta}$ and $m^{\alpha\beta}$) are related to their covariant components ($\sigma_{\alpha\beta}$ and $m_{\alpha\beta}$) by the formula

$$\sigma_{\alpha\beta} = g_{\alpha\beta}\,\sigma^{\alpha\beta}, \quad m_{\alpha\beta} = g_{\alpha\beta}\,m^{\alpha\beta}. \tag{4.2.13}$$

The Christoffel symbols on the deformed surface are given by $\Gamma^{\gamma}_{\alpha\beta} = \mathbf{g}^{\gamma} \cdot \mathbf{g}_{\alpha,\beta}$ and we have

$$\begin{gathered} \Gamma^1_{11} = 0, \;\; \Gamma^1_{12} = \frac{r'}{r}, \;\; \Gamma^1_{21} = 0, \;\; \Gamma^1_{22} = 0, \\ \Gamma^2_{11} = -\frac{rr'}{\lambda_2^2}, \;\; \Gamma^2_{12} = 0, \;\; \Gamma^2_{21} = 0, \;\; \Gamma^2_{22} = \frac{\lambda_2'}{\lambda_2} = \frac{r'r'' + z'z''}{r'^2 + z'^2}. \end{gathered} \tag{4.2.14}$$

The relative curvature κ is given by

$$\kappa = \kappa_{\alpha\beta}\,\mathbf{G}^{\alpha} \otimes \mathbf{G}^{\beta}, \;\; \kappa_{\alpha\beta} = -b_{\alpha\beta} = -\mathbf{n} \;\cdot\; \mathbf{g}_{\alpha\beta},$$

$$\mathbf{n} = \frac{1}{2}\,\epsilon^{\alpha\beta}\mathbf{g}_\alpha \times \mathbf{g}_\beta, \quad \epsilon^{\alpha\beta}\sqrt{g} = e^{\alpha\beta}, \tag{4.2.15}$$

where $\mathbf{n}$ is a unit normal such that $\mathbf{n}$, $\mathbf{g}_\alpha$, and $\mathbf{g}_\beta$ form an orthogonal basis for the deformed surface and $e^{\alpha\beta}$ is the unit alternator ($e^{11} = e^{22} = 0$, $e^{12} = -e^{21} = 1$).

Then

$$\begin{gathered} b_{11} = -\frac{rz'}{\sqrt{r'^2 + z'^2}}, \quad b_{12} = b_{21} = 0, \quad b_{22} = \frac{(r'z'' - z'r'')}{\sqrt{r'^2 + z'^2}}, \\ \mathbf{n} = \frac{1}{r\sqrt{r'^2 + z'^2}}(rz'\mathbf{e}_r - rr'\mathbf{e}_z) = \frac{z'\mathbf{e}_r - r'\mathbf{e}_z}{\sqrt{r'^2 + z'^2}}, \\ \kappa_{11} = \frac{rz'}{\lambda_2}, \quad \kappa_{22} = \frac{r'z'' - z'r''}{\lambda_2}. \end{gathered} \tag{4.2.16}$$

4.2.2 Equilibrium equations

In general, the behaviour of an incompressible hyperelastic material can be represented in terms of a strain-energy function. In this work, we assume that the strain-energy function U is a function of both stretches and curvature of the material surface.

$$U = U(\lambda_1, \lambda_2, \kappa). \tag{4.2.17}$$

More specifically, we shall assume that the strain-energy function has the form

$$U = w(\lambda_1, \lambda_2) + cf(\kappa_{11}, \kappa_{22}), \tag{4.2.18}$$

where the second term takes the form

$$f(\kappa_{11}, \kappa_{22}) = \frac{1}{R^4}(\kappa_{11} - R)^2 + \kappa_{22}^2 + \frac{1}{R^2}\kappa_{22}(\kappa_{11} - R), \tag{4.2.19}$$

and is chosen using Koiter's model for hard materials (Koiter 1996). The choice of constant c will be made based on comparison with the 3D theory in the small thickness limit.

4.2.3 Euler Lagrangian equations

We derive the equilibrium equations for the thin-walled tube by minimising the energy functional given by

$$L[\mathbf{u}] = \int_{-L}^{L} 2\pi RH\{w(\lambda_1, \lambda_2) + cf(\kappa_{11}, \kappa_{22})\}dZ - \int_{-L}^{L} P\pi r^2 z' dZ, \tag{4.2.20}$$

where the dependent variable $\mathbf{u}$ is given by $\mathbf{u} = (r, z)$.

Equivalently, we may minimise

$$L[\mathbf{u}] = \int_{-L}^{L} L[\mathbf{u}, \mathbf{u}', \mathbf{u}''] \, dZ, \tag{4.2.21}$$

where

$$L[\mathbf{u}, \mathbf{u}', \mathbf{u}''] = w(\lambda_1, \lambda_2) + cf(\kappa_{11}, \kappa_{22}) - \frac{P}{2RH} r^2 z'. \tag{4.2.22}$$

In order to obtain the equilibrium equations for the membrane surface, we assume that the equilibria are described by the Euler-Lagrangian equations associated with the variational problem given in (2.3.6):

$$\frac{\partial L}{\partial u_\alpha} - \frac{\partial}{\partial x_i}\left(\frac{\partial L}{\partial u_{\alpha,i}}\right) - \frac{\partial^2}{\partial x_i \partial x_j}\left(\frac{\partial L}{\partial u_{\alpha,ij}}\right) = 0. \tag{4.2.23}$$

Taking $\boldsymbol{u} = (r, z)$ we get

$$\frac{\partial L}{\partial r} - \left(\frac{\partial L}{\partial r'}\right)' + \left(\frac{\partial L}{\partial r''}\right)'' = 0, \quad \left(\frac{\partial L}{\partial z'}\right)' - \left(\frac{\partial L}{\partial z''}\right)'' = 0, \tag{4.2.24}$$

where $x_1 = Z$ and L is defined in (4.2.22). It can be shown that

$$\begin{aligned}
\frac{\partial L}{\partial r} &= w_1 \frac{1}{R} - \frac{P}{RH} r z' + c f_1 \frac{z'}{\lambda_2}, \\
\frac{\partial L}{\partial r'} &= w_2 \frac{r'}{\lambda_2} + c\left[-f_1 \frac{r r' z'}{\lambda_2^3} + f_2 \frac{z' \lambda_2'}{\lambda_2^2}\right], \\
\frac{\partial L}{\partial z'} &= w_2 \frac{z'}{\lambda_2} + c\left[f_1 \frac{r r'^2}{\lambda_2^3} - f_2 \frac{r' \lambda_2'}{\lambda_2^2}\right] - \frac{P r^2}{2RH},
\end{aligned} \tag{4.2.25}$$

$$\frac{\partial L}{\partial r''} = -cf_2\frac{z'}{\lambda_2}, \quad \frac{\partial L}{\partial z''} = cf_2\frac{r'}{\lambda_2}.$$

So, by setting the first variation to zero, we obtain the equilibrium equations in the form

$$w_1\frac{1}{R}+cf_1\frac{z'}{\lambda_2} -\frac{P}{RH}rz'-\left(w_2\frac{r'}{\lambda_2}\right)'+\left[c\left(f_1\frac{rr'z'}{\lambda_2^3}-f_2\frac{z'\lambda_2'}{\lambda_2^2}\right)\right]'-\left(cf_2\frac{z'}{\lambda_2}\right)''=0, \quad (4.2.26)$$

$$\left(w_2\frac{z'}{\lambda_2}\right)'+\left(c\,f_1\frac{rr'^2}{\lambda_2^3}-c\,f_2\frac{r'\lambda_2'}{\lambda_2^2}\right)'-\frac{P}{RH}rr'-\left(cf_2\frac{r'}{\lambda_2}\right)''=0, \quad (4.2.27)$$

where

$$w_1=\frac{\partial w}{\partial\lambda_1}, \quad f_1=\frac{\partial f}{\partial\kappa_{11}}, \quad f_2=\frac{\partial f}{\partial\kappa_{22}}, etc, \quad (4.2.28)$$

and a prime denotes differentiation with respect to Z.

One of the conservation laws can be obtained by integrating (4.2.27) and is given by

$$w_2\frac{z'}{\lambda_2}+c\left(f_1\frac{rr'^2}{\lambda_2^3}-f_2\frac{r'\lambda_2'}{\lambda_2^2}\right)-\frac{Pr^2}{2RH}-\left(cf_2\frac{r'}{\lambda_2}\right)'=C_1. \quad (4.2.29)$$

From the invariance of the energy functional with respect to translations in Z, we obtain, using Noether's Theorem,

$$L-\frac{\partial L}{\partial r'}\,r'-\frac{\partial L}{\partial z'}\,z'-\frac{\partial L}{\partial r''}\,r''-\frac{\partial L}{\partial z''}\,z''+r'\left(\frac{\partial L}{\partial r''}\right)'+z'\left(\frac{\partial L}{\partial z''}\right)'=\text{constant}, \quad (4.2.30)$$

which gives

$$w+cf-w_2\lambda_2+cf_2\frac{z'r''}{\lambda_2}-cf_2\frac{r'z''}{\lambda_2}-r'z''\,\frac{cf_2}{\lambda_2}+z'r''\,\frac{cf_2}{\lambda_2}=C_2. \quad (4.2.31)$$

Then (4.2.31) can be reduced to have

$$w+cf-\lambda_2w_2+\frac{2c\,f_2}{\lambda_2}(z'r''-r'z'')=C_2. \quad (4.2.32)$$

From $r'\times(4.2.26)-z'\times(4.2.27)$, we obtain

$$w_1r'+cf_1\frac{r'z'}{\lambda_2}-r'\left(w_2\frac{r'}{\lambda_2}\right)'-z'\left(w_2\frac{z'}{\lambda_2}\right)'+cr'\left(f_1\frac{rr'z'}{\lambda_2^3}-f_2\frac{z'\lambda_2'}{\lambda_2^2}\right)'$$

$$-cz'\left(f_1\frac{rr'^2}{\lambda_2^3}-f_2\frac{r'\lambda_2'}{\lambda_2^2}\right)'-cr'\left(f_2\frac{z'}{\lambda_2}\right)''+cz'\left(f_2\frac{r'}{\lambda_2}\right)''=0, \tag{4.2.33}$$

or equivalently

$$w_1\lambda_1'+cf_1\frac{r'z'}{\lambda_2}-(\lambda_2w_2)'+w_2\lambda_2'$$

$$+c\left[f_1\frac{rr'}{\lambda_2^3}-f_2\frac{\lambda_2'}{\lambda_2^2}-2\left(\frac{cf_2}{\lambda_2}\right)'\right](-r'z''+z'r'')-\frac{cf_2}{\lambda_2}(r'z'''-z'r''')=0. \tag{4.2.34}$$

From $z'\times(4.2.26)+r'\times(4.2.27)$, we obtain

$$w_1z'+cf_1\frac{z'^2}{\lambda_2}-Pr\lambda_2^2-z'(w_2\frac{r'}{\lambda_2})'+cz'(f_1\frac{rr'z'}{\lambda_2^3}-f_2\frac{z'\lambda_2'}{\lambda_2^2})'$$

$$-z'(cf_2\frac{z'}{\lambda_2})''+r'(w_2\frac{z'}{\lambda_2})'\lambda_2)'+cr'(f_1\frac{rr'^2}{\lambda_2^3}-f_2\frac{r'\lambda_2'}{\lambda_2^2})'-r'(cf_2\frac{r'}{\lambda_2})''=0, \tag{4.2.35}$$

or equivalently

$$-w_2\lambda_2\phi'+w_1z'+cf_1\frac{z'^2}{\lambda_2}-Pr\lambda_2^2+c\ f_1\frac{rr'\lambda_2'}{\lambda_2^2}-c\ f_2\frac{\lambda_2'^2}{\lambda_2}+$$

$$c(f_1\frac{rr'}{\lambda_2^3})'\lambda_2^2+c\lambda_2^2(f_2\frac{\lambda_2'}{\lambda_2^2})'-c\ \frac{f_2}{\lambda_2}(r'r'''+z'z''')-c(\frac{f_2}{\lambda_2})'\lambda_2=0. \tag{4.2.36}$$

Differentiating (4.2.32) with respect to Z, we obtain

$$w_1\lambda_1'+w_2\lambda_2'+cf_1\kappa_{11}'+cf_2\kappa_{22}'-(\lambda_2w_2)'+2c(\frac{f_2}{\lambda_2})'(z'r''-r'z'')$$

$$+2c\frac{f_2}{\lambda_2}(z'r'''-r'z''')=0, \tag{4.2.37}$$

where

$$\kappa_{11}'=\frac{z'r'}{\lambda_2}+\frac{rr'}{\lambda_2^3}(r'z''-z'r''),\quad \kappa_{22}'=\frac{\lambda_2'}{\lambda_2^2}(z'r''-r'z'')+\frac{1}{\lambda_2}(r'z'''-z'r'''). \tag{4.2.38}$$

With the use of (4.2.38), the equation (4.2.37) becomes

$$w_1\lambda_1'+cf_1\frac{r'z'}{\lambda_2}-(\lambda_2w_2)'+w_2\lambda_2'+$$

$$c(f_1\frac{rr'}{\lambda_2^3}-\frac{f_2\lambda_2'}{\lambda_2^2}-2(\frac{cf_2}{\lambda_2})')(z'r''-r'z'')-\frac{cf_2}{\lambda_2}(r'z'''-z'r''')=0. \tag{4.2.39}$$

We note that (4.2.34) represents equilibrium in the meridional direction, whereas (4.2.36) represents equilibrium in the radial direction. It can be shown that (4.2.34) is the same as (4.2.39). Thus (4.2.34) can be replaced by (4.2.39) as

$$\begin{aligned}
&(w_1 - \lambda_2 w_{12})\lambda_2 \sin\phi - w_{22}\lambda - 2\lambda_2' + c((-2(1-\kappa_{11}) + \kappa_{22}) \\
&(\lambda_2 \sin\phi\cos\phi + \lambda_1 \sin\phi\frac{\kappa_{22}}{\lambda_2} + (2\kappa_{22} - (1-\kappa_{11}))(-\lambda_2\phi'' - \lambda_2'\phi')) \\
&+2c(2(\lambda_2\phi'' - \lambda_2'\phi') + (\lambda_2 \sin\phi\cos\phi + \lambda_1 \sin\phi\frac{\kappa_{22}}{\lambda_2}))\lambda_2\phi' \\
&+2c(2\kappa_{22} - (1-\kappa_{11}))\lambda_2'\phi' + 2c(2\kappa_{22} - (1-\kappa_{11}))\lambda_2\phi'' = 0, \qquad (4.2.40)
\end{aligned}$$

where $\sin\phi = \frac{r'}{\lambda_2},\ \cos\phi = \frac{z'}{\lambda_2},\ \kappa_{22} = \frac{r'z'' - z'r''}{\lambda_2} = -\lambda_2\phi',\ \kappa_{11} = \frac{rz'}{\lambda_2}$.

4.2.4 Conditions at infinity

Here we are interested in localized bulging solutions in which the tube has a constant radius r_∞ and constant axial stretch z_∞ far away from the localized bulge if it exists. Hence we impose the following conditions

$$\lim_{Z\to\infty} r(Z) = r_\infty, \quad \lim_{Z\to\infty} z(Z) = z_\infty. \qquad (4.2.41)$$

It then follows that

$$\begin{aligned}
&r' \to 0,\ \ z' \to z_\infty,\ \ \lambda_1 \to r_\infty,\ \ \lambda_2 \to z_\infty,\ \ \phi \to 0, \\
&\kappa_{11} \to r_\infty,\ \ \kappa_{22} \to 0 \quad \text{as} \quad Z \to \pm\infty. \qquad (4.2.42)
\end{aligned}$$

We are first imposing a uniform state of pre-stress on the material, associated with the pressure P, and then determining whether there exist other non-uniform solutions

which satisfy the governing equations but decay to the same constant radius and axial stretch at infinity. The constants C_1 and C_2 can be found by evaluating (4.2.29) and (4.2.32) in the limit $Z \to \infty$, as

$$C_1 = w_2^{(\infty)} - \frac{Pr_\infty^2}{2}, \quad \text{and} \quad C_2 = w^{(\infty)} + c(r_\infty - 1) - z_\infty w_2^{(\infty)}, \tag{4.2.43}$$

where the superscript (∞) denotes evaluation at $\lambda_1 = r_\infty, \quad \lambda_2 = z_\infty$. In the limit $Z \to \infty$, the equilibrium equation (4.2.26) becomes,

$$P\lambda_1\lambda_2 = w_1 + cf_1, \tag{4.2.44}$$

which gives the pressure P in terms of r_∞ and z_∞ as,

$$P = \frac{w_1^{(\infty)}}{r_\infty z_\infty} + \frac{2c(r_\infty - 1)}{r_\infty z_\infty}, \tag{4.2.45}$$

where we have used the result that $f_1 = 2(r_\infty - 1)$ when $Z \to \infty$. When $c = 0$, the constant C_2 and P are to be equivalent to $(3.1.13)_2$ and (3.1.15) respectively. Equation (4.2.45) allows us to use r_∞ and z_∞ as controlling parameters of the deformation instead of the pressure P. Figure 4.2.1 shows the connection between P and r_∞ when the axial stretch z_∞ is fixed at 1.1 for the Ogden strain-energy function. The curve for the Gent model is monotonic for $z_\infty = 1.1$ for all J_m. Figure 4.2.2 shows the connection between P and r_∞ for the Gent strain-energy function with $J_m = 97.2$. For an infinite tube with open ends the remote axial stretch z_∞ represents a pre strain of the material prescribed by the load applied at the end of the tube and is therefore treated as a constant. The significance of the constant C_1 in $(4.2.43)_1$ is therefore shown to be the scaled axial force applied at the ends of the tube and this depends on the value of r_∞ as well as the strain-energy function. For a tube with closed ends and no axial loading, where we assume that the ends are suitably far away from the localized bulge, we require that

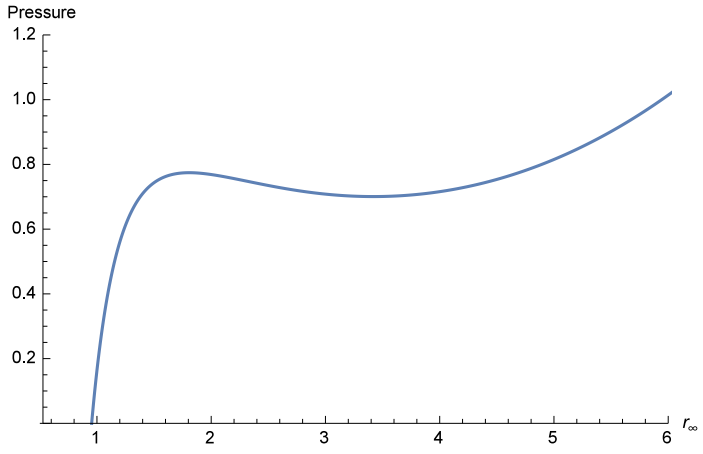

Figure 4.2.1: Pressure against r_∞ for the Ogden strain-energy function when $z_\infty = 1.1,\ c = 0.01$.

the force balance in the Z direction is zero, from which we can derive the condition $C_1 = 0$. For tubes with closed ends and no axial loading, we find the following relation from (4.2.29),

$$2z_\infty w_2(r_\infty, z_\infty) = r_\infty w_1(r_\infty, z_\infty) + 2c\, r_\infty(r_\infty - 1), \tag{4.2.46}$$

which can be used to determine z_∞ for any given r_∞. Therefore, for the case of fixed axial force, we may take r_∞ as the controlling parameter, with P determined by (4.2.45). The closed end relation (4.2.46) for the Gent material with $J_m = 30$ and Varga material becomes respectively

$$15(1 + r_\infty^4 z_\infty^2 - 2r_\infty^2 z_\infty^4) + c(-1 + r_\infty) r_\infty(-1 + r_\infty^4 z_\infty^2 + r_\infty^2 z_\infty^2(-33 + z_\infty)^2) = 0,$$

$$1 + r_\infty^2 z_\infty - 2r_\infty z_\infty^2 - c r_\infty^3 z_\infty + c r_\infty^2 z_\infty = 0, \tag{4.2.47}$$

which may be solved explicitly for r_∞ and are plotted in Figure 4.2.3. With C_1 and C_2 known, the integrals (4.2.29) and (4.2.32) are two coupled first-order non-linear

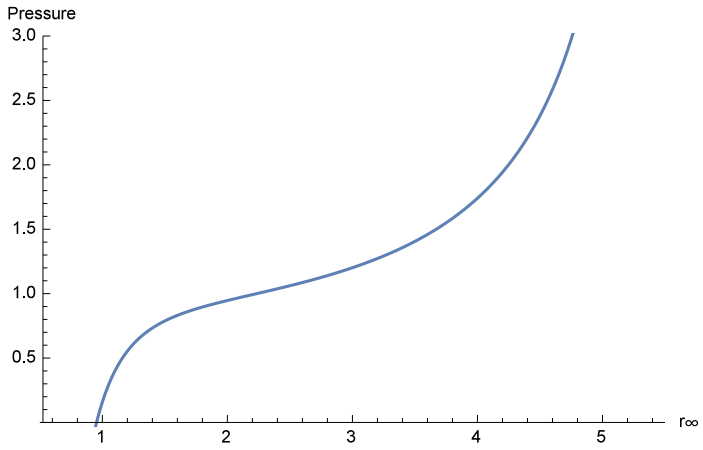

Figure 4.2.2: Pressure against r_∞ for the Gent strain-energy function with $J_m = 97.2$ when $z_\infty = 1.1,\ c = 0.01$.

differential equations for $\lambda_1,\ \lambda_2,$ and κ_{22}. Given the axial symmetry of the entire deformation together with the symmetry in the end condition (4.2.46), and the fact that our coordinate system can be set arbitrarily, we focus only on solutions which are symmetric about the origin $Z = 0$. The required conditions are therefore,

$$r'(0) = 0, \quad z'(0) = z'_0, \quad \phi(0) = 0, \quad \kappa_{22}(0) \neq 0. \tag{4.2.48}$$

To find the corresponding value r_0 for a given r_∞, (4.2.29) and (4.2.32) are evaluated at $Z = 0$, obtaining respectively,

$$w_2(r_0, z'_0) - w_2^{(\infty)} - \frac{1}{2}\left(\frac{w_1^{(\infty)}}{r_\infty z_\infty} + \frac{2c(r_\infty - 1)}{r_\infty z_\infty}\right)(r_0^2 - r_\infty^2) +$$

$$c\,\frac{\kappa_{22}(0)}{z'_0}(2\kappa_{22}(0) + \kappa_{11}(0) - 1) = 0, \tag{4.2.49}$$

$$w(r_0, z'_0) - w^{(\infty)} - z'_0 w_2(r_0, z'_0) + z_\infty w_2^{(\infty)} +$$

$$c((r_0-1)^2+\kappa_{22}(0)^2+\kappa_{22}(0)(r_0-1)) - c(r_\infty-1)^2 - 2c(2\kappa_{22}(0)+r_0-1)\kappa_{22}(0) = 0, \tag{4.2.50}$$

where $r_0 = r(0),\ z_0' = z'(0),\ \kappa_{22}(0) = -r''(0),\ \kappa_{11}(0) = r_0$. The corresponding equations when bending stiffness is neglected are given by (3.16) and (3.17). We see that the significance of the additional terms in (4.2.49) and (4.2.50) are therefore from the bending stiffness of the material. Since we have a system of two non-linear equations (4.2.49) and (4.2.50) with three unknowns r_0, z_0' and $\kappa_{22}(0)$, we can express $\kappa_{22}(0)$ and z_0' in terms of r_0 and apply the shooting method by adjusting the only unknown r_0 to satisfy the decaying condition as $Z \to \infty$.

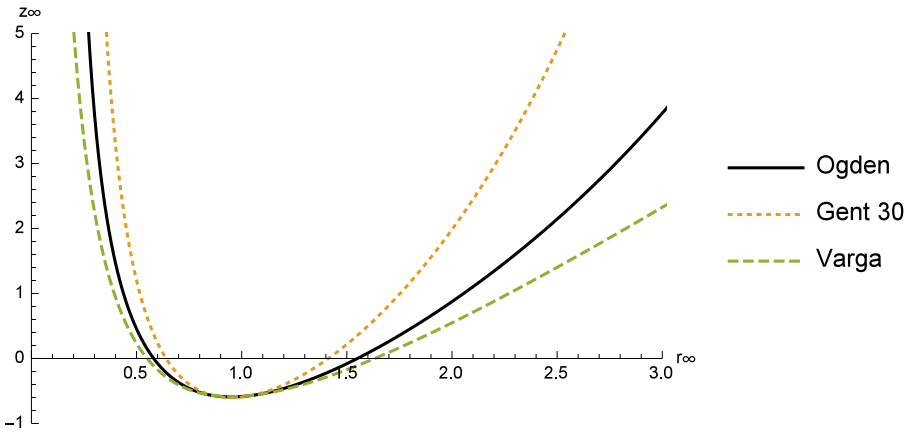

Figure 4.2.3: Connection between z_∞ and r_∞ for a tube with zero axial force. Solid, dotted and dashed lines represents Ogden, Gent 30 and Varga strain-energy functions respectively. All results correspond to c=0.01.

4.2.5 Koiter's shell model

Koiters non-linear shell theory is valid for modelling isotropic thin elastic shells undergoing infinitesimal deformations (Koiter 1996). According to Koiter's two-dimensional shell model the strain-energy per unit undeformed area is given by

$$U = \frac{1}{2}H\varepsilon.D[\varepsilon] + \frac{1}{24}H^3\rho.D[\rho], \tag{4.2.51}$$

where D is the tensor of linear plane-stress elastic moduli, H is the thickness of the shell prior to deformation, and ε and ρ respectively are surface tensors that characterise the change in metric and curvature of the shell mid surface induced by deformation. For soft materials such as rubber, a possible extension of (4.2.51) is

$$U = Hw(\lambda_1, \lambda_2) + \frac{1}{24}H^3\rho.D[\rho]. \tag{4.2.52}$$

In Steigmann (2012), Koiter's shell model (4.2.51) is derived from 3D non-linear elasticity and shown to furnish the leading order model in the small thickness limit when the bending and stretching energies are of the same order of magnitude. For an isotropic material, the elastic moduli and stress strain relations are given by

$$C_{ijkl} = \lambda\delta_{ij}\delta_{kl} + \mu(\delta_{ik}\delta_{jl} + \delta_{il}\delta_{jk}),$$

$$\sigma_{ij} = \lambda\delta_{ij}\epsilon_{kk} + 2\mu\epsilon_{ij}, \tag{4.2.53}$$

where λ and μ are Lam*é* constants and C_{ijkl} is the elasticity tensor which satisfies the symmetrises $C_{ijkl} = C_{klij} = C_{jikl}$. Solving $\sigma_{33} = 0$ for ϵ_{33} and substituting the expression back into $\sigma_{\alpha\beta}$, we obtain

$$\sigma_{\alpha\beta} = \frac{2\lambda\mu}{\lambda + 2\mu}\epsilon_{\gamma\gamma}\delta_{\alpha\beta} + 2\mu\epsilon_{\alpha\beta} = D^{\alpha\beta\gamma\delta}\epsilon_{\gamma\delta}, \tag{4.2.54}$$

where

$$D^{\alpha\beta\gamma\delta} = \frac{2\lambda\mu}{\lambda+2\mu}\delta_{\alpha\beta}\delta_{\gamma\delta} + \mu(\delta_{\alpha\gamma}\delta_{\beta\delta} + \delta_{\alpha\delta}\delta_{\beta\gamma}). \tag{4.2.55}$$

It then follows that

$$\rho \cdot D[\rho] = \frac{2\lambda\mu}{\lambda+2\mu}(tr\rho)^2 + 2\mu\ tr(\rho^2) = \frac{4\mu(\lambda+\mu)}{\lambda+2\mu}(tr\rho)^2 - 4\mu\ \det\rho. \tag{4.2.56}$$

For incompressible materials, $\lambda \to \infty$ and the above expression reduces to

$$\rho \cdot D[\rho] = 2\mu\{(\mathrm{tr}\rho)^2 + \mathrm{tr}(\rho^2)\} = 4\mu\{(\mathrm{tr}\rho)^2 - \det\rho\}. \tag{4.2.57}$$

4.2.6 Uniform inflation using 3D non-linear elasticity theory

One way to fix the constant c in (4.2.18) is to require the model to give the same prediction for the pressure in uniform inflation as the $3D$ exact theory in the thin-wall limit. We thus consider the uniform inflation of a long cylindrical tube. The axi-symmetric deformation is given by

$$r = r(R), \quad \theta = \Theta, \quad z = \lambda_z Z, \tag{4.2.58}$$

in terms of cylindrical polar coordinates, where λ_z is the axial extension ratio (or axial stretch), which is uniform. The undeformed and current configurations are defined by

$$A \le R \le B, \quad \text{and} \quad a \le r \le b, \tag{4.2.59}$$

respectively. Let $\lambda_1, \lambda_2, \lambda_3$ denote the principal stretches in the latitudinal, meridional and normal directions respectively such that

$$\lambda_1 = \frac{r}{R} = \lambda, \ \ \lambda_2 = \lambda_z, \quad \lambda_3 = (\lambda_1\lambda_2)^{-1}. \tag{4.2.60}$$

We use $\mathbf{e}_1, \mathbf{e}_2, \mathbf{e}_3$ to denote the unit basis vectors corresponding to the coordinates θ, z, r, respectively. The deformation gradient $\mathbf{F}$ is calculated according to

$$\mathbf{F} = \text{Grad } \mathbf{x} = r'\mathbf{e}_r \otimes \mathbf{e}_r + \frac{r}{R}\mathbf{e}_\theta \otimes \mathbf{e}_\theta + \lambda_z \mathbf{e}_z \otimes \mathbf{e}_z. \tag{4.2.61}$$

Incompressibility $\det \mathbf{F} = 1$ gives $rr' = R/\lambda_z$ from which we integrate to obtain

$$r = \sqrt{a^2 + \lambda_z^{-1}(R^2 - A^2)}. \tag{4.2.62}$$

As an example we consider the Mooney-Rivlin material (2.1.51). We have

$$\boldsymbol{\sigma} = -p\boldsymbol{I} + \mu_1 \boldsymbol{B} + \mu_2 \boldsymbol{B}^{-1}. \tag{4.2.63}$$

Thus, the non-zero stress components are

$$\begin{aligned} \sigma_{rr} &= -p + \mu_1 \frac{R^2}{\lambda_z^2 r^2} + \mu_2 \frac{\lambda_z^2 r^2}{R^2}, \\ \sigma_{\theta\theta} &= -p + \mu_1 \frac{r^2}{R^2} + \mu_2 \frac{R^2}{r^2}, \\ \sigma_{zz} &= -p + \mu_1 \lambda_z^2 + \mu_2 \lambda_z^{-2}. \end{aligned} \tag{4.2.64}$$

For the inflation problem, the equilibrium equation in the r-direction reduces to

$$\frac{\partial \sigma_{rr}}{\partial r} + \frac{\sigma_{rr} - \sigma_{\theta\theta}}{r} = 0, \tag{4.2.65}$$

which is to be solved subjected to the boundary conditions

$$\sigma_{rr}|_{r=a} = -P, \quad \sigma_{rr}|_{r=b} = 0. \tag{4.2.66}$$

It then follows that

$$\begin{aligned} P &= -\int_a^b [\mu_1 (\frac{R^2}{\lambda_z^2 r^2} - \frac{r^2}{R^2}) + \mu_2 (\frac{\lambda_z^2 r^2}{R^2} - \frac{R^2}{r^2})] \frac{dr}{r}, \\ &= (\mu_2 - \mu_1 \lambda_z^{-2})(\lambda_z \ln \frac{\mathrm{a}}{\mathrm{A}} - \lambda_z \ln \frac{\mathrm{b}}{\mathrm{B}} + \frac{\mathrm{B}^2}{2\mathrm{b}^2} - \frac{\mathrm{A}^2}{2\mathrm{a}^2}). \end{aligned} \tag{4.2.67}$$

Using the fact that the deformed thickness is necessarily $\lambda_3 H = H/(\lambda_1\lambda_z)$, we may write again

$$R = A + \frac{H}{2}, \quad a = \lambda_1 R - \frac{H}{2\lambda_1\lambda_z}, \quad b = \lambda_1 R + \frac{H}{2\lambda_1\lambda_z}. \tag{4.2.68}$$

We look for an asymptotic solution of the form

$$\frac{P}{\mu_1\lambda_z^{-2} - \mu_2} = p_1\frac{H}{R} + p_2(\frac{H}{R})^2 + p_3(\frac{H}{R})^3 + ... \tag{4.2.69}$$

By substituting (4.2.69) into (4.2.67) and equating the coefficients of like powers of H, we obtain

$$\frac{RP}{H(\mu_1\lambda_z^{-2} - \mu_2)} = \frac{\lambda_z^2\lambda_1^4 - 1}{\lambda_z\lambda_1^4} + \frac{\lambda_z^4\lambda_1^8 - 3\lambda_z^2\lambda_1^4 + 8\lambda_z\lambda_1^2 - 6}{12\lambda_z^3\lambda_1^8}\,(\frac{H}{R})^2, \tag{4.2.70}$$

where the higher order terms are neglected. For the Mooney-Rivlin material model, it can be easily shown that the leading order term in (4.2.69) agrees with its counterpart in (4.2.45) exactly. To compare the second term, we take the limit $\lambda_1 \to 1$ and $\lambda_z \to 1$ in (4.2.70) to obtain

$$\frac{RP}{H(\mu_1\lambda_z^{-2} - \mu_2)} = \frac{\lambda_z^2\lambda_1^4 - 1}{\lambda_z\lambda_1^4} + (\lambda_1 - 1)(\frac{H}{R})^2 + ..., \tag{4.2.71}$$

where we have set $\mu = \mu_1 - \mu_2$. It is then seen that (4.2.71) is consistent with (4.2.45) if

$$c = \frac{1}{2}\mu H^2. \tag{4.2.72}$$

4.3 Reformulation in the form of the classical shell theory

An elastic shell may be defined as a three-dimensional elastic body with a dimension $H/R \ll 1$ where H is a typical thickness in the thin direction and R is a typical length scale in the remainder of the body (Libai & Simmonds 1998). This enables us to consider the deformation of only the mid-plane of the elastic body through the thinner direction. An axisymmetric shell is such a shell which has symmetry around an axis. A membrane may then be defined as a shell which has negligible resistance to bending (Libai & Simmonds 1998).

The engineering shell theory is usually derived by considering equilibrium of an infinitesimal volume element, and it takes the form

$$\frac{d(rN_2)}{ds} - N_1\frac{dr}{ds} - \hat{Q}\kappa_2 = 0, \tag{4.3.1}$$

$$N_1\kappa_1 + N_2\kappa_2 + \frac{1}{r}\frac{d\hat{Q}}{ds} = P, \tag{4.3.2}$$

$$\frac{d(rM_2)}{ds} - M_1\frac{dr}{ds} + \hat{Q} = 0. \tag{4.3.3}$$

See, for instance, Pamplona & Calladine (1993), Pozrikidis (2001), Blyth & Pozrikidis (2004) or Liu et al. (2006). In the above equations, s is the arc length in the deformed configuration, $N_1,\ N_2,\ M_1,\ M_2$ are principal stress resultants and bending moments, $Q = \hat{Q}/r$ is the transverse shear tension and $\kappa_1,\ \kappa_2$ are the principal curvatures given by

$$\kappa_1 = \frac{\kappa_{11}}{r^2}, \quad \kappa_2 = \frac{\kappa_{22}}{\lambda_2^2}. \tag{4.3.4}$$

Equations (4.3.1) and (4.3.2) represent equilibrium in the tangential and normal directions, respectively. Let us take

$$N_i = Jh\sigma_{ii} = \frac{JR}{r\sqrt{r'^2 + z'^2}}\sigma_{ii}, \quad M_i = Jhm_{ii} = \frac{JR}{r\sqrt{r'^2 + z'^2}}m_{ii}, \text{ no sum on } i. \quad (4.3.5)$$

Equations (4.3.1)-(4.3.3) suggest the use of

$$\lambda_1, \ \lambda_2, \ \phi, \ \kappa_{22}, \ \hat{Q} \quad (4.3.6)$$

as the dependent variables. We now show that the above form can be derived from Steigmann and Ogden's variational formulation. The equilibrium equations given by Steigmann & Ogden (1999) related to a cylindrical elastic surface take the form

$$G^{-\frac{1}{2}} \left(G^{\frac{1}{2}} \mathbf{P}^{\alpha}\right)_{, \alpha} = -PJ\mathbf{n}, \quad J = \lambda_1\lambda_2, \quad (4.3.7)$$

where

$$\begin{aligned} \mathbf{P}^{\alpha} &= \mathbf{T}^{\alpha} - \mathbf{L}^{\alpha}, \\ \mathbf{T}^{\alpha} &= J\sigma^{\alpha\beta}\mathbf{g}_{\beta} + Jm^{\gamma\beta}\Gamma^{\alpha}_{\gamma\beta}\mathbf{n}, \\ \mathbf{L}^{\alpha} &= G^{-\frac{1}{2}}(G^{\frac{1}{2}}\mathbf{M}^{\beta\alpha})_{,\beta}, \\ \mathbf{M}^{\beta\alpha} &= -J\mathbf{m}^{\beta\alpha}\mathbf{n}. \end{aligned} \quad (4.3.8)$$

The vectors $\mathbf{P}^{\alpha}$ and $\mathbf{M}^{\beta\alpha}$ can be represented in terms of components relative to the basis $\{\mathbf{g}_{\alpha}, \ \mathbf{n}\}$. Since $G = \det(\mathbf{G}_{\alpha} \cdot \mathbf{G}_{\beta}) = R^2$ is a constant, the equilibrium equations reduce to

$$\mathbf{P}^{\alpha}_{, \alpha} = -PJ\mathbf{n}. \quad (4.3.9)$$

The unit normal in the current configuration is

$$\mathbf{n} = \frac{1}{\sqrt{g}}(\mathbf{g}_1 \times \mathbf{g}_2) = \frac{1}{\lambda_2}(z'\mathbf{e}_r - r'\mathbf{e}_z), \text{ and } \frac{\partial \mathbf{n}}{\partial \theta} = \frac{z'}{\lambda_2}\mathbf{e}_{\theta}. \quad (4.3.10)$$

Furthermore,

$$\mathbf{g}_1 = r\mathbf{e}_\theta, \quad \mathbf{g}_2 = \lambda_2 \mathbf{e}_z, \tag{4.3.11}$$

$$\mathbf{e}_s = \frac{1}{\lambda_2}(r'\mathbf{e}_r + z'\mathbf{e}_z), \quad \mathbf{e}_s' = -\kappa_2\lambda_2\mathbf{n}, \quad \mathbf{n}' = \kappa_2\lambda_2\mathbf{e}_s, \quad \kappa_1 = \frac{z'}{r\lambda_2}, \quad \kappa_2 = -\frac{\phi'}{\lambda_2}. \tag{4.3.12}$$

The principal directions of the deformation correspond to the lines of meridional and normal to the deformed surface.

We have

$$\mathbf{P}^1 = J\sigma^{11}\mathbf{g}_1 + Jm^{\gamma\beta}\Gamma^1_{\gamma\beta}\mathbf{n} + \frac{\partial}{\partial\theta}(Jm^{11}\mathbf{n}) = J\sigma^{11}r\mathbf{e}_\theta + Jm^{11}\frac{z'}{\lambda_2}\mathbf{e}_\theta, \tag{4.3.13}$$

$$\mathbf{P}^2 = J\sigma^{22}\mathbf{g}_2 + Jm^{\gamma\beta}\Gamma^2_{\gamma\beta}\mathbf{n} + (Jm^{22}\mathbf{n})' = J\sigma^{22}\lambda_2\mathbf{e}_s - Jm^{11}\frac{rr'}{\lambda_2^2}\mathbf{n}$$

$$+Jm^{22}\frac{\lambda_2'}{\lambda_2}\mathbf{n} + (Jm^{22}\mathbf{n})'. \tag{4.3.14}$$

From (4.3.9)

$$\frac{\partial}{\partial\theta}(\mathbf{P}^1) = -J\sigma^{11}r\mathbf{e}_r - Jm^{11}\frac{z'}{\lambda_2}\mathbf{e}_r, \tag{4.3.15}$$

$$(\mathbf{P}^2)' = (J\sigma^{22}\lambda_2)'\mathbf{e}_s - J\sigma^{22}\lambda_2^2\kappa_2\mathbf{n} - (Jm^{11}\frac{rr'}{\lambda_2^2})'\mathbf{n} - Jm^{11}\frac{rr'}{\lambda_2^2}\kappa_2\lambda_2\mathbf{e}_s$$

$$+(Jm^{22}\frac{\lambda_2'}{\lambda_2})\mathbf{n} + Jm^{22}\frac{\lambda_2'}{\lambda_2}\kappa_2\lambda_2\mathbf{e}_s + (Jm^{22})'\kappa_2\lambda_2\mathbf{e}_s + (Jm^{22})''\mathbf{n}$$

$$+(Jm^{22}\kappa_2\lambda_2)'\mathbf{e}_s - Jm^{22}\kappa_2\lambda_2\kappa_2\lambda_2\mathbf{n},$$

$$= \mathbf{e}_s\{(J\sigma^{22}\lambda_2)' - Jm^{11}\frac{rr'}{\lambda_2}\kappa_2 + Jm^{22}\lambda_2'\kappa_2 + (Jm^{22})'\kappa_2\lambda_2 + (Jm^{22}\kappa_2\lambda_2)'\}$$

$$\mathbf{n}\{-J\sigma^{22}\lambda_2^2\kappa_2 - (Jm^{11}\frac{rr'}{\lambda_2^2})' + (Jm^{22}\frac{\lambda_2'}{\lambda_2})' + (Jm^{22})'' - Jm^{22}\kappa_2^2\lambda_2^2\},$$

$$= \mathbf{e}_s\{[\lambda_2(J\sigma^{22} + \kappa_2 Jm^{22})]' - Jm^{11}\frac{rr'}{\lambda_2}\kappa_2 + Jm^{22}\lambda_2'\kappa_2$$

$$+(Jm^{22})'\kappa_2\lambda_2\} + \mathbf{n}\{-\kappa_2\lambda_2^2(J\sigma^{22} + \kappa_2 Jm^{22}) - (Jm^{11}\frac{rr'}{\lambda_2^2})'$$

$$+(Jm^{22}\frac{\lambda_2'}{\lambda_2})' + (Jm^{22})''\},$$

$$= \mathbf{e}_s\{[\lambda_2(J\sigma^{22} + \kappa_2 Jm^{22})]' + \kappa_2[(Jm^{22}\lambda_2)' - Jm^{11}\frac{rr'}{\lambda_2}]\} \tag{4.3.16}$$

$$+\mathbf{n}\{-\kappa_2\lambda_2^2(J\sigma^{22} + \kappa_2 Jm^{22}) + [\frac{1}{\lambda_2}(Jm^{22}\lambda_2)' - Jm^{11}\frac{rr'}{\lambda_2^2}]'\}.$$

It then follows that

$$\mathbf{P}^{\alpha}_{,\,\alpha} = \mathbf{e}_s\{-(rJ\sigma^{11} + Jm^{11}\frac{z'}{\lambda_2})\frac{r'}{\lambda_2} + [\lambda_2(J\sigma^{22} + \kappa_2 Jm^{22})]' + \kappa_2[(Jm^{22}\lambda_2)'$$

$$-Jm^{11}\frac{rr'}{\lambda_2}]\} + \mathbf{n}\{-(rJ\sigma^{11} + Jm^{11}\frac{z'}{\lambda_2})\frac{z'}{\lambda_2} - \kappa_2\lambda_2^2(J\sigma^{22}$$

$$+\kappa_2 Jm^{22}) + [\frac{1}{\lambda_2}(Jm^{22}\lambda_2)' - Jm^{11}\frac{rr'}{\lambda_2^2}]'\},$$

$$= \mathbf{e}_s\{[\lambda_2(J\sigma^{22} + \kappa_2 Jm^{22})]' - \frac{rr'}{\lambda_2}[J\sigma^{11} + \kappa_1 Jm^{11}] + \kappa_2[(Jm^{22}\lambda_2)' \tag{4.3.17}$$

$$-Jm^{11}\frac{rr'}{\lambda_2^2}]\} + \mathbf{n}\{-\kappa_2\lambda_2^2(J\sigma^{22} + \kappa_2 Jm^{22}) - r^2\kappa_1[J\sigma^{11} + \kappa_1 Jm^{11}]$$

$$+\frac{1}{\lambda_2}\frac{1}{\lambda_2}(Jm^{22}\lambda_2)' - Jm^{11}\frac{rr'}{\lambda_2^2}]'\}.$$

Thus, the equilibrium equation $\mathbf{P}^{\alpha}_{,\,\alpha} = -PJ\mathbf{n}$ reduces to

$$[\lambda_2(J\sigma^{22} + \kappa_2 Jm^{22})]' - \frac{rr'}{\lambda_2}[J\sigma^{11} + \kappa_1 Jm^{11}] + \kappa_2[(Jm^{22}\lambda_2)' - Jm^{11}\frac{rr'}{\lambda_2^2}] = 0, \tag{4.3.18}$$

$$-\kappa_2\lambda_2^2(J\sigma^{22} + \kappa_2 Jm^{22}) - r^2\kappa_1[J\sigma^{11} + \kappa_1 Jm^{11}] + [\frac{1}{\lambda_2}(Jm^{22}\lambda_2)' - Jm^{11}\frac{rr'}{\lambda_2^2}]' = -P\lambda_1\lambda_2. \tag{4.3.19}$$

To compare with (4.3.1) and (4.3.2), we rewrite the above equation as

$$\frac{1}{\lambda_2}[R\lambda_2(J\sigma^{22} + \kappa_2 Jm^{22})]' - \frac{Rrr'}{\lambda_2^2}[J\sigma^{11} + \kappa_1 Jm^{11}]$$

$$-\kappa_2 R[(Jm^{11}\frac{rr'}{\lambda_2^2} - \frac{1}{\lambda_2}(Jm^{22}\lambda_2)'] = 0, \tag{4.3.20}$$

$$\frac{\kappa_2\lambda_2}{\lambda_1}(J\sigma^{22} + \kappa_2 Jm^{22}) + \frac{r^2\kappa_1}{\lambda_1\lambda_2}[J\sigma^{11} + \kappa_1 Jm^{11}] + \frac{R}{r\lambda_2}[Jm^{11}\frac{rr'}{\lambda_2}$$

$$-\frac{1}{\lambda_2}(Jm^{22}\lambda_2)']' = P. \tag{4.3.21}$$

We see that these two equations become (4.3.1) and (4.3.2) if we take

$$N_1 = \frac{Rr}{\lambda_2}[J\sigma^{11} + \kappa_1 Jm^{11}], \quad N_2 = \frac{\lambda_2}{\lambda_1}[J\sigma^{22} + \kappa_2 Jm^{22}], \tag{4.3.22}$$

and

$$\hat{Q} = Jm^{11}\frac{Rrr'}{\lambda_2^2} - \frac{R}{\lambda_2}(Jm^{22}\lambda_2)'. \tag{4.3.23}$$

Now

$$\begin{gathered} J\sigma_{11} = \lambda_1 w_1 H, \quad J\sigma_{22} = \lambda_2 w_2 H, \quad J\sigma^{11} = \frac{w_1 H}{Rr}, \\ J\sigma^{22} = \frac{w_2 H}{\lambda_2}, Jm^{11} = \frac{\lambda_2}{Rr}M_1 = H\frac{\partial U}{\partial \kappa_{11}} = Hcf_1, \\ Jm^{22} = \frac{r}{R\lambda_2}M_2 = H\frac{\partial U}{\partial \kappa_{22}} = Hcf_2. \end{gathered} \tag{4.3.24}$$

Thus, we have

$$\hat{Q} = Hcf_1\frac{Rrr'}{\lambda_2^2} - \frac{HR}{\lambda_2}(cf_2\lambda_2)', \tag{4.3.25}$$

which is also consistent with (4.3.3). Alternatively, $\hat{Q}$ can be written as

$$\begin{aligned} \hat{Q} = c(\kappa_{22} + 2\lambda_1\cos\phi - 2)\frac{\lambda_1\sin\phi}{\lambda_2} - c\lambda_2\left(\frac{2\kappa_{22} + \lambda_1\cos\phi - 1}{\lambda_2}\right)' \\ -2c\frac{\lambda_2'}{\lambda_2}(2\kappa_{22} + \lambda_1\cos\phi - 1). \end{aligned} \tag{4.3.26}$$

With these facts established, we can now write down the system of first-order ordinary differential equations for finding fully non-linear localized bulging solutions for hyperelastic thin walled tubes. First, we have

$$\lambda_1' = \frac{r'}{R} = \frac{\lambda_2}{R}\sin\phi, \tag{4.3.27}$$

$$\phi' = -\frac{\kappa_{22}}{\lambda_2}, \tag{4.3.28}$$

$$\kappa_{22}' = -\lambda_2'\phi' - \lambda_2\phi'' = \frac{\lambda_2'}{\lambda_2}\kappa_{22} - \lambda_2\phi''. \tag{4.3.29}$$

The equilibrium equation (4.2.40) can then be solved with (4.3.26) and (4.3.29) to express λ_2' and ϕ'' in terms of $\lambda_1, \lambda_2, \phi, \kappa_{22}$ and $\hat{Q}$. We obtain

$$\begin{aligned}
\lambda_2' &= -((-\lambda_2\hat{Q} + 6\kappa_{22}\lambda_2\hat{Q} + \lambda_1\lambda_2\cos\phi\,\hat{Q} - 2c\,\lambda_1\sin\phi \\
&\quad +8c\,\kappa_{22}\lambda_1\sin\phi - 2c\,\kappa_{22}^2\lambda_1\sin\phi + 2w_1\lambda_2^2\sin\phi - 2w_{12}\lambda_2^3\sin\phi \\
&\quad +4c\,\lambda_1^2\cos\phi\sin\phi - 8c\,\kappa_{22}\lambda_1^2\cos\phi\sin\phi - 5c\,\lambda_2^2\cos\phi\sin\phi \\
&\quad +4c\,\kappa_{22}\lambda_2^2\cos\phi\sin\phi - 2c\,\lambda_1^3\cos^2\phi\sin\phi \\
&\quad +5c\,\lambda_1\lambda_2^2\cos^2\phi\sin\phi)/(c - 8c\,\kappa_{22}\lambda_1\cos\phi + c\,\lambda_1^2\cos^2\phi)), \qquad (4.3.30)
\end{aligned}$$

$$\begin{aligned}
\phi'' &= -((-c\kappa_{22}\hat{Q}\lambda_2 + 6c\kappa_{22}^2\hat{\lambda}_2 + \hat{Q}w_{22}\lambda_2^3 + c\kappa_{22}^2\hat{Q}\lambda_1\lambda_2\cos\phi \\
&\quad +5c^2\kappa_{22}^2\lambda_1\sin\phi - 4c^2\kappa_{22}^3\lambda_1\sin\phi - cw_1\lambda_2^2\sin\phi + 4c\kappa_{22}w_1\lambda_2^2\sin\phi \\
&\quad +2cw_{22}\lambda_1\lambda_2^2\sin\phi + cw_{12}\lambda_2^3\sin\phi - 4c\kappa_{22}w_{12}\lambda_2^3\sin\phi \\
&\quad -5c^2\kappa_{22}^2\lambda_1^2\cos\phi\sin\phi + 2c^2\lambda_2^2\kappa_{22}^3\cos\phi\sin\phi - 8c^2\kappa_{22}\lambda_2^2\cos\phi\sin\phi \\
&\quad +2c^2\kappa_{22}^2\lambda_2^2\cos\phi\sin\phi + cw_1\lambda_1\lambda_2^2\cos\phi\sin\phi - 2cw_{22}\lambda_1^2\lambda_2^2\cos\phi\sin\phi \\
&\quad -cw_{12}\lambda_1\lambda_2^3\cos\phi\sin\phi + cw_{22}\lambda_2^4\cos\phi\sin\phi \\
&\quad -4c^2\lambda_1\lambda_2^2\cos\phi^2\sin\phi + 8c^2\kappa_{22}\lambda_1\lambda_2^2\cos^2\phi\sin\phi \\
&\quad +2c^2\lambda_1^2\lambda_2^2\cos^3\phi\sin\phi)/(c\lambda_2^2(c - 8c\kappa_{22} + 12c\kappa_{22}^2 - 2cw_{22}\lambda_2^2 \\
&\quad -2c\lambda_1\cos\phi + 8c\kappa_{22}\lambda_1\cos\phi + c\lambda_1^2\cos^2\phi))). \qquad (4.3.31)
\end{aligned}$$

Finally, equation (4.3.21) can be written as

$$\begin{aligned}
\hat{Q}' &= \lambda_1\lambda_2 P - (\frac{c\kappa_{22}(-1 + \lambda_1\cos\phi + 2\kappa_{22})}{\lambda_2} + w_2)\frac{\kappa_{22}}{\lambda_2} \\
&\quad - \cos\phi(c\cos\phi(-2 + 2\lambda_1\cos\phi + \kappa_{22}) + w_1), \qquad (4.3.32)
\end{aligned}$$

where the pressure P is given by (4.2.45). Equations (4.3.27) -(4.3.30) and (4.3.32) represent a system of first-order ordinary differential equations for the variables $\lambda_1, \lambda_2, \phi, \kappa_{22}$ and $\hat{Q}$.

4.4 Weakly Non-Linear Analysis

When the elastic tube is inflated by an internal pressure, the tube inflates cylindrically until the pressure reaches a critical value. At this point, where $r_\infty = r_{cr}$, a bifurcation occurs and the cylindrical configuration becomes unstable. A weakly non-linear analysis may be conducted to determine the near-critical behaviour. We derive the amplitude equation for the radius variation along the axis using the weakly non-linear solutions of $\lambda_1, \lambda_2, \phi, \kappa_{22}$ and $\hat{Q}$. For near-critical localized solutions, we use the scalings in Fu et al. (2008) and the ordinary differential equations (4.3.27) -(4.3.30) and (4.3.32) to deduce that

$$\lambda_1 - r_\infty = O(\epsilon),\ \lambda_2 - z_\infty = O(\epsilon),\ \phi = O(\epsilon^{3/2}),\ \kappa_{22} = O(\epsilon^2),\ \hat{Q} = O(\epsilon^{3/2}), \quad (4.4.1)$$

where r_∞ and z_∞ are the radius of the bulge and axial stretch at infinity respectively. Thus, we shall look for an asymptotic solution of the form

$$\begin{aligned}
\lambda_1 &= r_\infty + \epsilon y_1(s) + \epsilon^2 y_2(s) + \epsilon^3 y_3(s),\\
\lambda_2 &= z_\infty + \epsilon z_1(s) + \epsilon^2 z_2(s) + \epsilon^3 z_3(s),\\
\phi &= \epsilon^{\frac{3}{2}}(\alpha_1(s) + \epsilon\alpha_2(s) + \epsilon^2\alpha_3(s)),\\
\kappa_{22} &= \epsilon^2(\gamma_1(s) + \epsilon\gamma_2(s) + \epsilon^2\gamma_3(s)),\\
Q &= \epsilon^{\frac{3}{2}}(\Gamma_1(s) + \epsilon\Gamma_2(s) + \epsilon^2\Gamma_3(s)),
\end{aligned} \quad (4.4.2)$$

where y_1, z_1, etc. are unknowns to be determined by the perturbation analysis. As before, s is a far distance variable defined by $s = \sqrt{\epsilon}Z$. Coefficients of ϵ can be obtained by substituting these asymptotic expressions into the dynamical system (4.3.27)-(4.3.30),(4.3.32), and expanding the latter as power series in ϵ. At order $\epsilon^{3/2}$, we obtain

two equations for $y_1'(s)$ and $\alpha_1(s)$, which may be written as

$$A \begin{pmatrix} y_1'(s) \\ \\ \alpha_1(s) \end{pmatrix} = \begin{pmatrix} 0 \\ \\ 0 \end{pmatrix}, \tag{4.4.3}$$

where

$$A = \begin{pmatrix} 1 & -z_\infty \\ \dfrac{z_\infty(2c - w_1^{(\infty)} + r_\infty w_{11}^{(\infty)})}{r_\infty(2c(-1+r_\infty) + w_1^{(\infty)} - z_\infty w_{12}^{(\infty)})} & \dfrac{2c - 2cr_\infty - w_1^{(\infty)} + z_\infty w_{12}^{(\infty)}}{w_{22}^{(\infty)}} \end{pmatrix}. \tag{4.4.4}$$

Then det A = 0 yields the bifurcation condition $\omega(r_\infty) = 0$ where

$$\omega(r_\infty) = \frac{-r_\infty \left((2c(-1+r_\infty) + w_1^{(\infty)} - z_\infty (w_{12}^{(\infty)})^2\right)^2}{r_\infty w_{22}^{(\infty)}(2c(-1+r_\infty) + w_1^{(\infty)} - z_\infty w_{12}^{(\infty)})}$$
$$\frac{+z_\infty^2 w_{22}^{(\infty)}(2c - w_1^{(\infty)} + r_\infty w_{11}^{(\infty)}))}{r_\infty w_{22}^{(\infty)}(2c(-1+r_\infty) + w_1^{(\infty)} - z_\infty w_{12}^{(\infty)})}. \tag{4.4.5}$$

The matrix equation (4.4.3) has then a non-trivial solution for y_1 and α_1. When $c = 0$, this bifurcation condition is found to be equivalent to what was obtained by Fu et al. (2008). Equation (4.4.5) can be solved for different strain-energy functions W, along with any specified z_∞, to find the bifurcation value of r_∞. For the Varga material, $\omega(r_\infty)$ is given by

$$\omega(r_\infty) = \frac{-z_\infty^2(-2 + 2(-1+c)r_\infty^2 z_\infty - 4cr_\infty^3 z_\infty + (-1+c)^2 r_\infty^4 z_\infty^2}{2r_\infty(-2 + cr_\infty^3 z_\infty + r_\infty^2(z_\infty - cz_\infty)}$$
$$\frac{-2(-1+c)cr_\infty^5 z_\infty^2 + c^2 r_\infty^6 z_\infty^2))}{2r_\infty(-2 + cr_\infty^3 z_\infty + r_\infty^2(z_\infty - cz_\infty)}. \tag{4.4.6}$$

Figure 4.4.1 shows $\omega(r_\infty)$ for different strain-energy functions. Gent material predicts two bifurcation values 1.69710 and 4.94332 when $J_m = 30$, and 1.63603 and 9.057674 when $J_m = 97$. We observe that when J_m decreases the two bifurcation values move towards each other. When $z_\infty = 1.1$, we also observe that Varga and Ogden materials

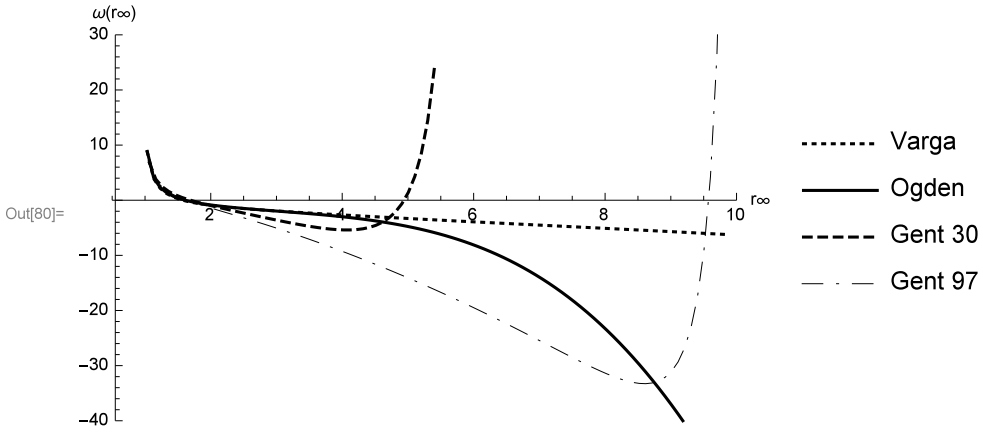

Figure 4.4.1: Function $\omega(r_\infty)$ for different strain-energy functions when $c = 0.01$ and $z_\infty = 1.1$.

each predicts one bifurcation value, given by $r_\infty = 1.57855$ and 1.61542, respectively. However, as z_∞ increases, we observed only one bifurcation point for the Ogden material until z_∞ reaches 2.5 and then it predicts two bifurcation points at $r_\infty = 1.14303$ and 4.3465. The case of fixed axial force Gent material with $J_m = 30$ substantially changes the distance between the two critical points of $\omega(r_\infty)$, as shown in Figure 4.4.2. Figure 4.4.3 shows how the solution of $\omega(\lambda_1, \lambda_2) = 0$ varies with respect to c for the Gent model with $J_m = 30$. The solid line corresponding to $c = 0$ is graphically equivalent to the case of no bending stiffness as shown in Figure 3.1.4. It shows that for each fixed axial stretch, the value of λ_1 decreases with increased in c at the first bifurcation point. We observe that λ_1 takes the values 1.69807, 1.68809 and 1.66551 for $c = 0,\ 0.1$ and 0.3 respectively when $z_\infty = 1.1$ for the Gent model with $J_m = 30$. Proceeding to the next

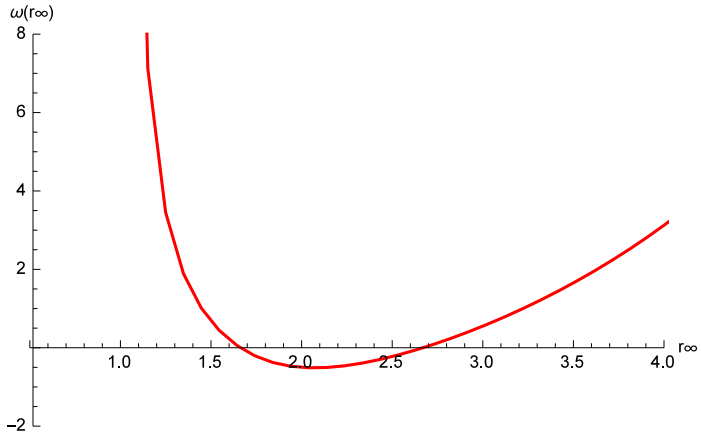

Figure 4.4.2: Function $\omega(r_\infty)$ for the Gent strain-energy function with $J_m = 30$ when the axial force is fixed at zero.

order, we find that $y_2'(s)$ and $\alpha_2(s)$ satisfy the inhomogeneous system

$$A \begin{pmatrix} y_2'(s) \\ \\ \alpha_2(s) \end{pmatrix} = \begin{pmatrix} k_1(s) \\ \\ k_2(s) \end{pmatrix}, \tag{4.4.7}$$

where $k_1(s)$ and $k_2(s)$ contains $y_1(s), z_1(s), \alpha_1(s), \gamma_1(s), \Gamma_1(s)$ and their derivatives. We can further show that

$$\begin{aligned} z_1(s) &= \frac{z_\infty(2c - w_1 + r_\infty w_{11})y_1(s)}{r_\infty(-2c + 2cr_\infty + w_1 - z_\infty w_{12})}, \\ \Gamma_1(s) &= \frac{-c\, y_1'(s)}{z_\infty^2 w_{22}}((2r_\infty - 2r_\infty^2 + z_\infty^2)w_{22} + (-1 + r_\infty) \\ &\qquad (2c(-1 + r_\infty)w_1 - z_\infty w_{12})), \\ \alpha_1(s) &= \frac{y_1'(s)}{z_\infty}, \\ \gamma_1(s) &= -y_1''(s). \end{aligned} \tag{4.4.8}$$

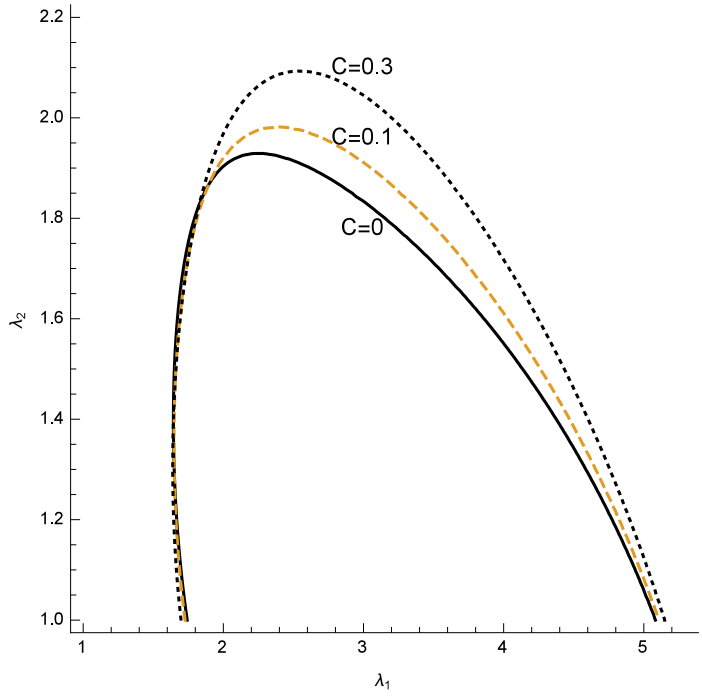

Figure 4.4.3: Bifurcation condition $\omega(r_\infty) = 0$ for the Gent model with $J_m = 30$ for different values of c when the axial force is zero.

Now $k_1(s)$ and $k_2(s)$ only contain $y_1(s)$ and its derivatives. As the matrix A is singular as discussed above, we now need to impose a solvability condition in order to find a solution to (4.4.7). We take the dot product of (4.4.7) with the left eigenvector of A as discussed in Section (3.1.3), resulting in a zero in the left hand side of the resulting equation. We then obtain the amplitude equation from the right hand side of (4.4.7) as in the same form of (3.1.29) where the function $\omega(r_\infty)$ is given by (4.4.5). The expression for $\gamma(r_\infty)$ is too long and so is not written out here (see Appendix A). We then differentiate the amplitude equation with respect to Z and expand the resulting equation around r_{cr}, a root of the bifurcation condition $\omega(r_\infty) = 0$. In the near critical

post bifurcation analysis, $r_\infty = r_{cr} + \epsilon r_1$, where ϵ is a small positive number and r_1 is a negative constant. Neglecting terms of order higher than ϵ^2, we obtain the localized solution

$$y_1(s) = \frac{\omega'(r_{cr})(r_\infty - r_{cr})}{\gamma(r_{cr})} \operatorname{sech}^2\left(\frac{\sqrt{\omega'(r_{cr})(r_\infty - r_{cr})}s}{2}\right), \tag{4.4.9}$$

where $\omega'(r_{cr}) = d\omega(r_{cr})/dr_{cr}$ and bulging solution exists only to the left of the bifurcation point r_{cr} satisfying

$$\omega'(r_{cr})(r_\infty - r_{cr}) > 0. \tag{4.4.10}$$

For all materials that we have considered so far, $\omega'(r_{cr})$ is always negative corresponding to the first bifurcation point and so bifurcation into the above localized solution must necessarily be subcritical. For the Gent material with $J_m = 30$, we have $\omega'(r_{cr}) = -3.5855$, $\gamma(r_{cr}) = -1.4448$ while for the Ogden material $\omega'(r_{cr}) = -3.09342$, $\gamma(r_{cr}) = -1.26788$. So, the localized solution (4.4.9) represents a bulge. We now can write down the following expressions that can be used as an initial guess in finding the exact localized bulging solutions

$$\begin{gathered}
\lambda_1(Z) = r_\infty - \frac{d}{\gamma(r_{cr})} \operatorname{sech}^2\frac{\sqrt{d}Z}{2}, \\
\lambda_2(Z) = z_\infty + \frac{z_\infty(w_1 - r_{cr}w_{11})}{r_{cr}(c\, r_{cr} + w_1 - z_\infty w_{12})} (\lambda_1(Z) - r_\infty), \\
\phi(Z) = -\frac{d^{3/2}}{\gamma(r_{cr})} \operatorname{sech}^2\frac{\sqrt{d}Z}{2} \tanh\frac{\sqrt{d}Z}{2}, \\
\kappa_{22}(Z) = -\frac{\phi'(Z)}{\lambda_2(Z)}, \\
Q(Z) = \frac{c(-r_{cr}^2 + z_\infty^2)w_{22} + c\, r_{cr}(c\, r_{cr} + w_1 - z_\infty w_{12})}{z_\infty w_{22}} \phi(Z),
\end{gathered} \tag{4.4.11}$$

where $d = \omega'(r_{cr})(r_\infty - r_{cr})$. It can be easily shown that $\lambda_1(0) = r_0,\ \lambda_2(0) = z_0'\ , \phi(0) = 0,\ \kappa_{22}(0) = -r''(0),$ and $\hat{Q}(0) = 0$ for any strain-energy function. The third and the

fifth of these coming from the fact that the deformed tube is locally flat at $Z = 0$ as we impose $r_0' = 0$ as part of the symmetry conditions.

4.5 Fully Non-Linear Solutions

Here we discuss two methods to find the fully non-linear localized bulging solutions, namely the shooting method and the Finite Difference Method as for the membrane case.

4.5.1 Shooting method

We rewrite equations (4.2.49) and (4.2.50) derived in Section 4.2 as

$$w_2(r_0, z_0') - w_2^{(\infty)} - \frac{P}{2}(r_0^2 - r_\infty^2) + c\,\frac{\kappa_{22}(0)}{z_0'}(2\kappa_{22}(0) + \kappa_{11}(0) - 1) = 0, \tag{4.5.1}$$

$$\begin{aligned} &w(r_0, z_0') - w^{(\infty)} + c((r_0 - 1)^2 + \kappa_{22}^2(0) + \kappa_{22}(0)(r_0 - 1)) \\ &-c\,(r_\infty - 1)^2 - z_0' w_2(r_0, z_0') + z_\infty \hat{w}_2^{(\infty)} - 2c\,(2\kappa_{22}(0) + r_0 - 1)\kappa_{22}(0) \\ &-2c(2\kappa_{22}(0) + r_0 - 1)\kappa_{22}(0) = 0. \end{aligned} \tag{4.5.2}$$

These two equations involve three unknowns r_0, z_0' and $\kappa_{22}(0)$. In the shooting method, r_0 is to be guessed and z_0' and $\kappa_{22}(0)$ are related to r_0 by (4.5.1) and (4.5.2). Then for each specified r_∞ and a guess for r_0, we have to solve (4.5.1) and (4.5.2) to find the corresponding z_0' and $\kappa_{22}(0)$. A reasonable starting guess for r_0 is required to ensure the success of the shooting method. The weakly non-linear result presented in

the previous section provides a very good initial guess for r_0. Therefore we use these results to guess a value for r_0 and solve (4.5.1) and (4.5.2) for z_0' and $\kappa_{22}(0)$. Then as in Section 3.2.1, we decrease r_∞ in small steps, using the solution from the previous step as the initial guess for the current step. We have attempted to solve the system of first order differential equations (4.3.27)-(4.3.30) and (4.3.32) derived in the previous section using the shooting method described above. Unfortunately, we have not been able to find a convergent result. This is left as future work.

4.5.2 Finite Difference Method

In this section we apply the Finite Difference Method to find the fully non-linear solutions for the system of first order non-linear differential equations derived in Section 4.3. Rewrite our system of ordinary differential equations as

$$\begin{aligned}
\lambda_1' &= \lambda_2 \sin\phi, \\
\lambda_2' &\text{ as given in (4.3.30)}, \\
\phi' &= -\frac{\kappa_{22}}{\lambda_2}, \\
\kappa_{22}' &= \frac{\lambda_2'}{\lambda_2}\kappa_{22} - \lambda_2\phi'', \\
\hat{Q}' &= \lambda_1\lambda_2 P - \Big(\frac{c\kappa_{22}(-1+\lambda_1\cos\phi+2\kappa_{22})}{\lambda_2} + w_2\Big)\frac{\kappa_{22}}{\lambda_2} \\
&\quad - \cos\phi\big(c\cos\phi(-2+2\lambda_1\cos\phi+\kappa_{22}) + w_1\big),
\end{aligned} \tag{4.5.3}$$

where prime denotes the differentiation with respect to Z. Our goal is to write these equations in a form that can be solved numerically for the unknown values of the dependent variables $\lambda_1, \lambda_2, \phi, \kappa_{22}$ and $\hat{Q}$ at specified values of the independent variable

Z. For implementation of the Finite Difference Method to solve the system of differential equations (4.5.3), 1D grid discretization of the domain with n cells is presented in Figure 4.5.1. The domain length is taken as L, with n cells in the domain, with $n-1$ internal

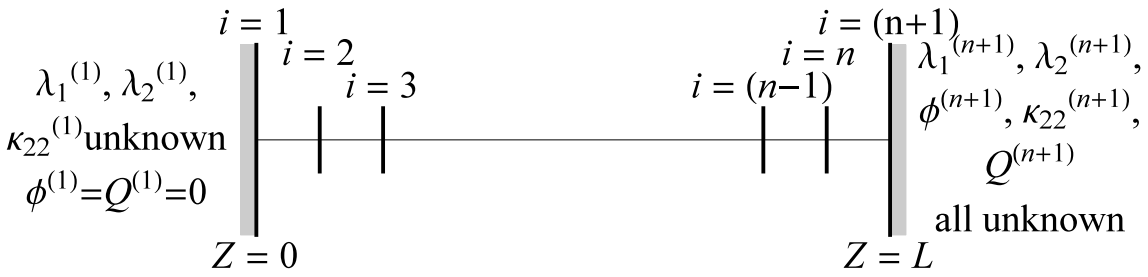

Figure 4.5.1: Finite difference discretization.

nodes and two boundary nodes. The length of each cell is then L/N. The first order central differencing formulae are used to approximate the equations (4.5.3). We now write $\lambda_1^{(i)}$, $\lambda_2^{(i)}$, $\phi^{(i)}$, $\kappa_{22}^{(i)}$ and $\hat{Q}^{(i)}$ to represent λ_1, λ_2, ϕ, κ_{22} and $\hat{Q}$ at the node i respectively. The left boundary values of ϕ and $\hat{Q}$ are known, given by

$$\phi^{(1)} = \hat{Q}^{(1)} = 0. \tag{4.5.4}$$

The rest of the left boundary values and all the right boundary values are unknown. Finite difference approximations (2.4.4) of the governing equations (4.5.3) at the second node are given by

$$\frac{\lambda_1^{(3)} - \lambda_1^{(1)}}{2h} = \lambda_2^{(2)} \sin\phi^{(2)},$$

$$\frac{\lambda_2^{(3)} - \lambda_2^{(1)}}{2h} = f(\lambda_1^{(2)}, \lambda_2^{(2)}, \phi^{(2)}, \kappa_{22}^{(2)}, \hat{Q}^{(2)}),$$

$$\frac{\phi^{(3)}-\phi^{(1)}}{2h}=\frac{-\kappa_{22}^{(2)}}{\lambda_2^{(2)}},$$
$$\frac{\kappa_{22}^{(3)}-\kappa_{22}^{(1)}}{2h}=\frac{\lambda_2^{(3)}-\lambda_2^{(1)}}{2h}\kappa_{22}^{(2)}-\lambda_2^{(2)}\phi''^{(2)},$$
$$\frac{\hat{Q}^{(3)}-\hat{Q}^{(1)}}{h}=\lambda_1^{(2)}\lambda_2^{(2)}P-\{\frac{c\kappa_{22}^{(2)}(-1+\lambda_1^{(2)}\cos\phi^{(2)}+2\kappa_{22}^{(2)})}{\lambda_2^{(2)}}$$
$$+w_2(\lambda_1^{(2)},\lambda_2^{(2)})\}\frac{\kappa_{22}^{(2)}}{\lambda_2^{(2)}}\cos\phi^{(2)}(c\cos\phi^{(2)}(-2+2\lambda_1^{(2)}\cos\phi^{(2)}$$
$$+\kappa_{22}^{(2)})+w_1(\lambda_1^{(2)},\lambda_2^{(2)}), \tag{4.5.5}$$

where f is a function of $\lambda_1^{(2)},\lambda_2^{(2)},\phi^{(2)},\kappa_{22}^{(2)},\hat{Q}^{(2)}$ which can be calculated using (4.3.30), and the expression of ϕ'' is given in (4.3.31). It can be easily shown that due to the symmetric property of ϕ and $\hat{Q}$, we have

$$-\phi^{(0)}=\phi^{(2)}\quad\text{and}\quad-\hat{Q}^{(0)}=\hat{Q}^{(2)}. \tag{4.5.6}$$

Therefore finite difference approximations of the third and fifth equations of (4.5.3) at the first node are respectively

$$\frac{\phi^{(2)}}{h}=\frac{-\kappa_{22}^{(1)}}{\lambda_2^{(1)}},$$
$$\frac{\hat{Q}^{(2)}}{h}=\lambda_1^{(1)}\lambda_2^{(1)}P-\{\frac{c\kappa_{22}^{(1)}(-1+\lambda_1^{(1)}\cos\phi^{(1)}+2\kappa_{22}^{(1)})}{\lambda_2^{(1)}}$$
$$+w_2(\lambda_1^{(1)},\lambda_2^{(1)})\}\frac{\kappa_{22}^{(1)}}{\lambda_2^{(1)}}-\cos\phi^{(1)}(c\cos\phi^{(1)}(-2$$
$$+2\lambda_1^{(1)}\cos\phi^{(1)}+\kappa_{22}^{(1)})+w_1(\lambda_1^{(1)},\lambda_2^{(1)}). \tag{4.5.7}$$

We may use the Taylor expansions

$$u_{i+1}=u_i+hu_i'+\frac{u_i''}{2}h^2+O(h^3),$$
$$u_{i+2}=u_i+2\,hu_i'+\frac{u_i''}{2}(2h)^2+O(h^3), \tag{4.5.8}$$

to obtain

$$u_i' = \frac{4u_{i+1} - u_{i+2} - 3u_i}{2h} + O(h^2). \tag{4.5.9}$$

We now use the above approximation for the first, second and fourth equations of (4.5.3) at the first node as

$$\begin{aligned} \frac{4\lambda_1^{(2)} - \lambda_1^{(3)} - 3\lambda_1^{(1)}}{2h} &= \lambda_2^{(1)} \sin\phi^{(1)}, \\ \frac{4\lambda_2^{(2)} - \lambda_2^{(3)} - 3\lambda_2^{(1)}}{2h} &= f(\lambda_1^{(1)}, \lambda_2^{(1)}, \phi^{(1)}, \kappa_{22}^{(1)}, \hat{Q}^{(1)}), \\ \frac{4\kappa_{22}^{(2)} - \kappa_{22}^{(3)} - 3\kappa_{22}^{(1)}}{2h} &= \frac{\lambda_2^{(3)} - \lambda_2^{(1)}}{2h}\kappa_{22}^{(2)} - \lambda_2^{(2)}\phi''^{(2)}. \end{aligned} \tag{4.5.10}$$

Applying finite difference approximations (2.4.4) at every internal node along with (4.5.7) and (4.5.10), $5n$ coupled algebraic equations with $5n + 3$ unknowns can be found. Three more equations are derived in the next section.

4.5.3 Decaying conditions

As $Z \to \infty$, we may look for an asymptotic solution of the form

$$\begin{aligned} \lambda_1 &= r_\infty + \epsilon y_1(Z) + ..., \\ \lambda_2 &= z_\infty + \epsilon z_1(Z) + ..., \\ \phi &= \epsilon\phi(Z) + ..., \\ \kappa_{22} &= \epsilon\gamma(Z) + ..., \\ \hat{Q} &= \epsilon\Gamma(Z) + ... \end{aligned} \tag{4.5.11}$$

Substitute (4.5.11) into the system of ordinary differential equations (4.5.3) and expand asymptotically in terms of ϵ. Considering the coefficients of ϵ, the system of linear differential equations can be written as a matrix equation,

$$\mathbf{u}' = M(r_\infty)\mathbf{u}, \tag{4.5.12}$$

where the column vector $\mathbf{u}$ and the matrix $M(r_\infty)$ are given by

$$\mathbf{u} = \begin{pmatrix} y_1 \\ z_1 \\ \phi \\ \gamma_{22} \\ \Gamma \end{pmatrix}, \quad M(r_\infty) = \begin{pmatrix} 0 & 0 & z_\infty & 0 & 0 \\ 0 & 0 & a_{23} & 0 & a_{25} \\ 0 & 0 & 0 & \frac{-1}{z_\infty} & 0 \\ 0 & 0 & a_{43} & 0 & a_{45} \\ a_{51} & a_{52} & 0 & a_{54} & 0, \end{pmatrix}, \tag{4.5.13}$$

with

$$a_{23} = \frac{2c\, r_\infty - 4c\, r_\infty^2 + 2c\, r_\infty^3 + 5c\, z_\infty^2 - 5c\, r_\infty z_\infty^2 - 2z_\infty^2 w_1^{(\infty)} + 2z_\infty^3 w_{12}^{(\infty)}}{c - 2c\, r_\infty + cr_\infty^2 - 2z_\infty^2 w_{22}^{(\infty)}},$$

$$a_{25} = \frac{z_\infty - r_\infty z_\infty}{c - 2c\, r_\infty + cr_\infty^2 - 2z_\infty^2 w_{22}^{(\infty)}},$$

$$a_{43} = z_\infty\Big(\frac{2c^2 - 4c^2\, r_\infty + 2c^2 r_\infty^2 + 2c\, r_\infty w_{22}^{(\infty)} - 2c\, r_\infty^2 w_{22}^{(\infty)}}{c(c - 2c\, r_\infty + cr_\infty^2 - 2z_\infty^2 w_{22}^{(\infty)})}$$

$$\frac{+c\, z_\infty^2 w_{22}^{(\infty)} - c\, w_1^{(\infty)} + c\, r_\infty w_1^{(\infty)} + c\, z_\infty w_{12}^{(\infty)} - c\, r_\infty z_\infty w_{12}^{(\infty)}}{c(c - 2c\, r_\infty + cr_\infty^2 - 2z_\infty^2 w_{22}^{(\infty)})}\Big), \tag{4.5.14}$$

$$a_{45} = \frac{z_\infty^2 w_{22}^{(\infty)}}{c(c - 2c\, r_\infty + cr_\infty^2 - 2z_\infty^2 w_{22}^{(\infty)})},$$

$$a_{51} = \frac{-2 + w_1^{(\infty)} - r_\infty w_{11}^{(\infty)}}{r_\infty},$$

$$a_{52} = \frac{-2 + 2c\, r_\infty + w_1^{(\infty)} - z_\infty w_{12}^{(\infty)}}{z_\infty}, \quad a_{54} = \frac{-c\, z_\infty - w_2^{(\infty)}}{z_\infty}.$$

We expect that for sufficiently large values of Z, the asymptotic behaviour of the solution is governed by the linearized system (4.5.12) (Nagatou 2003).

Looking for a solution of the form $\boldsymbol{u} = \boldsymbol{\eta}\, e^{\omega Z}$, we obtain $(M(r_\infty) - \omega I)\boldsymbol{\eta} = \mathbf{0}$, which indicates that ω must be an eigenvalue of $M(r_\infty)$ and η is an associate eigenvector. We have

$$\frac{1}{\omega}\det(M(r_\infty) - \omega I) = \frac{-1}{c\,\lambda_1(c - 2c\lambda_1 + c\lambda_1^2 - 2w_{22}^{(\infty)}\lambda_2^2)}[c\,(-2w_{22}^{(\infty)}$$

$$\omega^2 + c(2+\omega^2)^2)\lambda_1^3 + (-2c + w_1^{(\infty)})w_{22}^{(\infty)}\lambda_2^2 - 2c\lambda_1^2(-2w_1^{(\infty)}$$

$$-w_1^{(\infty)}\omega^2 - w_{22}^{(\infty)}\omega^2 + c(2+\omega^2)^2 + w_{12}^{(\infty)}(2+\omega^2)\lambda_2)$$

$$+\lambda_1((w_2^{(\infty)} - c(2+\omega^2))^2 + (-2w_1^{(\infty)}w_{12}^{(\infty)} + w_2^{(\infty)}w_{22}^{(\infty)}\omega^2$$

$$+2cw_{12}^{(\infty)}(2+\omega^2))\lambda_2 + ((w_{12}^{(\infty)})^2 - w_{22}^{(\infty)}(w_{11}^{(\infty)} + 2c\,\omega^2(-1+\omega^2)))\lambda_2^2)]. \qquad (4.5.15)$$

Since the right hand side depends on ω through ω^2, using $\beta = \omega^2$, (4.5.15) may be written as

$$\frac{1}{\omega}\det(M(r_\infty) - \omega I)c\lambda_1(c - 2c\lambda_1 + c\lambda_1^2 - 2w_{22}^{(\infty)}\lambda_2^2) =$$

$$\beta^2(-c^2\,\lambda_1 + 2c^2\lambda_1^2 - c^2\,\lambda_1^3 + 2c\,w_{22}^{(\infty)}\lambda_1\lambda_2^2) + \beta(-4c^2\lambda_1$$

$$+2cw_1^{(\infty)}\lambda_1 + 8c^2\lambda_1^2 - 2cw_1^{(\infty)}\lambda_1^2 - 2cw_{22}^{(\infty)}\lambda_1^2 - 4c^2\lambda_1^3$$

$$+2c\,w_{22}^{(\infty)}\lambda_1^3 - 2cw_{12}^{(\infty)}\lambda_1\lambda_2 - w_2^{(\infty)}w_{22}^{(\infty)}\lambda_1\lambda_2 + 2c\,w_{12}^{(\infty)}\lambda_1^2\lambda_2$$

$$-2c\,w_{22}^{(\infty)}\lambda_1\lambda_2^2) - 4c^2\lambda_1 + 4cw_1^{(\infty)}\lambda_1 - (w_1^{(\infty)})^2\lambda_1 + 8c^2\,\lambda_1^2$$

$$-4cw_1^{(\infty)}\lambda_1^2 - 4c^2\lambda_1^3 - 4cw_{12}^{(\infty)}\lambda_1\lambda_2 + 2w_1^{(\infty)}w_{12}^{(\infty)}\lambda_1\lambda_2 + 4cw_{12}^{(\infty)}\lambda_1^2\lambda_2$$

$$+2cw_{22}^{(\infty)}\lambda_2^2 - w_1^{(\infty)}w_{22}^{(\infty)}\lambda_2^2 - (w_{12}^{(\infty)})^2\lambda_1\lambda_2^2 + w_{11}^{(\infty)} - w_{22}^{(\infty)}\lambda_1\lambda_2^2 = 0. \qquad (4.5.16)$$

The right hand side of (4.5.16) takes the form $a\beta^2 + b\beta + \hat{c} = 0$, where

$$a = -c^2\ \lambda_1 + 2c^2\lambda_1^2 - c^2\ \lambda_1^3 + 2c\ w_{22}^{(\infty)}\lambda_1\lambda_2^2,$$

$$b = -4c^2\lambda_1 + 2cw_1^{(\infty)}\lambda_1 + 8c^2\lambda_1^2 - 2cw_1^{(\infty)}\lambda_1^2 - 2cw_{22}^{(\infty)}\lambda_1^2$$

$$-4c^2\lambda_1^3 + 2cw_1^{(\infty)}\lambda_1 + 8c^2\lambda_1^2 - 2cw_1^{(\infty)}\lambda_1^2 - 2cw_{22}^{(\infty)}\lambda_1^2$$

$$-4c^2\lambda_1^3 - 2c\ w_{22}^{(\infty)}\lambda_1\lambda_2^2, \tag{4.5.17}$$

$$\hat{c} = -4c^2\lambda_1 + 4cw_1^{(\infty)}\lambda_1 - (w_1^{(\infty)})^2\lambda_1 + 8c^2\ \lambda_1^2 - 4cw_1^{(\infty)}\lambda_1^2$$

$$-4c^2\lambda_1^3 - 4cw_{12}^{(\infty)}\lambda_1\lambda_2 + 2w_1^{(\infty)}w_{12}^{(\infty)}\lambda_1\lambda_2 + 4cw_{12}^{(\infty)}\lambda_1^2\lambda_2$$

$$-4cw_1^{(\infty)}\lambda_1^2 - 4c^2\lambda_1^3 - 4cw_{12}^{(\infty)}\lambda_1\lambda_2 + 2w_1^{(\infty)}w_{12}^{(\infty)}\lambda_1\lambda_2 + 4cw_{12}^{(\infty)}\lambda_1^2\lambda_2.$$

Thus, $M(r_\infty)$ has five eigenvalues, given by

$$-\sqrt{\beta_2} < -\sqrt{\beta_1} < 0 < \sqrt{\beta_1} < \sqrt{\beta_2}, \tag{4.5.18}$$

with $\beta_1 > 0,\ \beta_2 > 0$, and β_1 and β_2 given by

$$\beta_1 = -\frac{b}{2a} - \sqrt{\left(\frac{b}{2a}\right)^2 - \frac{\hat{c}}{a}}, \quad \beta_2 = -\frac{b}{2a} + \sqrt{\left(\frac{b}{2a}\right)^2 - \frac{\hat{c}}{a}}. \tag{4.5.19}$$

We observe that since we expect localized bulging to occur before any standing wave mode, we must necessarily have $b/a < 0$ and $\hat{c}/a > 0$. In the limit $\hat{c}/a \to 0$, the two eigenvalues $\sqrt{\beta_1}$ and $-\sqrt{\beta_1}$ also become zero. Thus 0 becomes a triple eigenvalue when

$\hat{c} = 0$, which is the new bifurcation condition given by $\omega(r_\infty) = 0$, where

$$\begin{aligned}\omega(r_\infty) = \sqrt{\beta_1} \;=\; & [-4c^2 r_\infty + 8c^2 r_\infty^2 - 4c^2 r_\infty^3 - 2c\, r_\infty^2 w_{22}^{(\infty)} + 2c\, r_\infty^3 w_{22}^{(\infty)} \\ & -2c r_\infty z_\infty^2 w_{22}^{(\infty)} - r_\infty z_\infty w_{22}^{(\infty)} w_2^{(\infty)} + 2c\, r_\infty w_1^{(\infty)} - 2c\, r_\infty^2 w_1^{(\infty)} \\ & -2c\, r_\infty z_\infty w_{12}^{(\infty)} + 2c\, r_\infty^2 z_\infty w_{12}^{(\infty)} + \{(r_\infty(r_\infty(2c\, r_\infty^2(2c \\ & -w_{22}^{(\infty)}) + 2c\, z_\infty^2 w_{22}^{(\infty)} + 2c(2c - w_1^{(\infty)}) + z_\infty(w_2^{(\infty)} w_{22}^{(\infty)} \\ & +2c\, w_{12}^{(\infty)}) + 2c\, r_\infty(-4c + w_{22}^{(\infty)} + w_1^{(\infty)} - z_\infty w_{12}^{(\infty)}))^2 \\ & -4c(c - 2c\, r_\infty + c r_\infty^2 - 2z_\infty^2 w_{22}^{(\infty)} - z_\infty^2 w_{22}^{(\infty)})(4c^2\, r_\infty^3 \\ & +z_\infty^2 w_{22}^{(\infty)}(-2c + w_1^{(\infty)}) - 4c\, r_\infty^2(2c - w_1^{(\infty)} + z_\infty w_{12}^{(\infty)}) \\ & +r_\infty((-2c + w_1^{(\infty)})^2 + z_\infty(4c\, w_{12}^{(\infty)} - 2w_1^{(\infty)} w_{12}^{(\infty)}) \\ & +z_\infty^2((w_{12}^{(\infty)})^2 - w_{22}^{(\infty)} w_{11}^{(\infty)})))))\}^{1/2}]/ \\ & (2c\, r_\infty(c - 2c\, r_\infty + c\, r_\infty^2 - 2z_\infty^2 w_{22}^{(\infty)})). \end{aligned} \tag{4.5.20}$$

The bifurcation condition given in (4.5.20) is identical to that given in (4.4.5) which had been derived previously by using a different method.

Denote the five right eigenvectors and the five left eigenvectors associated with the five eigenvalues in (4.5.18) by

$$\mathbf{r}^{(-2)}, \quad \mathbf{r}^{(-1)}, \quad \mathbf{r}^{(0)}, \quad \mathbf{r}^{(1)}, \quad \mathbf{r}^{(2)}$$

and

$$\mathbf{l}^{(-2)}, \quad \mathbf{l}^{(-1)}, \quad \mathbf{l}^{(0)}, \quad \mathbf{l}^{(1)}, \quad \mathbf{l}^{(2)},$$

respectively. Then for sufficiently large values of Z our decaying solution $\mathbf{u}$ must necessarily be a linear combination of the two decaying eigen solutions

$$\mathrm{e}^{-\sqrt{\beta_1} Z}\mathbf{r}^{(-1)} \quad \text{and} \quad \mathrm{e}^{-\sqrt{\beta_2} Z}\mathbf{r}^{(-2)}.$$

Since the right eigenvector associated with any given eigenvalue is orthogonal to all the left eigenvectors associated with the other eigenvalues, the decaying condition may be written as

$$\mathbf{u} \cdot \mathbf{l}^{(k)} = 0, \quad k = 0, 1, 2.$$

Thus, if we write

$$\mathbf{l}^{(0)} = [n_{31}, n_{32}, n_{33}, n_{34}, n_{35}]^T,$$

$$\mathbf{l}^{(1)} = [n_{11}, n_{12}, n_{13}, n_{14}, n_{15}]^T,$$

$$\mathbf{l}^{(2)} = [n_{21}, n_{22}, n_{23}, n_{24}, n_{25}]^T,$$

then the decaying condition may be written as

$$(\lambda_1^{(n+1)} - r_\infty) + (\lambda_2^{(n+1)} - z_\infty)n_{12} + \phi^{(n+1)}n_{13} + \kappa_{22}^{(n+1)}n_{14} + Q^{(n+1)}n_{15} = 0, \quad (4.5.21)$$

$$(\lambda_1^{(n+1)} - r_\infty) + (\lambda_2^{(n+1)} - z_\infty)n_{22} + \phi^{(n+1)}n_{23} + \kappa_{22}^{(n+1)}n_{24} + Q^{(n+1)}n_{25} = 0, \quad (4.5.22)$$

$$(\lambda_1^{(n+1)} - r_\infty) + (\lambda_2^{(n+1)} - z_\infty)n_{32} + \phi^{(n+1)}n_{33} + \kappa_{22}^{(n+1)}n_{34} + Q^{(n+1)}n_{35} = 0. \quad (4.5.23)$$

We have

$$n_{11} = 1,$$

$$n_{12} = z_\infty w_{22}^{(\infty)}(-cr_\infty - w_1^{(\infty)} + z_\infty w_{12}^{(\infty)})/M,$$

$$n_{13} = -(z_\infty \beta_1 (z_\infty (cz_\infty(-1 + 2\beta_1) - w_2^{(\infty)} w_{22}^{(\infty)} - c(-1 + r_\infty),$$

$$(c(r_\infty - \beta_1 + r_\infty \beta_1) + w_1^{(\infty)}) - z_\infty w_{12}^{(\infty)}))/M, \quad (4.5.24)$$

$$n_{14} = c(2z_\infty^2 \beta_1 w_{22}^{(\infty)} - (-1 + r_\infty)(c(r_\infty - \beta_1 + r_\infty \beta_1)$$

$$+ w_1^{(\infty)} - z_\infty w_{12}^{(\infty)}))/M,$$

$$n_{15} = -(z_\infty^2 \beta_1 w_{22}^{(\infty)})/M.$$

Similarly, $[n_{21}, n_{22}, n_{23}, n_{24}, n_{25}]^T$ can be obtained by replacing $\sqrt{\beta_1}$ by $\sqrt{\beta_2}$ in (4.5.24). The eigenvector $[n_{31}, n_{32}, n_{33}, n_{34}, n_{35}]^T$ is given by

$$n_{31} = 1,$$

$$n_{32} = z_\infty w_{22}^{(\infty)}(-cr_\infty - w_1^{(\infty)} + z_\infty w_{12}^{(\infty)})/g_1,$$

$$n_{33} = 0, \tag{4.5.25}$$

$$n_{34} = -c(-1 + r_\infty)(c\, r_\infty + w_1^{(\infty)} - z_\infty w_{12}^{(\infty)}))/g_2,$$

$$n_{35} = 0,$$

where

$$\begin{aligned} g_1 \;=\; & \{-2c^2 r_\infty + 2c^2 r_\infty^2 + 2c^2\beta_1 - 5c^2 r_\infty \beta_1 + 3c^2 r_\infty^2 \beta_1 + \\ & c^2\beta_1^2 - 2c^2 r_\infty^2 \beta_1^2 + \beta_1(2c(r_\infty - r_\infty^2 + z_\infty^2 - z_\infty^2\beta_1) \\ & + z_\infty w_2^{(\infty)}) w_{22}^{(\infty)} + (w_1^{(\infty)})^2 + 2cz_\infty w_{12}^{(\infty)} - 3cr_\infty z_\infty w_{12}^{(\infty)} \\ & + 2cz_\infty \beta_1 w_{12}^{(\infty)} - 2cr_\infty z_\infty \beta_1 w_{12}^{(\infty)} + z_\infty^2 (w_{12}^{(\infty)})^2 \\ & + w_1^{(\infty)}(c(-2 + 3r_\infty - 2\beta_1 + 2r_\infty\beta) - 2z_\infty w_{12}^{(\infty)})\}, \end{aligned} \tag{4.5.26}$$

and

$$\begin{aligned} g_2 \;=\; & \{-2c^2 r_\infty + 2c^2 r_\infty^2 + (w_1^{(\infty)})^2 + 2c\; z_\infty w_{12}^{(\infty)} - 3c\; r_\infty z_\infty w_{12}^{(\infty)} \\ & + z_\infty^2 (w_{12}^{(\infty)})^2 + w_1^{(\infty)}(c(-2 + 3r_\infty) - 2z_\infty w_{12}^{(\infty)}\}. \end{aligned} \tag{4.5.27}$$

4.5.4 Connection with the scalings and eigenvectors in the weakly non-linear theory

We denote by $[n_{41}, n_{42}, n_{43}, n_{44}, n_{45}]^T$ the right eigenvector associated with the eigenvalue $-\sqrt{\beta_1}$. The components satisfy the equations

$$\begin{aligned}
-\sqrt{\beta_1}n_{41} + z_\infty n_{43} &= 0,\\
-\sqrt{\beta_1}n_{42} + a_{23}n_{43} + a_{25}n_{45} &= 0,\\
-\sqrt{\beta_1}n_{43} - \frac{1}{z_\infty}n_{44} &= 0,\\
-\sqrt{\beta_1}n_{44} + a_{43}n_{43} + a_{45}n_{45} &= 0,\\
-\sqrt{\beta_1}n_{45} + a_{51}n_{41} + a_{52}n_{42} + a_{54}n_{44} &= 0,
\end{aligned} \tag{4.5.28}$$

where $\sqrt{\beta_1} = 0$ gives the bifurcation condition. Using these equations, we may show that in the limit $\sqrt{\beta_1} \to 0$,

$$n_{42} = O(n_{41}), n_{43} = O(\sqrt{\beta_1}n_{41}), n_{44} = O(\beta_1 n_{41}), n_{45} = O(\sqrt{\beta_1}n_{41}). \tag{4.5.29}$$

It follows that when $r_\infty = r_{cr} + \epsilon r_1$, $n_{41} = O(\epsilon)$. Then $\beta_1 = O(\epsilon)$, and so we have $n_{42} = O(\epsilon)$, $n_{43} = O(\epsilon^{3/2})$, $n_{44} = O(\epsilon^2)$ and $n_{45} = O(\epsilon^{3/2})$. We used these scalings in Section 4.4.

4.5.5 Computer programming

We have written a Mathematica code to solve the finite difference equations derived in Section 4.5.2. In this section we explain how the program is written and works. We

choose the domain of the Z variable to be [0, L], where L is the length of the tube. Finite Difference Method is sufficiently accurate when the step size $h = \frac{Z_{max} - Z_{min}}{n}$ is very small. Therefore we choose $n = 650$. $Z_{max} = L(< 60)$, and $Z_{min} = 0$ are used as input parameters. We have a set of $5n$ finite difference equations with $5n + 5$ unknowns. Then the code solves these equations in conjunction with the two initial conditions (4.5.4) and three decaying conditions (4.5.22)-(4.5.24). The behaviour of dynamical systems are highly sensitive to initial conditions: small differences in initial conditions yield widely diverging outcomes for such dynamical systems. Since the weakly non-linear solution (4.4.11) should provide a very good approximation for the exact solution when r_∞ is close to r_{cr}, we start from a case for which r_∞ is close to the critical value (say $r_\infty = r_{cr} - 0.02$), and use the weakly non-linear solution as a initial guess to find the exact solution. Once a solution is found, we then decrease r_∞ in small steps and always use the solution from the previous step as the initial guess for the current step. In Figure 4.5.2 we have shown a typical result from such a calculation. There is good agreement between the weakly non-linear solution and the exact solution obtained from the finite difference scheme, which shows that our numerical code is correct. Unfortunately, we find it difficult to obtain convergent solutions for values of r_∞ further away from its critical value. Since each solution takes quite a few hours to obtain on Mathematica, the convergence issue is still under investigation.

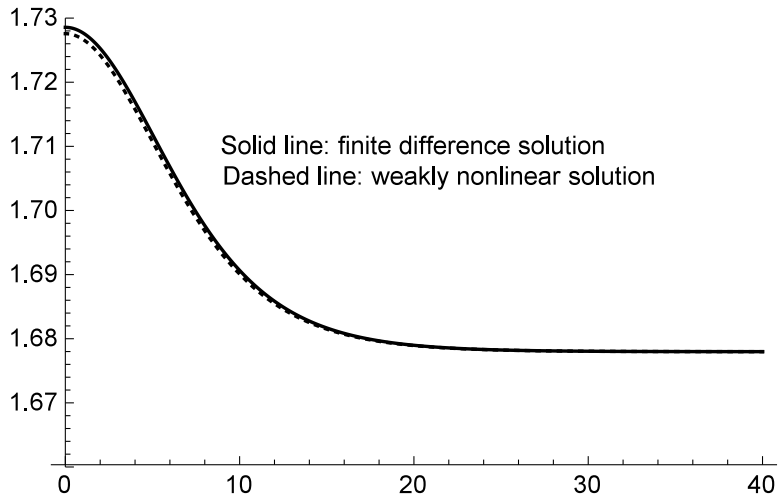

Figure 4.5.2: Profile of $r(Z)$ when $r_\infty = r_{cr} - 0.02$. The solutions corresponds to the Gent material model with $J_m = 30$ and $c = 0.001$, $r_{cr} = 1.69798$, $z_\infty = 1.1$, $L = 40$ and $n = 460$.

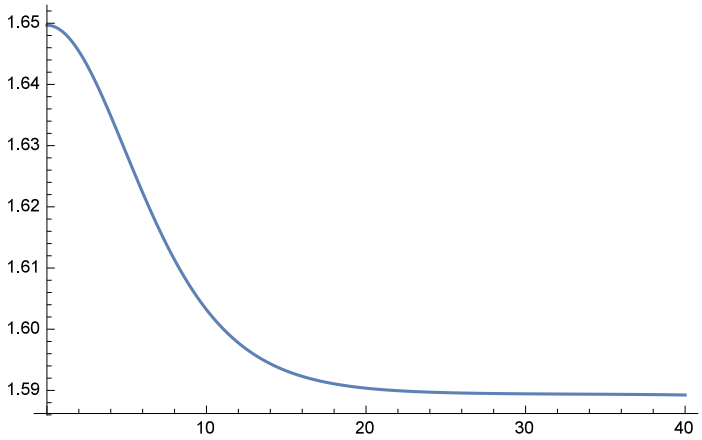

Figure 4.5.3: Profile of $r(Z)$ when $r_\infty = 1.58944$. The solutions corresponds to the Gent material model with $J_m = 30$ and $c = 0.001$, $z_\infty = 1.1$, $L = 40$ and $n = 460$.

4.6 Pressure-Volume Curve

We now show that the turning point of the uniform inflation pressure-volume curve corresponds to the bifurcation point for the case of a closed end tube (fixed axial force). To show this, we first define a volume measure v,

$$v = r_\infty^2 z_\infty, \tag{4.6.1}$$

which for uniform inflation is the volume change per unit volume in the reference configuration. Closed end condition is given by (4.2.46), that is

$$2z_\infty w_2(r_\infty, z_\infty) = r_\infty w_1(r_\infty, z_\infty) + 2c\, r_\infty(r_\infty - 1). \tag{4.6.2}$$

On differentiating (4.6.2) with respect to r_∞, viewing z_∞ as a function of r_∞, we obtain

$$\frac{dz_\infty}{dr_\infty} = \frac{z_\infty(2c - w_1^{(\infty)} - 4c\, r_\infty - w_{11}^{(\infty)} r_\infty + 2w_{12}^{(\infty)} z_\infty)}{-2cr_\infty + w_1^{(\infty)} r_\infty + 2c\, r_\infty^2 - w_{12}^{(\infty)} r_\infty z_\infty + 2w_{22}^{(\infty)} r_\infty^2}. \tag{4.6.3}$$

Differentiating the pressure given by

$$P = \frac{w_1^{(\infty)}}{r_\infty z_\infty} + \frac{2c(r_\infty - 1)}{r_\infty z_\infty}, \tag{4.6.4}$$

and (4.6.1) with respect to r_∞ yields

$$\frac{dv}{dr_\infty} = 2r_\infty z_\infty - r_\infty^2 \frac{z_\infty(2c - w_1^{(\infty)} - 4c\, r_\infty - w_{11}^{(\infty)} r_\infty + 2w_{12}^{(\infty)} z_\infty)}{-2cr_\infty + w_1^{(\infty)} r_\infty + 2c\, r_\infty^2 - w_{12}^{(\infty)} r_\infty z_\infty + 2w_{22}^{(\infty)} r_\infty^2}, \tag{4.6.5}$$

$$\begin{aligned}\frac{dP}{dr_\infty} &= \frac{-2(4c^2 r_\infty^3 + (-2c + w_1^{(\infty)}) w_{22}^{(\infty)} z_\infty^2 - 4cr_\infty^2(2c - w_1^{(\infty)} + w_{12}^{(\infty)} z_\infty)}{z_\infty r_\infty^2(2cr_\infty^2 + 2w_{22}^{(\infty)} z_\infty^2 + r_\infty(-2c + w_1^{(\infty)} - w_{12}^{(\infty)} z_\infty))}. \\ &+ \frac{r_\infty((-2c + w_1^{(\infty)})^2 + (4cw_{12}^{(\infty)} - 2w_1^{(\infty)} w_{12}^{(\infty)}) z_\infty + ((w_{12}^{(\infty)})^2 - w_{11}^{(\infty)} w_{22}^{(\infty)}) z_\infty^2)}{z_\infty r_\infty^2(2cr_\infty^2 + 2w_{22}^{(\infty)} z_\infty^2 + r_\infty(-2c + w_1^{(\infty)} - w_{12}^{(\infty)} z_\infty))}.\end{aligned} \tag{4.6.6}$$

It can then be shown that, using the chain rule,

$$\frac{dP}{dv} = \frac{-2(4c^2r_\infty^3 + (-2c + w_1^{(\infty)})w_{22}^{(\infty)}z_\infty^2 - 4cr_\infty^2(2c - w_1^{(\infty)}))}{r_\infty^3 z_\infty^2((8c + w_{11}^{(\infty)})r_\infty^2 + 4w_{22}^{(\infty)}z_\infty^2 + r_\infty(-6c + 3w_1^{(\infty)} - 4w_{12}^{(\infty)}z_\infty))}$$

$$+\frac{+w_{12}^{(\infty)}z_\infty)r_\infty((-2c + w_1^{(\infty)})^2}{r_\infty^3 z_\infty^2((8c + w_{11}^{(\infty)})r_\infty^2 + 4w_{22}^{(\infty)}z_\infty^2 + r_\infty(-6c + 3w_1^{(\infty)} - 4w_{12}^{(\infty)}z_\infty))}$$

$$+\frac{+(4cw_{12}^{(\infty)} - 2w_1^{(\infty)}w_{12}^{(\infty)})z_\infty + ((w_{12}^{(\infty)})^2 - w_{11}^{(\infty)}w_{22}^{(\infty)})z_\infty^2)}{r_\infty^3 z_\infty^2((8c + w_{11}^{(\infty)})r_\infty^2 + 4w_{22}^{(\infty)}z_\infty^2 + r_\infty(-6c + 3w_1^{(\infty)} - 4w_{12}^{(\infty)}z_\infty))}. \quad (4.6.7)$$

Alternatively

$$\frac{1}{2}\frac{dP}{dv}(r_\infty^3 z_\infty^2(8c + w_{11}^{(\infty)})r_\infty^2 + 4w_{22}^{(\infty)}z_\infty^2 + r_\infty(-6c + 3w_1^{(\infty)} - 4w_{12}^{(\infty)}z_\infty)) =$$

$$-(4c^2r_\infty^3 + (-2c + w_1^{(\infty)})w_{22}^{(\infty)}z_\infty^2 - 4cr_\infty^2(2c - w_1^{(\infty)} + w_{12}^{(\infty)}z_\infty)$$

$$+r_\infty((-2c + w_1^{(\infty)})^2 + (4cw_{12}^{(\infty)} - 2w_1^{(\infty)}w_{12}^{(\infty)})z_\infty + ((w_{12}^{(\infty)})^2 - w_{11}^{(\infty)}w_{22}^{(\infty)})z_\infty^2). \quad (4.6.8)$$

In view of the expression (4.4.5), this may be written as

$$\frac{1}{2}\frac{dP}{dv}(r_\infty^3 z_\infty^2(8c + w_{11}^{(\infty)})r_\infty^2 + 4w_{22}^{(\infty)}z_\infty^2 + r_\infty(-6c + 3w_1^{(\infty)} - 4w_{12}^{(\infty)}z_\infty))$$

$$= \omega(r_\infty)w_{22}^{(\infty)}r_\infty(w_1^{(\infty)} + 2c(-1 + r_\infty) - w_{12}^{(\infty)})z_\infty). \quad (4.6.9)$$

Therefore, the bifurcation points for a closed tube occur at the turning points of the pressure-volume curve which can be seen in Figure 4.6.1. That is

$$\frac{\partial P}{\partial v} \propto \omega(r_\infty, z_\infty). \quad (4.6.10)$$

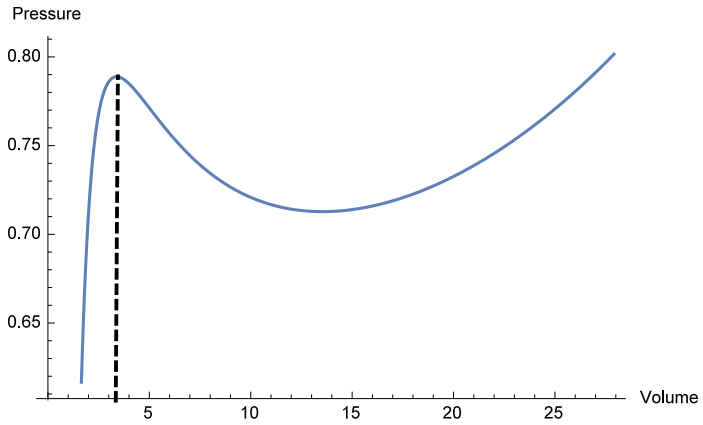

Figure 4.6.1: Pressure-volume curve when the axial force is zero and $c = 0.01$. The solid line represents the pressure volume curve and dashed line represents the volume at critical values of r_∞ and z_∞.

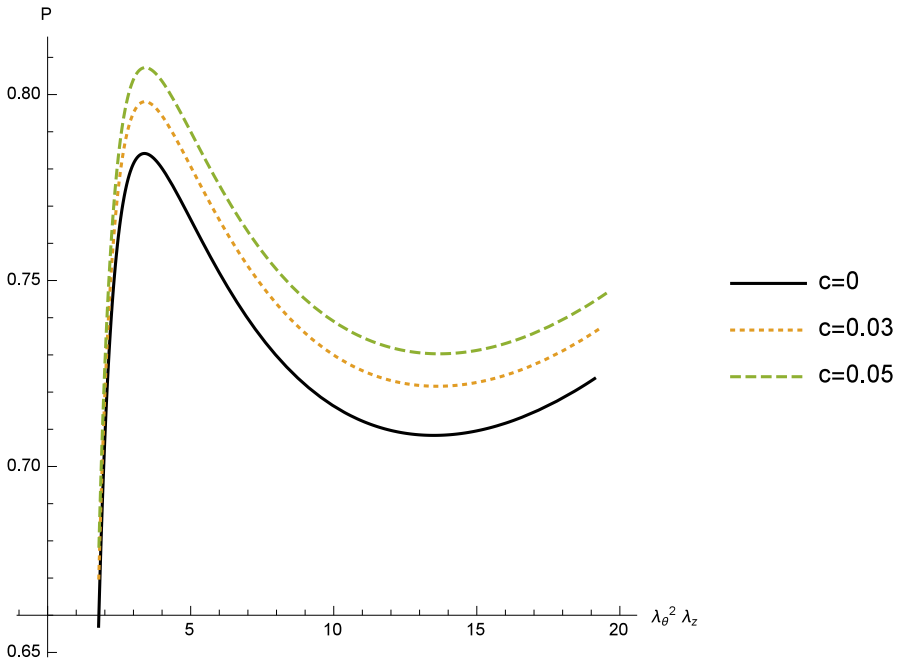

Figure 4.6.2: Variation of pressure with respect to the volume of a tube with fixed axial force for the Ogden material model. Different values of c are considered.

We observe that in Figure 4.6.2 the critical pressure would increase with respect to increase in c. Therefore we can conclude that the critical pressure increases when we incorporate bending stiffness in the model. For the case of an open ends with fixed z_∞, we may differentiate P with respect to r_∞, obtaining

$$\frac{dP}{dr_\infty} = \frac{r_\infty w_{11}^{(\infty)} - w_1^{(\infty)} + 2c}{r_\infty^2}. \tag{4.6.11}$$

Then the bifurcation condition $\omega(r_\infty) = 0$ may be written as

$$(2c(-1 + r_\infty) + w_1^{(\infty)} - z_\infty w_{12}^{(\infty)})^2 - z_\infty^2 r_\infty^2 w_{22}^{(\infty)} \frac{dP}{dr_\infty} = 0. \tag{4.6.12}$$

Therefore if a bifurcation point exists, it must come before the maximum of the pressure volume curve.

4.6.1 Kink solution

From the qualitative analysis of dynamical systems, we know that a smooth solitary wave solution of a system of ordinary differential equations corresponds to a smooth homoclinic orbit (Pearce and Fu 2010). Similarly, a smooth heteroclinic orbit corresponds to a kink wave solution of the ordinary differential equations. According to the above analysis, in this section, we consider the existence and the explicit expressions of the kink solution for the system derived in Section 4.3. When the cylindrical tube is inflated by an internal pressure, a localized bulge forms and with continued inflation, the radius of the bulge will increase monotonically until it reaches a maximum. At this point, the bulge flattens out at its centre and starts to propagate in both directions. At this stage, the bulge can be viewed as two kink solutions stitched together and each

consists of two uniform states, (r_∞, z_∞) and (r_0, z_0') respectively, joined by a smooth transition region.

When the solution flattens out at $Z = 0$, we have $r_0' = 0$ and $r_0'' = 0$, see Pearce & Fu (2010). By the definition of $\kappa_{22} = (r'z'' - z'r'')/\lambda_2$, it is clear that $\kappa_{22}(0) = 0$. Subject to these requirements the equilibrium equations (4.2.49) and (4.2.50) become

$$w_2(r_0, z_0') - w^{(\infty)} - \frac{1}{2}\left(\frac{w_1^{(\infty)}}{r_\infty z_\infty} + \frac{2c(r_\infty - 1)}{r_\infty z_\infty}\right)(r_0^2 - r_\infty^2) = 0, \tag{4.6.13}$$

$$w(r_0, z_0') - w^{(\infty)} - z_0' w_2(r_0, z_0') + z_\infty w_2^{(\infty)} + c(r_0 - 1)^2 - c(r_\infty - 1)^2 = 0. \tag{4.6.14}$$

Differentiating (4.6.13) and (4.6.14) with respect to r_∞, viewing z_0' and r_0 as functions of r_∞ we obtain,

$$\begin{aligned}(w_1(r_0, z_0') - z_0' w_{12}(r_0, z_0') + 2c(r_0 - 1))\frac{\partial r_0}{\partial r_\infty} - z_0' w_{22}(r_0, z_0')\frac{\partial z_0'}{\partial r_\infty}\\ -w_1^{(\infty)} + z_\infty w_{12}^{(\infty)} + z_\infty w_{22}^{(\infty)}\frac{\partial z_\infty}{\partial r_\infty} + 2c(r_\infty - 1) = 0,\end{aligned} \tag{4.6.15}$$

$$\begin{aligned}(w_{12}(r_0, z_0') - Pr_0)\frac{\partial r_0}{\partial r_\infty} + w_{22}(r_0, z_0')\frac{\partial z_0'}{\partial r_\infty} +\\ Pr_\infty - w_{12}^{(\infty)} - w_{22}^{(\infty)}\frac{\partial z_\infty}{\partial r_\infty} - \frac{(r_0^2 - r_\infty^2)}{2}\frac{\partial P}{\partial r_\infty} = 0.\end{aligned} \tag{4.6.16}$$

At the turning point, $\frac{\partial r_0}{\partial r_\infty} \to \infty$. By taking this limit in (4.6.15) and (4.6.16), and using the chain rule we obtain

$$w_1(r_0, z_0') - z_0' w_{12}(r_0, z_0') - z_0' w_{22}(r_0, z_0')\frac{\partial z_0'}{\partial r_\infty} + 2c(r_0 - 1) = 0, \tag{4.6.17}$$

$$w_{12}(r_0, z_0') - Pr_0 + w_{22}(r_0, z_0')\frac{\partial z_0'}{\partial r_\infty} = 0. \tag{4.6.18}$$

On eliminating $\dfrac{\partial z_0'}{\partial r_\infty}$ from the two equations above, we obtain

$$w_1(r_0, z_0') - \frac{r_0 z_0'}{r_\infty z_\infty}(\hat{w}_1^{(\infty)} + 2c(r_\infty - 1)) + 2c(r_0 - 1) = 0. \tag{4.6.19}$$

We may now solve (4.6.19) with (4.6.13), (4.6.14) and a specified z_∞ for the three unknowns $r_\infty,\ z_0'$ and r_0 for the tube with open ends to find the kink amplitude. For the case of closed end tubes, (4.6.19) can be solved with (4.6.13), (4.6.14) and the closed end condition (4.6.2) for the four unknowns $r_0,\ z_0',\ r_\infty$ and z_∞.

We now show that the two uniform states (r_∞, z_∞) and (r_0, z_0') satisfy the Maxwell equal-area rule as in other related localization problems (Ericksen 1975, Chater & Hutchinson 1984). The geometric representation of Maxwell's equal area rule is that the value of the pressure $P = P_k$ line cuts the pressure volume curve in such a way that the magnitude of the areas between the line and the curve above and below the line are equal. This rule may be represented analytically as

$$\int_{v_1}^{v_2} P(v)\, dv = P_k(v_2 - v_1), \tag{4.6.20}$$

where v_1 and v_2, given by

$$v_1 = r_\infty^2 z_\infty, \quad v_2 = r_0^2 z_0', \tag{4.6.21}$$

are the two volumes corresponding to the two uniform solutions (r_∞, z_∞) and (r_0, z_0') of the kink solutions respectively. Figure 4.6.3 shows the pressure volume curve for a typical closed ends tube modelled by the Gent strain-energy function with $J_m = 30$, along with the line P_k which satisfies the equal area rule. This pressure volume curve is typical for rubber-like materials as discussed in Carroll (1987) and Gent (2005). We now demonstrate that the equal area condition (4.6.20) gives the same condition for the kinked solution as (4.6.19). Define the strain-energy function depending on the volume as

$$\hat{w}(v) = w(r_\infty(v), z_\infty(v)) + c(r_\infty(v) - 1)^2. \tag{4.6.22}$$

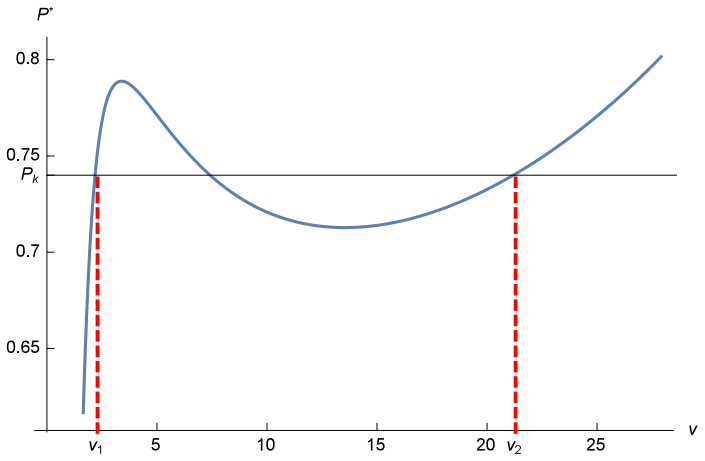

Figure 4.6.3: Pressure-volume curve for a closed end tube.

It can be shown using the chain rule

$$\frac{d\hat{w}}{dv} = \frac{\partial \hat{w}}{\partial r_\infty}\frac{dr_\infty}{dv} + \frac{\partial \hat{w}}{\partial z_\infty}\frac{dz_\infty}{dv} + 2c(r_\infty - 1)\frac{dr_\infty}{dv}, \tag{4.6.23}$$

and

$$v = r_\infty^2 z_\infty$$
$$\frac{d\hat{w}}{dv} = \frac{(\hat{w}_1^{(\infty)} + 2c(r_\infty - 1))}{2r_\infty z_\infty} = \frac{1}{2}P. \tag{4.6.24}$$

Using the Maxwell area rule (4.6.20), (4.6.24) becomes

$$P_k(v_2 - v_1) = 2(\hat{w}(v_2) - \hat{w}(v_1)), \tag{4.6.25}$$

where

$$P_k = P|_{v=v_1} = \frac{\hat{w}_1(r_0, z_0') + 2c(r_0 - 1)}{r_0 z_0'} = P|_{v=v_2} = \frac{\hat{w}_1^{(\infty)} + 2c(r_\infty - 1)}{r_\infty z_\infty}. \tag{4.6.26}$$

Substituting (4.6.21) and $(4.6.26)_2$ into (4.6.25) along with equilibrium equation (4.2.32)

we obtain

$$\left(\frac{w_1^{(\infty)}}{r_\infty z_\infty}+\frac{2c(r_\infty-1)}{r_\infty z_\infty}\right)(r_0^2 z_0'-r_\infty^2 z_\infty)=2(-c(r_0-1)^2+c(r_\infty-1)^2$$
$$+z_0' w_2(r_0,z_0')-z_\infty {w_2}^{(\infty)}). \tag{4.6.27}$$

We can then use the other equilibrium equation (4.2.29) to express w_2 in terms of w_1, which then reduces (4.6.27) to the kink solution (4.6.19).

4.6.2 Conclusion

In this chapter a non-linear analysis was conducted for thin-walled tubes, defining the strain-energy function as a function of the principal stretches as well as the bending stiffness. Euler-Lagrangian equations (2.3.6) were used to derive two integrals of the equilibrium equations. Dynamical system (4.3.27-4.3.30) and (4.3.32) was derived using the Steigmann & Ogden (1997) theory. Using weakly non-linear analysis, bifurcation condition $\omega(r_\infty)=0$ was derived for any strain-energy function and it was shown that $\omega'(r_{cr})$ is always negative at the first bifurcation point which correspondents to the bulging solution. A shooting method and a finite difference scheme were formulated that can be used to determine fully non-linear bulging solutions.

Our mathematical model proposed in (4.2.18) can be used to predict the formation of aneurysms in arteries since an artery can also be modelled as a cylindrical tube subject to an axial pre-stretch and an internal pressure. We calculated the bifurcation pressure for the membrane and the cylindrical shell given in (3.1.15) and (4.2.45) respectively for some specific values of z_∞. We showed that pressure takes the value 0.757337 for the membrane when $z_\infty=1.1$ and it is 0.764476 and 0.829018 for the thin walled tube

for $c = 0.01$ and 0.1 respectively. These values were calculated for the Ogden material. For the Gent material with $J_m = 30$, pressure takes the values 0.851803, 0.858847 and 0.921345 when $c = 0, 0.01$ and 0.1 respectively. We can show that this is true for any strain-energy function. We can see from this fact that there is a significant increase in bifurcation pressure when bending stiffness is taken into account. Therefore wall thickness may become a key parameter for the bifurcation pressure in uniform inflation. Our present study may be relevant to understanding the formation process of arterial aneurysms since they are caused by weakening or thinning in arterial walls, which makes localised bulging possible.

5 Analysis of Localised Bulging Based on the 3D Theory of Non-Linear Elasticity

5.1 Introduction

In this chapter, we study localized bulging with the aid of the exact theory of non-linear elasticity. When the tube is of arbitrary thickness, any non-linear analysis would become extremely difficult, if not intractable, but fortunately, the dynamical systems theory's view provides us with a means to determine the bifurcation point analytically. To sketch the idea, suppose that we consider an axially symmetric perturbation superimposed on a uniformly inflated cylindrical tube. The incremental boundary value problem is readily available from the classical paper by Haughton & Ogden (1979b). Suppose now further that the perturbation depends on the axial coordinate z through $\mathrm{e}^{\alpha z}$. The constant α can be determined by solving a reduced eigenvalue problem. We observe that part of Haughton & Ogden (1979b)'s numerical computation was concerned with solutions of this eigenvalue problem when α is replaced by $-\mathrm{i}\alpha$ where $\mathrm{i} = \sqrt{-1}$. It can be shown that the distribution of the eigenvalues of α is symmetric with respect to both axes in the complex α-plane (since in the eigenvalue problem α appears through α^2 and all the coefficient functions are real). Suppose that we characterize the uniform inflation using the azimuthal stretch λ_a on the inner surface. When λ_a is increased only slightly above 1, it can be shown that there are five real eigenvalues of α of the form $0, \pm\alpha_1, \pm\alpha_2$ such that $0 < \alpha_1 < \alpha_2$; see Figure 5.1.1. As λ_a increases,

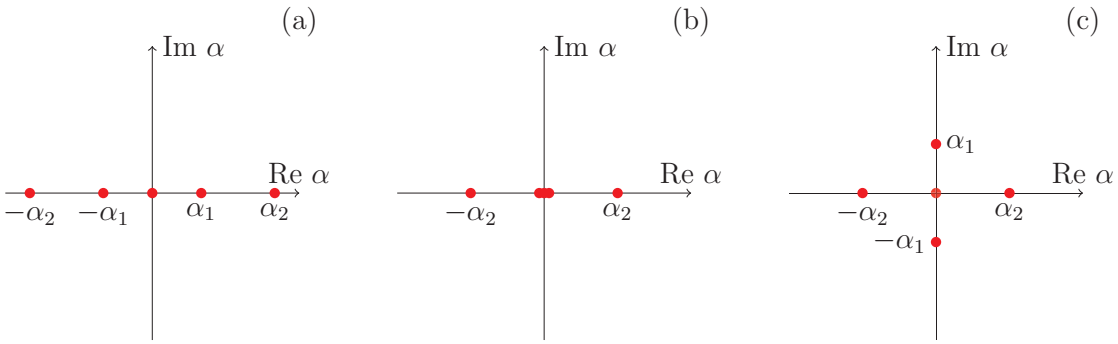

Figure 5.1.1: Movement of the five eigenvalues that are initially real as the azimuthal stretch increases. The three plots (a), (b) and (c) correspond to when the azimuthal stretch is smaller than, equal to, or greater than its critical value, respectively. Localized bulging occurs when α_1 vanishes, making zero a triple eigenvalue.

the two real eigenvalues $\pm\alpha_1$ will move towards the origin. When they eventually coalesce at the origin, zero becomes a triple eigenvalue which signals the initiation of a bifurcation into a localized solitary-wave type solution; see, for instance, Kirchgassner (1982) and Mielke (1991). When λ_a is increased further, the two eigenvalues $\pm\alpha_1$ would move onto the imaginary axis. The exponential $\mathrm{e}^{\alpha z}$ then becomes sinusoidal, and this is the situation addressed by Haughton & Ogden (1979b). It is clear from this deduction that localized bulging must necessarily occur before any bifurcation into periodic patterns. This fact is consistent with all experimental observations.

It will be shown that with the internal pressure P and resultant axial force F viewed as functions of the azimuthal stretch on the inner surface and the axial stretch, the bifurcation condition for the initiation of a localized bulge is that the Jacobian of the vector function (P, F) should vanish. The bifurcation condition is valid for all loading

conditions, and in the special case of fixed resultant axial force it gives the expected result that the initiation pressure for localized bulging is precisely the maximum pressure in uniform inflation. It is shown that even if localized bulging cannot take place when the axial force is fixed, it is still possible if the axial stretch is fixed instead. The explicit bifurcation condition also provides a means to quantify precisely the effect of bending stiffness on the initiation pressure. It is shown that the (approximate) membrane theory gives good predictions for the initiation pressure, with a relative error less than 5%, for thickness/radius ratios up to 0.67. A two-term asymptotic bifurcation condition for localized bulging that incorporates the effect of bending stiffness is proposed, and is shown to be capable of giving extremely accurate predictions for the initiation pressure for thickness/radius ratios up to as large as 1.2.

A paper based on this chapter has been accepted to *Journal of the Mechanics and Physics of Solids* (Fu et al 2016).

5.2 Problem formulation

Our point of departure is the paper by Haughton & Ogden (1979b). We first recall some results from this paper which are necessary for our subsequent analysis.

Consider a hyperelastic cylindrical tube that initially has inner radius A and outer radius B. When it is uniformly stretched in the axial direction and inflated by an internal pressure P, the inner and outer radii become a and b, respectively. In terms

of cylindrical polar coordinates, the deformation is given by

$$r^2 = \lambda_z^{-1}(R^2 - A^2) + a^2, \quad \theta = \Theta, \quad z = \lambda_z Z, \tag{5.2.1}$$

where (R, Θ, Z) and (r, θ, z) are the coordinates in the undeformed and deformed configurations, respectively, and λ_z is the stretch in the axial direction which is assumed to be a constant throughout this paper.

With incompressibility taken into account, the three principal stretches are given by

$$\lambda_1 \equiv \lambda = \frac{r}{R}, \quad \lambda_2 = \lambda_z, \quad \lambda_3 = 1/(\lambda_1\lambda_2),$$

where the first equation defines λ as a function of r (with R eliminated using $(5.2.1)_1$). Following Haughton & Ogden (1979b), we have identified the indices $1, 2, 3$ with the θ-, z-, and r-directions, respectively.

We assume that the constitutive behavior of the tube is described by a strain-energy function $W(\lambda_1, \lambda_2, \lambda_3)$. In terms of the reduced strain-energy function w defined by

$$w(\lambda, \lambda_z) = W(\lambda, \lambda_z, \lambda^{-1}\lambda_z^{-1}), \tag{5.2.2}$$

the internal pressure is given by

$$P = \int_{\lambda_b}^{\lambda_a} \frac{w_1}{\lambda^2\lambda_z - 1} d\lambda, \tag{5.2.3}$$

where $w_1 = \partial w/\partial\lambda$, and the two limits λ_a and λ_b are defined by

$$\lambda_a = \frac{a}{A}, \quad \lambda_b = \frac{b}{B},$$

and are related to each other by

$$\lambda_a^2\lambda_z - 1 = \frac{B^2}{A^2}(\lambda_b^2\lambda_z - 1). \tag{5.2.4}$$

The three principal stresses are

$$\sigma_{ii} = \sigma_i - \bar{p}, \quad \sigma_i = \lambda_i \frac{\partial W}{\partial \lambda_i}, \text{ no summation on } i, \tag{5.2.5}$$

where $\bar{p}$ is the pressure associated with the constraint of incompressibility.

The resultant axial force at any cross section is independent of Z and is given by

$$F(\lambda_a, \lambda_z) \equiv 2\pi \int_a^b \sigma_{22} r dr - \pi a^2 P = \pi A^2 (\lambda_a^2 \lambda_z - 1) \int_{\lambda_b}^{\lambda_a} \frac{2\lambda_z w_2 - \lambda w_1}{(\lambda^2 \lambda_z - 1)^2} \lambda d\lambda, \tag{5.2.6}$$

where $w_2 = \partial w / \partial \lambda_z$ and we have shown F explicitly as a function of λ_a and λ_z (the λ_b in the equation is eliminated using (5.2.4)).

The volume ratio v, that is the internal volume in the deformed configuration divided by the internal volume in the undeformed configuration, is given by $v = \lambda_z \lambda_a^2$. This quantity is a function of λ_a only since λ_z is either fixed or eliminated with the use of $F =$ constant. Thus, once the strain-energy function is specified, we may easily plot the dependence of P on v. In particular, when $F = C$ applies, a pressure maximum in such a plot would correspond to

$$\left. \frac{dP}{d\lambda_a} \right|_{\text{fixed} F} = \frac{\partial P}{\partial \lambda_a} + \frac{\partial P}{\partial \lambda_z} \frac{d\lambda_z}{d\lambda_a} = 0. \tag{5.2.7}$$

The ordinary derivative in the above expression can be eliminated by solving

$$\frac{\partial F}{\partial \lambda_a} + \frac{\partial F}{\partial \lambda_z} \frac{d\lambda_z}{d\lambda_a} = 0. \tag{5.2.8}$$

It thus follows that at a pressure maximum we have

$$\frac{\partial P}{\partial \lambda_a} - \frac{\partial P}{\partial \lambda_z} \frac{\partial F}{\partial \lambda_a} \left(\frac{\partial F}{\partial \lambda_z} \right)^{-1} = 0. \tag{5.2.9}$$

This equation can then be solved in conjunction with $F(\lambda_a, \lambda_z) = C$ to find the values of λ_a and λ_z at which a pressure maximum in uniform inflation is attained. When these

two equations do not have a solution, the pressure will be a monotonic function of the internal volume. One practical way to determine whether a pressure maximum exists or not is to draw the contour plots of the two equations together in the (λ_a, λ_z)-plane. If, for instance, there are two intersections, the pressure has both a maximum and a minimum. The existence of a pressure maximum in uniform inflation is known as a *limit-point* instability. For most commonly used materials models, equation (5.2.9) together with $F = 0$ has two roots, corresponding to the fact that the pressure versus volume curve has an N shape with a maximum and a minimum. Notable exceptions are the neo-Hookean and Mooney-Rivlin material models.

In a similar manner, we may consider the variation of F with respect to λ_z when P is fixed and the latter fact is used to express λ_a in terms of λ_z. In this case the F will reach a maximum when

$$\frac{\partial F}{\partial \lambda_z} - \frac{\partial F}{\partial \lambda_a}\frac{\partial P}{\partial \lambda_z}\left(\frac{\partial P}{\partial \lambda_a}\right)^{-1} = 0. \tag{5.2.10}$$

We remark that in writing down (5.2.9) and (5.2.10) we have implicitly assumed that $\partial F/\partial \lambda_z$ and $\partial P/\partial \lambda_a$ are non-zero. It can be shown that in the undeformed state when $\lambda_a = \lambda_z = 1$ this is indeed the case since we then have

$$\frac{\partial F}{\partial \lambda_z} = 3\mu\pi(1 - A^2), \quad \frac{\partial P}{\partial \lambda_a} = 2\mu\pi(1 - A^2),$$

where μ is the ground state shear modulus. It seems that none of the well-known constitutive assumptions guarantee that this is the case for all deformations, but it is known that under the membrane assumption $\partial P/\partial \lambda_a$ is at least positive before the condition for localized bulging is satisfied (Fu & Ilichev 2015). In the present 3D setting, for each material model that we use the above assumption is checked numerically by inspecting the contour plots of $\partial F/\partial \lambda_z = 0$ and $\partial P/\partial \lambda_a = 0$ in the (λ_a, λ_z)-plane.

We have verified that this assumption is always satisfied at least before the bifurcation condition for localized bulging is satisfied.

It can be seen that both (5.2.9) and (5.2.10) imply the following equation:

$$J(P,F) \equiv \frac{\partial P}{\partial \lambda_a}\frac{\partial F}{\partial \lambda_z} - \frac{\partial P}{\partial \lambda_z}\frac{\partial F}{\partial \lambda_a} = 0, \tag{5.2.11}$$

which states that the Jacobian of the vector function (P, F) vanishes. It will be shown later that this is in fact the bifurcation condition for the initiation of a localized bulge.

To study the bifurcation of the primary deformation determined above, we consider an axially symmetric perturbation of the form

$$\dot{\boldsymbol{r}} = u(r,z)\boldsymbol{e}_r + v(r,z)\boldsymbol{e}_z,$$

where $\dot{\boldsymbol{r}}$ denotes the perturbation of the position vector $\boldsymbol{r}$, and $\boldsymbol{e}_r$ and $\boldsymbol{e}_r$ are base vectors in the r- and θ-directions, respectively. The linearized incremental equilibrium equations that are not satisfied automatically are

$$\chi_{3j,j} + \frac{1}{r}(\chi_{33} - \chi_{11}) = 0, \quad \chi_{2j,j} + \frac{1}{r}\chi_{23} = 0, \tag{5.2.12}$$

where the incremental stress tensor (χ_{ij}) is given by

$$\chi_{ij} = \mathcal{B}_{jilk}\eta_{kl} + \bar{p}\eta_{ji} - p^*\delta_{ji}. \tag{5.2.13}$$

In the last equation, p^* is the incremental pressure field, the $\boldsymbol{\eta}$, with components η_{kl}, is the gradient of incremental displacement and is given by

$$\boldsymbol{\eta} = \begin{bmatrix} \frac{u}{r} & 0 & 0 \\ 0 & v_z & v_r \\ 0 & u_z & u_r \end{bmatrix}, \tag{5.2.14}$$

and the $\mathcal{B}_{jilk}$'s are the instantaneous elastic moduli given by

$$\mathcal{B}_{iijj} = \mathcal{B}_{jjii} = \lambda_i \lambda_j W_{ij}, \quad \text{no summation on } i \text{ or } j,$$

$$\mathcal{B}_{ijij} = \frac{\lambda_i W_i - \lambda_j W_j}{\lambda_i^2 - \lambda_j^2}\lambda_i^2, \quad \lambda_i \neq \lambda_j, \quad \text{no summation on } i \text{ or } j,$$

$$\mathcal{B}_{ijji} = \mathcal{B}_{ijij} - \lambda_i W_i, \quad i \neq j, \quad \text{no summation on } i \text{ or } j,$$

where $W_i = \partial W/\partial \lambda_i$, $W_{ij} = \partial^2 W/\partial \lambda_i \partial \lambda_j$ etc.

The incompressibility condition takes the form

$$\operatorname{tr} \boldsymbol{\eta} = u_r + v_z + \frac{u}{r} = 0, \tag{5.2.15}$$

and the incremental boundary conditions are

$$(\boldsymbol{\chi n} - P\boldsymbol{\eta}^T \boldsymbol{n})\big|_{r=a} = 0, \quad \boldsymbol{\chi n}|_{r=b} = 0, \tag{5.2.16}$$

which reflect the fact that the internal boundary $r = a$ is subjected to a *hydrostatic* pressure P whereas the outer boundary $r = b$ is traction-free.

Written out explicitly, the equilibrium equations (5.2.12) take the form

$$p_r^* = (r\mathcal{B}'_{1133} - \mathcal{B}_{1111})\frac{u}{r^2} + (r\mathcal{B}'_{3333} + r\bar{p}' + \mathcal{B}_{3333})\frac{u_r}{r} + \mathcal{B}_{3333}u_{rr} + \mathcal{B}_{2323}u_{zz}$$
$$+(r\mathcal{B}'_{2233} + \mathcal{B}_{2233} - \mathcal{B}_{1122})\frac{v_z}{r} + (\mathcal{B}_{2233} + \mathcal{B}_{3223})v_{rz}, \tag{5.2.17}$$

$$p_z^* = \mathcal{B}_{3232}v_{rr} + (r\mathcal{B}'_{3232} + \mathcal{B}_{3232})\frac{v_r}{r} + \mathcal{B}_{2222}v_{zz} + (\mathcal{B}_{2233} + \mathcal{B}_{3223})u_{rz}$$
$$+(r\mathcal{B}'_{3223} + r\bar{p}' + \mathcal{B}_{3223} + \mathcal{B}_{1122})\frac{u_z}{r}, \tag{5.2.18}$$

and the associated boundary conditions (5.2.16) become

$$v_r + u_z = 0, \quad \text{on } \ r = a, b, \tag{5.2.19}$$

$$(\mathcal{B}_{3333} - \mathcal{B}_{2233} + \lambda_3 W_3)u_r + (\mathcal{B}_{1133} - \mathcal{B}_{2233})\frac{u}{r} - p^* = 0, \quad \text{on } \ r = a, b. \tag{5.2.20}$$

In the above equations, a subscript denotes partial differentiation with respect to the implied coordinate (e.g. $p^*_r = \partial p^*/\partial r$), and the primes denote d/dr.

For our illustrative calculations, we shall use three representative material models: the Ogden material model (Ogden 1972), the Gent material model (Gent 1996), and an arterial model, for which the strain-energy function is given, respectively, by

$$W = \mu \sum_{r=1}^{3} \mu^*_r (\lambda_1^{\alpha_r} + \lambda_2^{\alpha_r} + \lambda_3^{\alpha_r} - 3)/\alpha_r, \tag{5.2.21}$$

$$W = -\frac{\mu}{2} J_m \ln(1 - \frac{J_1}{J_m}), \quad J_1 = \lambda_1^2 + \lambda_2^2 + \lambda_3^2 - 3, \tag{5.2.22}$$

and

$$W = \frac{\mu}{2(1-k+k\alpha)} \left\{ (1-k)J_1 + k\mathrm{e}^{\alpha J_1} - k \right\}, \tag{5.2.23}$$

where μ is the shear modulus for infinitesimal deformations,

$$\alpha_1 = 1.3, \quad \alpha_2 = 5.0, \quad \alpha_3 = -2.0, \quad \mu^*_1 = 1.491, \quad \mu^*_2 = 0.003, \quad \mu^*_3 = -0.023,$$

and J_m, k, α are material constants. We shall take $J_m = 97.2$ which is typical for rubbers, and $k = 1/2, \alpha = 1/4$ which is a simple choice that gives us the desired behaviour that when the axial force is fixed the pressure does not have a maximum in uniform inflation. Without the first term $(1-k)J_1$ on the right hand side, equation (5.2.23) has been postulated by Delfino *et al* (1997) as a possible model for arteries. This first term is added to represent the contribution from the matrix material. Although both the Gent and Ogden models are believed to be excellent models for rubber materials, it will be shown that they give different predictions for localized bulging in the large stretches regime.

5.3 Numerical determination of the bifurcation condition

As outlined in the Introduction, we now look for a solution of the form

$$u = f(r)\mathrm{e}^{\alpha z}, \quad w = g(r)\mathrm{e}^{\alpha z}, \quad p^* = h(r)\mathrm{e}^{\alpha z}. \tag{5.3.1}$$

On substituting this into the incremental equations and boundary conditions, and then eliminating $g(r)$ and $h(r)$ in favor of $f(r)$, we find that $f(r)$ satisfies a single fourth-order ordinary differential equation and two boundary conditions, which are numbered in Haughton(1979b) as (53), (54), and (55), respectively. For our purpose, it is more convenient to rewrite them in matrix form as

$$\frac{d\boldsymbol{y}}{dr} = A(r,\alpha)\boldsymbol{y}, \quad a \le r \le b, \tag{5.3.2}$$

$$B(r,\alpha)\boldsymbol{y} = 0, \quad \text{on } \ r = a, b, \tag{5.3.3}$$

where $\boldsymbol{y} = [f, f', f'', f''']^T$, and the coefficient matrices A and B are given by

$$A = \begin{bmatrix} 0 & 1 & 0 & 0 \\ 0 & 0 & 1 & 0 \\ 0 & 0 & 0 & 1 \\ a_{41} & a_{42} & a_{43} & a_{44} \end{bmatrix}, \quad B = \begin{bmatrix} -1-\alpha^2 r^2 & r & r^2 & 0 \\ b_{21} & b_{22} & b_{23} & r^3\zeta(r) \end{bmatrix}, \tag{5.3.4}$$

with $\zeta(r) = \mathcal{B}_{3232}$, and

$$\begin{aligned}
r^4\zeta(r)a_{41} &= \alpha^2 r^2(\mathcal{B}_{1111} + \mathcal{B}_{2222}) - \alpha^2 r^3 \mathcal{B}'_{2222} - \alpha^4 r^4 \mathcal{B}_{2323} + \alpha^2 r^4(\mathcal{B}''_{3232} - \sigma''_{33}) \\
&\quad + \alpha^2 r^3 \mathcal{B}'_{3223} - 2\alpha^2 r^2 \mathcal{B}_{3223} + r^2 \mathcal{B}''_{3232} - 3r\mathcal{B}'_{3232} + 3\mathcal{B}_{3232}, \\
r^4\zeta(r)a_{42} &= 2\alpha^2 r^4 \mathcal{B}'_{3223} - \alpha^2 r^4 \mathcal{B}'_{2222} - \alpha^2 r^3 \mathcal{B}_{2222} + 2\alpha^2 r^3 \mathcal{B}_{3223} - r^3 \mathcal{B}''_{3232} \\
&\quad + 3r^2 \mathcal{B}'_{3232} - 3r\mathcal{B}_{3232} - \alpha^2 r^4 \mathcal{B}'_{3333} - \alpha^2 r^3 \mathcal{B}_{3333}, \\
r^4\zeta(r)a_{43} &= 2\alpha^2 r^4 \mathcal{B}_{3223} - \alpha^2 r^4 \mathcal{B}_{2222} - r^4 \mathcal{B}''_{3232} - 3r^3 \mathcal{B}'_{3232} + 3r^2 \mathcal{B}_{3232} - \alpha^2 r^4 \mathcal{B}_{3333}, \\
r^4\zeta(r)a_{44} &= -2r^4 \mathcal{B}'_{3232} - 2r^3 \mathcal{B}_{3232}, \\
b_{21} &= -\alpha^2 r^2 \left(-\mathcal{B}_{2222} + r\mathcal{B}'_{3232} + \mathcal{B}_{3232} - \sigma_3 - r\sigma'_{33}\right) - r\mathcal{B}'_{3232} + \mathcal{B}_{3232}, \\
b_{22} &= \alpha^2 r^3(\mathcal{B}_{2222} - \mathcal{B}_{3223} + \mathcal{B}_{3333} + \sigma_3) + r\left(r\mathcal{B}'_{3232} - \mathcal{B}_{3232}\right), \\
b_{23} &= r^2\left(r\mathcal{B}'_{3232} + 2\mathcal{B}_{3232}\right).
\end{aligned}$$

We have solved this eigenvalue problem using both the determinant and compound matrix methods. All of our numerical computations and algebraic manipulations are carried out with the aid of *Mathematica*. Using the determinantal method, we first solve $B(a, \alpha)\boldsymbol{y} = 0$ to find two linearly independent vectors, say $\boldsymbol{y}^{(1)}(a)$ and $\boldsymbol{y}^{(2)}(a)$. Next, we use each of these two vectors as an initial condition and integrate (5.3.2) from $r = a$ to $r = b$ to obtain two linearly independent solutions $\boldsymbol{y}^{(1)}(r)$ and $\boldsymbol{y}^{(2)}(r)$. Since a general solution can be written as a linear combination of these two solutions, satisfaction of the boundary condition at $r = b$ then requires that

$$E(\lambda_a, \alpha) \equiv \det\left\{B(b, \alpha)[\boldsymbol{y}^{(1)}(b), \boldsymbol{y}^{(2)}(b)]\right\} = 0, \tag{5.3.5}$$

where the first equation defines the function $E(\lambda_a, \alpha)$, and $[\boldsymbol{y}^{(1)}(b), \boldsymbol{y}^{(2)}(b)]$ denotes the 4×2 matrix formed by putting the two vectors $\boldsymbol{y}^{(1)}(b)$ and $\boldsymbol{y}^{(2)}(b)$ side by side. Eigenvalues of α are the roots of $E(\lambda_a, \alpha) = 0$. Thus, for each λ_a, we may we iterate

on α until the above error function is sufficiently small (typically smaller than 10^{-9}). In this way, the dependence of α on λ_a can be determined numerically. In the case of fixed axial force, the axial stretch λ_z is found to be a monotonically increasing function of λ_a, and can be taken as an independent parameter instead of λ_a.

As remarked in the Introduction, in general the eigen system (5.3.2) and (5.3.3) have both real and complex eigenvalues, but the distribution of eigenvalues of α in the complex α-plane must necessarily be symmetric with respect to both axes (since in the eigenvalue problem α appears through α^2 and all the coefficient functions are real). For our current purpose, however, we only need to examine the real eigenvalues. It is found that there are five real eigenvalues as discussed in the Introduction. In Figure 5.3.1, we have shown a typical plot showing the variation of α_1^2 and α_2^2 with respect to λ_z when $A = 0.9,\ F = 0$, and when the Gent material model is used. Note that λ_a is related to λ_z through $F = 0$ and is found to be an increasing function of λ_z. It is seen that α_1^2 is positive when $\lambda_z < 1.1889$ or $\lambda_z > 3.3313$. We have verified, with the aid of (5.2.9), that these two intervals correspond to the two ascending branches of the pressure versus volume curve in uniform inflation, and it is precisely when $\lambda_z = 1.1889$ or $\lambda_z = 3.3313$ that the pressure attains its maximum or minimum, respectively. Thus, in the case of fixed axial force, localized bulging occurs when pressure reaches its maximum in uniform inflation. This correspondence has previously been proved analytically when the tube is modeled as a membrane without any bending stiffness Fu & Ilichev (2015).

Figure 5.3.2 shows that the two outmost eigenvalues $\pm\alpha_2$ tend to infinity as the thickness tends to zero, which is consistent with the fact that when the membrane theory is used, there are only three real eigenvalues.

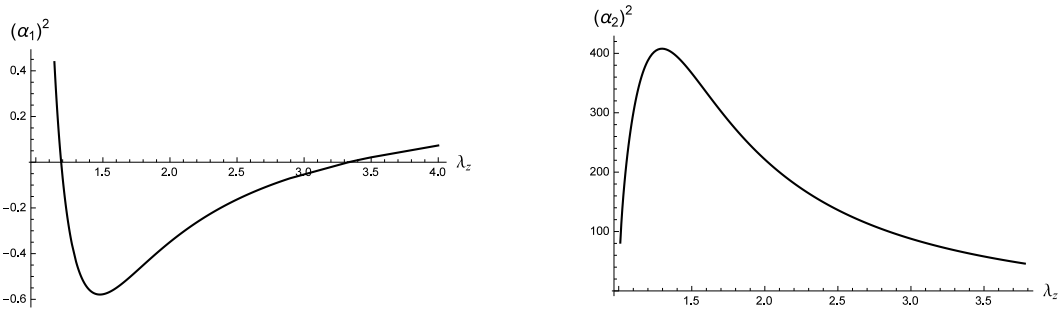

Figure 5.3.1: Variation of α_1^2 and α_2^2 with respect to λ_z when $A = 0.9,\ F = 0$, and when the Gent material model is used.

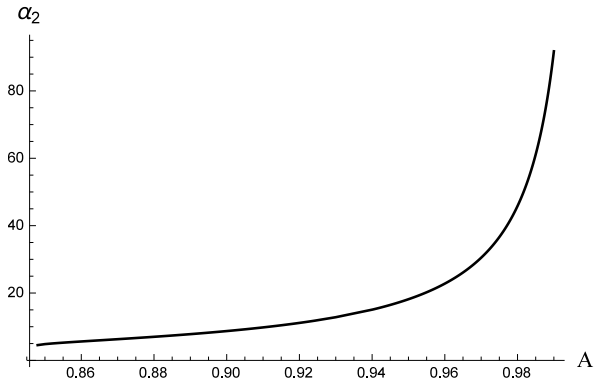

Figure 5.3.2: Variation of α_2 with respect to A showing the fact that it tends to infinity in the thin-wall limit.

5.4 An explicit expression for the bifurcation condition

The numerical procedure used in the previous section breaks down when α is exactly equal to zero. In this section, we derive an analytical expression for the condition under

which zero becomes a triple eigenvalue.

When α is small, we expand the coefficient matrix $A(r,\alpha)$ and $B(r,\alpha)$ in the form

$$A(r,\alpha) = A^{(0)}(r) + \alpha^2 A^{(1)}(r) + \cdots, \quad B(r,\alpha) = B^{(0)}(r) + \alpha^2 B^{(1)}(r) + \cdots, \quad (5.4.1)$$

and look for a solution of the form

$$\boldsymbol{y} = \boldsymbol{y}^{(0)} + \alpha^2 \boldsymbol{y}^{(1)} + \cdots, \quad f(r,\alpha) = f^{(0)}(r) + \alpha^2 f^{(1)}(r) + \cdots. \quad (5.4.2)$$

The explicit expressions for $A^{(0)}(r), B^{(0)}(r)$ etc are not written out here for the sake of brevity, and we recall that $f(r,\alpha)$ is the first element in $\boldsymbol{y}$. On substituting these expressions into (5.3.2) and (5.3.3), and equating the coefficients of α^0 and α^2 to zero, we obtain

$$\frac{d\boldsymbol{y}^{(0)}}{dr} = A^{(0)}(r)\boldsymbol{y}^{(0)}, \quad \frac{d\boldsymbol{y}^{(1)}}{dr} = A^{(0)}(r)\boldsymbol{y}^{(1)} + A^{(1)}(r)\boldsymbol{y}^{(0)}, \quad a \le r \le b, \quad (5.4.3)$$

$$B^{(0)}(r)\boldsymbol{y}^{(0)} = 0, \quad B^{(0)}(r)\boldsymbol{y}^{(1)} + B^{(1)}(r)\boldsymbol{y}^{(0)} = 0, \quad \text{on } r = a, b. \quad (5.4.4)$$

It can be deduced from $(5.4.3)_1$ that the fourth order differential equation satisfied by $f^{(0)}(r)$ can be rewritten in the compact form

$$\frac{d}{dr}\frac{1}{r}\frac{d}{dr}\left(r\zeta(r)\frac{d}{dr}\frac{1}{r}\frac{d}{dr}rf^{(0)}(r)\right) = 0, \quad (5.4.5)$$

so that a general solution can be deduced through straightforward integration and is given by

$$f^{(0)}(r) = c_1 r + c_2\frac{1}{r} + c_3\kappa_1(r) + c_4\kappa_2(r), \quad (5.4.6)$$

where c_1, c_2, c_3, c_4 are constants and

$$\kappa_1(r) = \frac{1}{r}\int_a^r t\int_a^t \frac{s}{\zeta(s)}dsdt, \quad \kappa_2(r) = \frac{1}{r}\int_a^r t\int_a^t \frac{1}{s\zeta(s)}dsdt, \quad (5.4.7)$$

recalling that the function $\zeta(r)$ is defined below (5.3.4). On substituting this solution into the leading-order boundary condition $(5.4.4)_1$, it is found that the coefficients c_3 and c_4 must necessarily vanish, but c_1 and c_2 are unrestricted. At the next order, the general solution is given by

$$f^{(1)}(r) = d_1 r + d_2 \frac{1}{r} + d_3\kappa_1(r) + d_4\kappa_2(r) + c_1\kappa_3(r) + c_2\kappa_4(r), \tag{5.4.8}$$

where d_1, d_2, d_3, d_4 are constants and the last two terms are particular integrals given by

$$\kappa_3(r) = \frac{1}{r}\int_a^r y \int_a^y \frac{1}{x\zeta(x)} \int_a^x t \int_a^t \omega_1(s) ds dt dx dy, \tag{5.4.9}$$

$$\kappa_4(r) = \frac{1}{r}\int_a^r y \int_a^y \frac{1}{x\zeta(x)} \int_a^x t \int_a^t \omega_2(s) ds dt dx dy, \tag{5.4.10}$$

with $\omega_1(s)$ and $\omega_1(s)$ defined by

$$\omega_1(r) = \mathcal{B}'_{1122} - \mathcal{B}'_{1133} + 3\mathcal{B}'_{2233} - 2\mathcal{B}'_{2222} - \mathcal{B}'_{3333} + 3\mathcal{B}'_{3223} + r(\mathcal{B}''_{3223} + \bar{p}'')$$

$$+\frac{1}{r}(\mathcal{B}_{1111} - 2\mathcal{B}_{1122} + 2\mathcal{B}_{2233} - \mathcal{B}_{3333})$$

$$\omega_2(r) = \frac{1}{r}(\mathcal{B}''_{3223} + \bar{p}'') + \frac{1}{r^2}(\mathcal{B}'_{1122} - \mathcal{B}'_{1133} - \mathcal{B}'_{2233} - \mathcal{B}'_{3333} - \mathcal{B}'_{3223})$$

$$+\frac{1}{r^3}(\mathcal{B}_{1111} - 2\mathcal{B}_{1122} + 2\mathcal{B}_{2233} - \mathcal{B}_{3333}).$$

On substituting (5.4.6) and (5.4.8) into the boundary condition $(5.4.4)_2$, we obtain a matrix equation of the form $M\boldsymbol{d} = 0$ where M is a 4×4 matrix which is not written out here for the sake of brevity, and $\boldsymbol{d}$ is the column vector formed from the four disposable constants c_1, c_2, d_3, d_4. It then follows that the condition for zero to become a triple eigenvalue is $\det M = 0$, which can be reduced to

$$\Omega(\lambda_a, \lambda_z) = 0, \tag{5.4.11}$$

where $\Omega(\lambda_a, \lambda_z)$ is given by

$$\begin{aligned}\Omega(\lambda_a,\lambda_z) &= 2\zeta(b)(F_1 - b^2F_2 + D_1(b) - b^2a^{-2}D_1(a) + D_2(a) - D_2(b)) \\ &\quad -2\zeta(a)(F_1 - a^2F_2 - D_1(a) + a^2b^{-2}D_1(b) + D_2(a) - D_2(b)) \\ &\quad +(1-a^{-2}b^2)D_1(a)(F_1 - D_2(b)) + 2F_3(F_2 + a^{-2}D_1(a) - b^{-2}D_1(b)) \\ &\quad +(1-a^2b^{-2})D_2(a)(b^2F_2 - D_1(b)) - 2F_4(F_1 + D_2(a) - D_2(b)),\end{aligned} \tag{5.4.12}$$

together with

$$F_1 = \int_a^b \omega_1(t)dt, \quad F_3 = \int_a^b t\left(\int_a^t \omega_1(s)ds\right)dt,$$
$$F_2 = \int_a^b \omega_2(t)dt, \quad F_4 = \int_a^b t\left(\int_a^t \omega_2(s)ds\right)dt.$$
$$D_1(r) = \mathcal{B}_{1122} - \mathcal{B}_{1133} - \mathcal{B}_{2233} + r\mathcal{B}'_{3223} + \mathcal{B}_{3333} + r\bar{p}' + \sigma_3,$$
$$D_2(r) = \mathcal{B}_{1122} - \mathcal{B}_{1133} - 2\mathcal{B}_{2222} + 3\mathcal{B}_{2233} + r\mathcal{B}'_{3223} + 2\mathcal{B}_{3223} - \mathcal{B}_{3333} + r\bar{p}' - \sigma_3.$$

The explicit bifurcation condition (5.4.11) is valid for all types of loading conditions imposed at the two ends. Guided by what is known in the case when the tube is modeled as a membrane and by the numerical calculations conducted in the previous sections, we anticipate that there is some connection between (5.2.11) and (5.4.11). It turns out that the contour plots of $\Omega(\lambda_a, \lambda_z) = 0$ and $J(P, F) = 0$ in the (λ_a, λ_z)-plane always coincide. We therefore conclude that (5.2.11) and (5.4.11) are equivalent bifurcation conditions.

5.5 Effects of bending stiffness

With an explicit bifurcation condition at our disposal, we are now in a position to quantify precisely the effects of bending stiffness on the initiation pressure. We first

summarize the main results when the tube is modeled as a membrane. When a membrane tube is subjected to uniform inflation, the strain energy per unit surface area is given by $Hw(\lambda_1, \lambda_2)$, where H is the thickness in the undeformed configuration, w has the same meaning as in (5.2.2), and λ_1 ($\equiv \lambda_m$) and λ_2 ($\equiv \lambda_z$) are the *constant* stretches in the azimuthal and axial directions, respectively. The bifurcation condition for the initiation of a localized bulge in an infinitely long tube without any imperfections is $\Omega^{(0)}(\lambda_m, \lambda_z) = 0$ with $\Omega^{(0)}(\lambda_m, \lambda_z)$ given by (5.6.2); see Fu *et al* (2008, eqn (6.2)). The pressure $P_{\rm mem}$ and axial force $F_{\rm mem}$ are given by

$$\frac{R_m}{H} P_{\rm mem} = \frac{w_1}{\lambda_1 \lambda_2}, \qquad \frac{F_{\rm mem}}{2\pi R_m H} = w_2 - \frac{\lambda_1 w_1}{2\lambda_2} \equiv \mu \hat{F}(\lambda_1, \lambda_2), \tag{5.5.1}$$

where the last equation defines the function $\hat{F}$. As discussed in Section 2, two commonly used loading conditions correspond to fixed axial stretch or fixed axial force, respectively. In the former case, the bifurcation condition $\Omega^{(0)}(\lambda_1, \lambda_2) = 0$ can be solved to find the value of λ_m, and hence the critical pressure, at which localized bulging takes place. In the latter case, $\hat{F} = \text{const}$ can be solved to express λ_2 as a function of λ_1. In the $\lambda_1\lambda_2$-plane, the curve corresponding to this function may be viewed as the *loading path* that starts from the point with coordinates $(1, 1)$. The contour plot of the bifurcation condition $\Omega^{(0)}(\lambda_1, \lambda_2) = 0$ gives another curve in the same plane. Localized bulging may take place only if these two curves have at least one intersection. In the case of fixed axial stretch, the loading path is simply a horizonal line in the $\lambda_1\lambda_2$-plane.

Figures 5.5.1 and 5.5.2 depict two typical situations when such intersections may or may not take place, respectively. Figure 5.5.1 (a,b) shows results typical of material models for which the pressure curve in uniform inflation has an N shape when the axial force is fixed. In this case, each of the two loading curves $\hat{F}(\lambda_1, \lambda_2) = 0, 2$ and the bifurcation condition $\Omega^{(0)}(\lambda_1, \lambda_2) = 0$ have two intersections, which correspond to

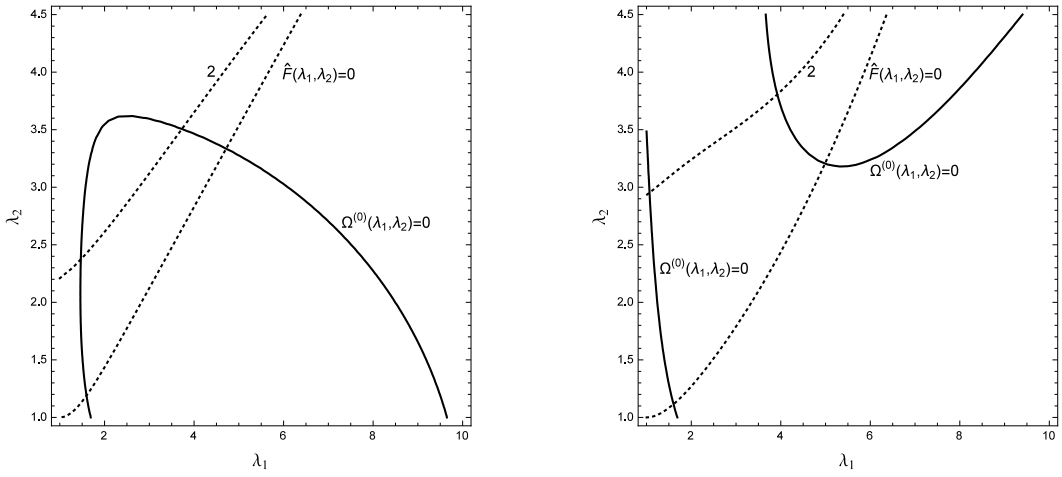

(a) (b)

Figure 5.5.1: Results for a Gent material with $J_m = 97.2$ (left figure) and for the Ogden material (right figure). In both figures the loading curve $\hat{F}(\lambda_1, \lambda_2) = 0$ or 2 (shown in dotted line) and bifurcation condition $\Omega^{(0)}(\lambda_1, \lambda_2) = 0$ have two intersections, but they differ in that according to the Gent model localized bulging becomes impossible when the axial force or axial stretch becomes sufficiently large, whereas according to the Ogden model localized bulging is always possible.

the pressure maximum and minimum in uniform inflation, respectively. However, the Gent and Ogden material models give different predictions in the high stretch regime: whereas according to the Ogden model localized bulging is always possible, the Gent model predicts that localized bulging becomes impossible when the axial force or axial stretch becomes sufficiently large. This is due to the fact that for the Gent material model the two branches of $\Omega^{(0)}(\lambda_1, \lambda_2) = 0$ are joined at a finite value of λ_z whereas for the Ogden material these two branches are never joined.

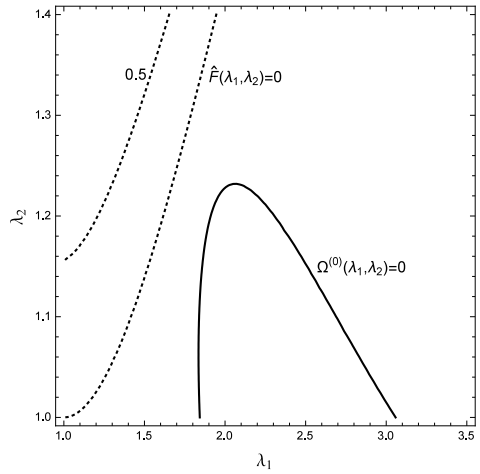

Figure 5.5.2: Results for the material model given by (5.2.23), showing the fact that $\hat{F}(\lambda_1, \lambda_2) = 0$ or 0.5 and $\omega(\lambda_1, \lambda_2)$ do not have any intersection and so localized bulging will not occur. However, localized bulging may still occur if it is the axial stretch that is held fixed during inflation.

In contrast, Figure 5.5.2 shows results corresponding to the material model given by (5.2.23), which are typical of material models for which the pressure does not have a maximum when the axial force is fixed. In this case, there are no intersections, which means that the pressure would be monotonic in uniform inflation. However, these results demonstrate the fact that even if localized bulging cannot take place in the case of fixed axial force, it may still occur in the case of fixed axial stretch. In the latter case the loading path in the $\lambda_a\lambda_z$-plane is simply a horizontal line and it has intersections with $\Omega^{(0)}(\lambda_1, \lambda_2) = 0$ provided λ_z does not exceed a threshold value (which is approximately equal to 1.23 in Figure 5.5.2).

We now proceed to discuss the effects of bending stiffness. We shall focus on the first

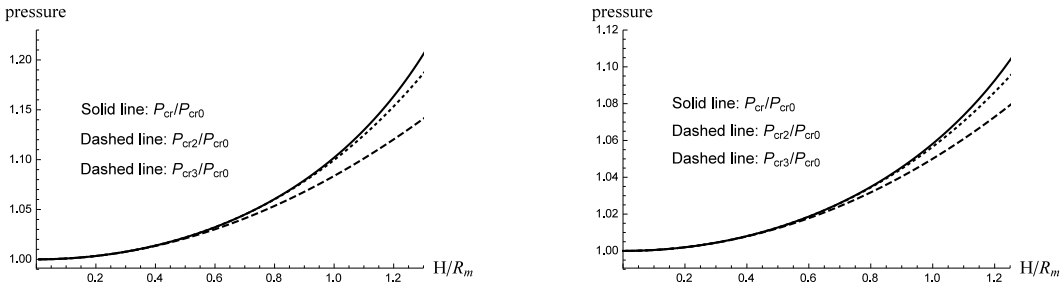

(a) (b)

Figure 5.5.3: Variation of $P_{\rm cr}/P_{\rm cr0}$ (solid line) and $P_{\rm cr1}/P_{\rm cr0}$ (dashed line) with respect to H/R when the axial force is fixed at 0. (a) When the Gent material model is used; (b) when the Ogden material model is used.

bifurcation point, and use $P_{\rm cr}$ and $P_{\rm cr0}$ to denote the critical pressures predicted by the exact theory and membrane theory, respectively. Figure 5.5.3 shows how good the membrane theory is in predicting the critical pressure for localized bulging when $F = 0$: it shows how the critical pressure $P_{\rm cr}$, normalized by $P_{\rm cr0}$, varies with respect to H/R (the dashed line and $P_{\rm cr1}$ in the figures will be defined in the next section). In the limit $H/R \to 0$, we have $P_{\rm cr}/P_{\rm mem} \to 1$ and so the membrane theory becomes exact. It can be seen that the membrane theory always under-predicts the initiation pressure, but due to the fact that the curve is very flat near $H/R = 0$ the error is less than 5% for values of H/R up to approximately 0.67.

Figure 5.5.4 shows how the contour plot of $\Omega(\lambda_a, \lambda_z) = 0$ evolves with respect to A (we have taken $B = 1$ without loss of generality). These results are based on the Gent material model with $J_m = 97.2$. The first curve corresponding to $A = 0.99$ is graphically indistinguishable from its membrane counterpart in Figure 5.5.1 (a). It

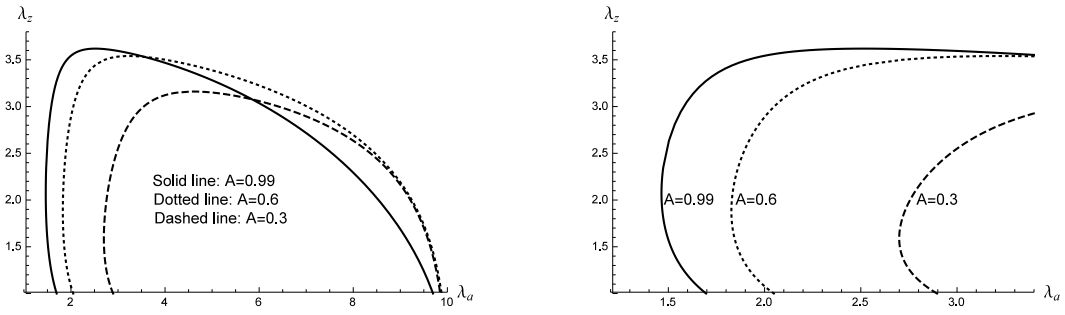

Figure 5.5.4: Evolution of the contour plot of $\Omega(\lambda_a, \lambda_z) = 0$ with respect to A when the Gent material model with $J_m = 97.2$ is used. The right plot shows a blow-up of the left plot near $\lambda_a = \lambda_z = 1$.

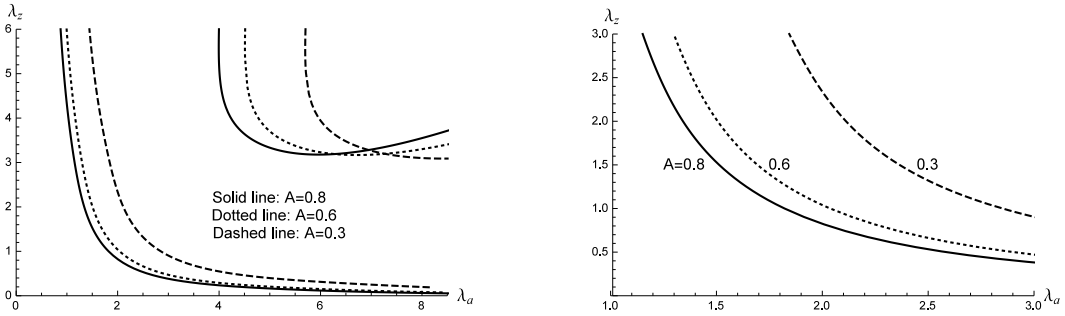

Figure 5.5.5: Evolution of the contour plot of $\Omega(\lambda_a, \lambda_z) = 0$ with respect to A when the Ogden material model is used. The right plot shows a blow-up of the left plot near $\lambda_a = \lambda_z = 1$.

shows clearly that for each fixed λ_z, the larger the wall thickness, the greater the critical value of λ_a. Similar behavior can be observed in Figure 5.5.5 when the Ogden material model is used.

Figure 5.5.6 offers a different perspective on the results of Figures 5.5.4 and 5.5.5 by

taking the horizontal axis as the normalized internal pressure defined by

$$\hat{P} = \frac{R}{\mu H} P, \tag{5.5.2}$$

where P is calculated using the expression (5.2.3). It shows that the normalized critical pressure is a decreasing function of the axial stretch. We also observe that at each fixed value of λ_z the normalized critical pressure would increase with respect to increase in the wall thickness, as expected, but such increases are almost negligible for values of A between 1 and 0.6. This is consistent with the observations made with regards Figure 5.5.3. Results shown in this figure can also be used directly to interpret the experimental results reported in Goncalves *et al* (2008). The authors in the latter paper conducted a series of experiments on localized bulging in thick-walled cylindrical tubes with H/R ranging from 0.25 to 0.5, and with λ_z fixed at a number of values in turn. All of their results show that the initiation pressure decreases with increased λ_z, which is consistent with our theoretical predictions displayed in Figure 5.5.6. To make a quantitative comparison with the results of Goncalves *et al* (2008), we consider the specimen that they numbered as B204. Using (5.5.2) together with their values for μ, A and B, and our Figure 5.5.6 to compute the dimensional initiation pressure (i.e. the values of P, rather than $\hat{P}$), we obtain 0.216, 0.189, and 0.168 (unit MPa) when λ_z is equal to $1, 1.16$ and 1.32, respectively. The corresponding values of the initiation pressure given by their Figure 5.5.4 are 0.194, 0.188, and 0.172. The agreement is very impressive, especially considering the fact that our choice of $J_m = 97.2$ do not necessarily fit their material. We observe, however, that in the above-mentioned paper the authors used a Mooney-Rivlin material model in their numerical simulations. It can be shown that according to this model, the critical pressure would increase when λ_z is increased, which would contradict their experimental results. Furthermore, the

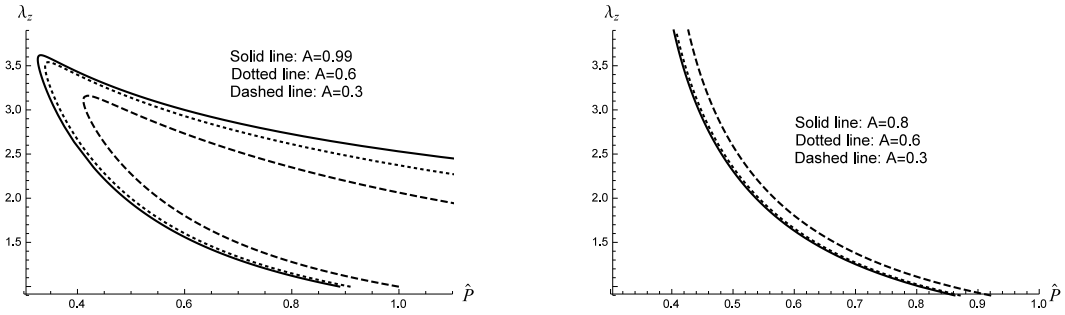

(a) (b)

Figure 5.5.6: Variation of λ_z with respect to the normalized pressure $\hat{P}$ when $F = 0$. (a) When the Gent material model is used; (b) when the Ogden material model is used.

Mooney-Rivlin material model is not suitable for modeling bulge initiation and propagation in another aspect: according to this model the diameter at the center of the bulge would grow for ever once the bulge has initiated (because the pressure versus volume curve does not have a minimum so that a Maxwell state corresponding to steady propagation cannot be reached).

5.6 A two-term approximation incorporating the effect of bending stiffness

Although (5.4.11), or equivalently (5.2.11), can be used to compute the exact initiation pressure for localized bulging for any given material model, it involves integrals that in general do not have closed-form expressions. In this section, we shall derive a two-term

approximation for this bifurcation condition that can be used to compute the initiation pressure with sufficient accuracy for values of H/R_m over a sufficiently large interval.

We first introduce the wall thickness $H = B - A$, averaged radius $R_m = (A + B)/2$, and define a dimensionless parameter ε through

$$\varepsilon = \frac{H}{R_m}.$$

We then have

$$A = R_m - \frac{H}{2}, \quad B = R_m + \frac{H}{2}, \quad a = r_m - \frac{h}{2}, \quad b = r_m + \frac{h}{2},$$

where h and r_m are the tube wall thickness and the averaged radius in the deformed configuration, respectively. We also have

$$\lambda_a = (\lambda_m - \frac{\varepsilon}{2\lambda_m\lambda_z})(1 - \frac{\varepsilon}{2})^{-1}, \quad \lambda_b = (\lambda_m + \frac{\varepsilon}{2\lambda_m\lambda_z})(1 + \frac{\varepsilon}{2})^{-1},$$

where λ_m is the azimuthal stretch at $r = r_m$ and we have replaced H/h by $\lambda_m\lambda_z$. At first sight, one may think that $H/h = \lambda_m\lambda_z$ is only valid to leading order, but it turns out that the above expressions satisfy the incompressibility condition (5.2.4) exactly.

With the use of the above expressions, it is found that the $\Omega(\lambda_a, \lambda_z)$ in (5.4.11) may be expanded as

$$\Omega(\lambda_a, \lambda_z) = \varepsilon^2 \frac{4}{\lambda_m^3\lambda_z^2}\Omega^{(0)} + \varepsilon^4 \frac{1}{6\lambda_m^7\lambda_z^4}\Omega^{(1)} + O(\varepsilon^6), \tag{5.6.1}$$

where $\Omega^{(0)}$ and $\Omega^{(1)}$ are given by

$$\Omega^{(0)} = \lambda_m(w_1 - \lambda_z w_{12})^2 + \lambda_z^2 w_{22}(w_1 - \lambda_m w_{11}), \tag{5.6.2}$$

$$
\begin{aligned}
\Omega^{(1)} \;=\;& 2\lambda_m(3+2\lambda_m^2\lambda_z)w_1^2 - 4\lambda_m^4\lambda_z(2-\lambda_m^2\lambda_z)w_1w_{11} - 8\lambda_m\lambda_z(1+\lambda_m^2\lambda_z)w_1w_{12} \\
&+6\lambda_z^2(1+\lambda_m^2\lambda_z)w_1w_{22} + 4\lambda_m^3\lambda_z^3w_{12}^2 + 2\lambda_m\lambda_z^2(1-\lambda_m^2\lambda_z)w_1w_{122} \\
&+2\lambda_m(1-\lambda_m^2\lambda_z)\left(\lambda_m^2(3-\lambda_m^2\lambda_z)w_1w_{111} - 2\lambda_m\lambda_z(1-\lambda_m^2\lambda_z)w_1w_{112}\right) \\
&\lambda_m^2\lambda_z(1-\lambda_m^2\lambda_z)^2\left(\lambda_z w_1w_{1122} - 2\lambda_m w_1w_{1112}\right) - 2\lambda_m^3(3-2\lambda_m^2\lambda_z)w_{11}^2 \\
&+\lambda_m\lambda_z(1+\lambda_m^2\lambda_z)\left(4\lambda_m(2-\lambda_m^2\lambda_z)w_{11}w_{12} - 6\lambda_z w_{11}w_{22}\right) \\
&+\lambda_m^2\lambda_z(1-\lambda_m^2\lambda_z)\left(4\lambda_m w_{11}w_{112} - 2\lambda_z w_{11}w_{122} + 3\lambda_z(1+\lambda_m^2\lambda_z)w_{111}w_{22}\right) \\
&+\lambda_m^3\lambda_z(\lambda_m^2\lambda_z-1)\left(2(3-\lambda_m^2\lambda_z)w_{111}w_{12} + 4\lambda_m\lambda_z^2w_{112}w_{12}\right) \\
&+\lambda_m^3\lambda_z^2(1-\lambda_m^2\lambda_z)^2(2w_{1112}w_{12} - w_{11}w_{1122} - w_{1111}w_{22}), \qquad (5.6.3)
\end{aligned}
$$

with all the partial derivatives of w evaluated at $\lambda_1 = \lambda_m$. As expected, the leading order result $\Omega^{(0)}(\lambda_m, \lambda_z) = 0$ is simply the bifurcation condition in the membrane approximation; see Fu *et al* [2008, eqn (4.8)]. With an error of order ε^4, the expression

$$\Omega^{(0)} + \frac{\varepsilon^2}{24\lambda_m^4\lambda_z^2}\Omega^{(1)} = 0 \qquad (5.6.4)$$

then gives a two-term approximation to the bifurcation condition that incorporates the effect of bending stiffness.

To the same order of accuracy, we may expand the right hand sides of (5.2.3) and (5.2.6) obtain

$$P = \varepsilon\frac{w_1}{\lambda_m\lambda_z} + \varepsilon^3\frac{K_1}{24\lambda_m^3\lambda_z^3} + O(\varepsilon^5), \qquad (5.6.5)$$

$$\frac{F}{\pi(B^2-A^2)} = w_2 - \frac{\lambda_m w_1}{2\lambda_z} + \varepsilon^2\frac{K_2}{48\lambda_m^3\lambda_z^3} + O(\varepsilon^4), \qquad (5.6.6)$$

where the coefficients K_1 and K_2 are defined by

$$
\begin{aligned}
K_1 \;=\;& 2\lambda_z w_1 + 2(\lambda_m^3\lambda_z^2 - \lambda_m\lambda_z)w_{11} + (1+\lambda_m^4\lambda_z^2 - 2\lambda_m^2\lambda_z)w_{111}, \\
K_2 \;=\;& (\lambda_m^2\lambda_z - 1)\left(2w_1 - 4w_{12}\lambda_z + 4w_{11}\lambda_m - 2w_{11}\lambda_m^3\lambda_z + w_{111}\lambda_m^2\right. \\
&\left.+2w_{112}\lambda_m^3\lambda_z^2 - 2w_{112}\lambda_m\lambda_z - w_{111}\lambda_m^4\lambda_z\right).
\end{aligned}
$$

As expected, the leading-order terms on the right hand sides of (5.6.5) and (5.6.6) correspond to the membrane approximation (5.5.1). The fact that the first correction term in (5.6.5) is of order ε^3 in some sense explains the excellent performance of the membrane theory as shown in Fig.5.5.3.

We note that an expansion similar to (5.6.5) was recently derived by Mangan & Destrade (2015). However, their expansion was in terms of H/A and their derivatives were evaluated at $\lambda_1 = \lambda_a$. As a result, their second term is quadratic in H/A.

On substituting (5.6.5) and (5.6.6) into the equivalent bifurcation condition (5.2.11) and keeping only the first two terms, we obtain

$$\Omega^{(0)} + \frac{\varepsilon^2}{24\lambda_m^3\lambda_z^2}\Omega^{(2)} = 0, \tag{5.6.7}$$

where $\Omega^{(2)}$ is given by

$$\begin{aligned}
\Omega^{(2)} \;=\;& 4w_1^2\lambda_m^2\lambda_z - (6-4\lambda_m^2\lambda_z)(w_{11}^2\lambda_m^2 + w_{12}^2\lambda_z^2) + 3w_{111}w_{22}\lambda_m\lambda_z^2(1-\lambda_m^4\lambda_z^2) \\
&+\lambda_m\lambda_z(1-\lambda_m^2\lambda_z)^2(2w_{1112}w_{12}\lambda_m\lambda_z - w_{1111}w_{22}\lambda_m\lambda_z - 4w_1w_{112}) \\
&+w_{12}\lambda_m^2\lambda_z(\lambda_m^2\lambda_z - 1)(2w_{111}\left(3-\lambda_m^2\lambda_z\right) + 4w_{112}\lambda_m\lambda_z^2) \\
&+w_{11}\lambda_m\lambda_z^2(-w_{1122}\lambda_m + 2w_{1122}\lambda_m^3\lambda_z + 2w_{122}\lambda_m^2\lambda_z - 6w_{22}\lambda_m\lambda_z - 2w_{122}) \\
&+4w_{11}w_{112}\lambda_m^2\lambda_z(1-\lambda_m^2\lambda_z) - 4w_{11}w_{12}\lambda_m\lambda_z(\lambda_m^2\lambda_z - 2)(\lambda_m^2\lambda_z + 1) \\
&+2\lambda_z(1-2\lambda_m^2\lambda_z)(2w_1w_{12} - w_1w_{1112}\lambda_m^2) + 2w_1\lambda_m\lambda_z^3(3w_{22} - w_{122}\lambda_m) \\
&+w_1\lambda_m^3\lambda_z(\lambda_m^2\lambda_z - 2)(4w_{11} + w_{1122}\lambda_z^2) + w_1\lambda_m\lambda_z^2(w_{1122} - 2w_{1112}\lambda_m^5\lambda_z) \\
&+2w_1\left\{w_{111}\lambda_m^2(1-\lambda_m^2\lambda_z)(3-\lambda_m^2\lambda_z) + w_{122}\lambda_z^2\right\} - w_{11}w_{1122}\lambda_m^6\lambda_z^4.
\end{aligned}$$

We note that although the first terms in (5.6.4) and (5.6.7) are identical, the second terms may differ from each other by a quantity of order ε^4.

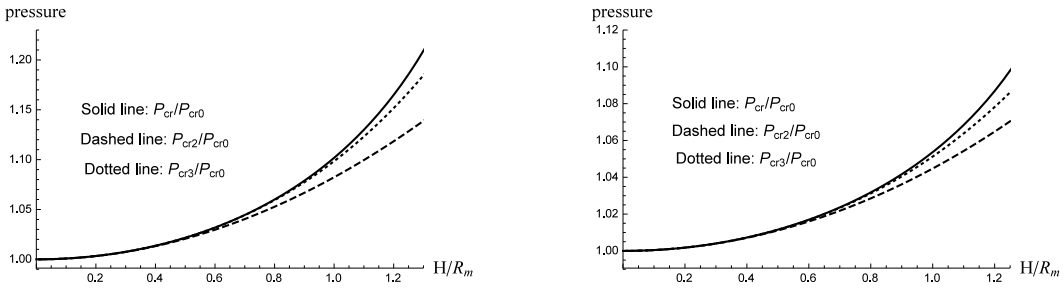

Figure 5.6.1: Comparison of the membrane theory with the exact theory and two other approximate theories that incorporate the effect of bending stiffness when the axial stretch λ_z is fixed at 1.1. (a) Results when the Gent material model is used; (b) results when the Ogden material model is used.

The two-term bifurcation condition (5.6.4) or (5.6.7), together with the associated two-term approximations (5.6.5) and (5.6.6) for the pressure and axial force, gives us a leading-order theory that incorporates the effect of bending stiffness. To demonstrate its accuracy, we have shown its performance in Figs 5.5.3 and 5.6.1 for the cases of fixed axial force and fixed axial stretch, respectively, with $P_{\rm cr2}$ denoting the critical pressure based on the approximation (5.6.7). It is found in all cases that against the exact result the relative error in predicting the initiation pressure is less than 5% for values of H/R_m up to as large as 1.2. Similar results are obtained for the cases when the axial stretch is fixed to be 1.2, 1.4 and 1.6, respectively.

In Figs 5.5.3 and 5.6.1 we have also shown the results when the values of λ_m and λ_z are calculated using the two-term approximations (5.6.7) and (5.6.6) but the critical pressure, denoted by $P_{\rm cr3}$, is calculated using a three-term expansion with the third

term given by

$$\frac{\varepsilon^5}{1920\lambda_m^5\lambda_z^5}\left(24\lambda_z^2 w_1 + 24\lambda_m\lambda_z^2(\lambda_m^2\lambda_z+1)(\lambda_m^2\lambda_z-1)w_{11} + \left(\lambda_m^2\lambda_z-1\right)^4 w_{11111}\right.$$

$$\left.+12\lambda_z(3\lambda_m^2\lambda_z+1)(\lambda_m^2\lambda_z-1)^2 w_{111} + 12\lambda_m\lambda_z(\lambda_m^2\lambda_z-1)^3 w_{1111}\right).$$

It is seen that there is significant improvement in the accuracy for the larger values of H/R_m. It is further found that with the values of λ_m and λ_z calculated using the two-term approximations but the critical pressure computed using the exact expression (5.2.3), the result in each case becomes graphically indistinguishable from the exact result for values of H/R_m up to as large as 1.33! To understand why the two-term bifurcation condition performs so well, we have shown in Fig.5.6.2 the contour plots of the exact bifurcation condition and its two-term approximation (5.6.7) for $\varepsilon = 0.22, 1.08$, respectively. It is seen that the two contour plots in each case are graphically indistinguishable in a sufficiently large part on the left; the two-term approximation only becomes increasingly poor in the large stretch regime as ε increases. Since it is the left part of the contour plot that is associated with the computation of the initiation pressure (see Fig.5.5.1 for two typical loading paths when the axial force is fixed and observe the fact when the axial stretch is fixed it is usually less than 2 in many applications), this explains why the two-term approximation (5.6.7) is almost exact as far as computation of the initiation pressure is concerned; the error mainly comes from the truncation of the power series expansion of the pressure.

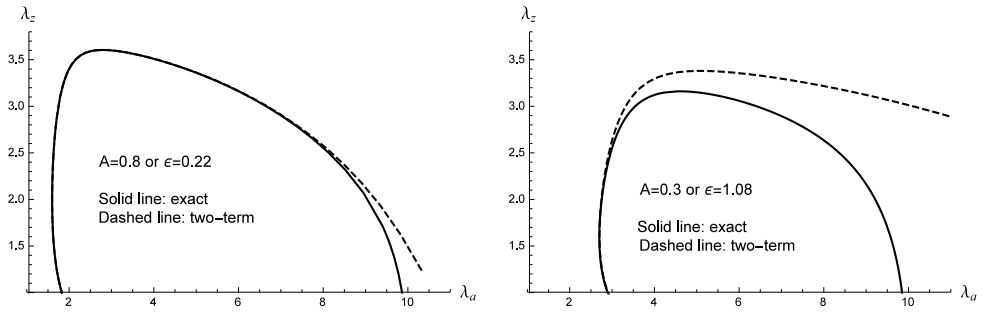

Figure 5.6.2: Comparison of the contour plots of the exact bifurcation condition and its two-term approximation (5.6.7) for $\varepsilon = 0.22, 1.08$.

5.7 Conclusion

In this chapter we have derived an explicit bifurcation condition for localized bulging in a cylindrical tube of arbitrary thickness with the aid of the exact 3D theory of non-linear elasticity. It is motivated by the fact that in some applications the cylindrical tube concerned may have walls thick enough so that the membrane theory may become invalid. Also, even if the membrane theory can be applied approximately it would be desirable to know precisely how good the approximation is. Using this explicit bifurcation condition, we are able to demonstrate that localized bulging is in fact possible for a cylindrical tube of arbitrary thickness. The initiation pressure varies linearly with respect to the wall thickness in the thin-wall limit, but this dependence becomes non-linear for thick-walled tubes. It is also demonstrated that the membrane theory is surprisingly accurate as far as prediction of the initiation pressure is concerned: the error involved is less than 5% for wall thickness/radius ratios up to 0.67. A two-term approximation of the exact bifurcation condition is proposed, and is shown to be almost exact as far as the determination of the initiation pressure is concerned. The

error mainly comes from the truncation of the power series expansion for the pressure: for thickness/radius ratios up to as large as 1.2, the relative error is less than 5% when two terms are kept in this expansion, and this error comes down to around 1% when three terms are kept in the expansion and to around 0.2% when the exact expression for the pressure is used. Thus, the two-term approximation of the exact bifurcation condition should be sufficient for all practical applications.

We conclude this chapter by highlighting the fact that contrary to popular belief, *absence of the limit point instability does not imply non-existence of localized bulging*. The limit point instability exclusively refers to the case of fixed resultant axial force (which is usually zero, as when a party balloon is inflated), but one can envisage a number of other loading conditions under which the resultant axial force is not fixed. In particular, for arteries it is more appropriate to assume that it is the axial stretch that is fixed. Based on the results in Figs 5.5.1 and 5.5.2, it is not hard to see that localized bulging is likely to be possible for ALL material models if the axial stretch is fixed to be below a certain threshold value that is dependent on the material model used. Whether localized bulging can take place or not can easily be verified by drawing the contour plot of the bifurcation condition as explained in the present chapter.

6 Conclusion and Perspectives

Localized bulging in an inflated cylindrical hyperelastic tube is characterized by three distinct phases: initiation, growth and propagation, which are also shared by a large variety of other localization problems in continuum mechanics. It is therefore a fundamental protypical problem whose understanding can help shed light on other more complicated localization problems. Although the first study on this problem was made as early as in 1891 by Mallock, it was only recently that this problem was recognized as a bifurcation problem and significant theoretical advances were made. However, in all these recent studies, the membrane assumption was made. Whereas this assumption is valid in many applications, there also exist situations where bending stiffness can be significant. The particular situation that motivated our present study is the mathematical modelling of the initiation of aneurysms in human arteries. In this context arteries are known to show noticeable bending stiffness in contrast with party balloons (Fung et al. 1979, Gasser et al. 2006).

There already exist a number of shell theories that take into account bending stiffness, but most of such theories were developed for hard and isotropic materials that exhibit linear constitutive behaviour. One noticeable exception is the theory developed by Steigmann and Ogden (1997, 1999) for materials with surface effects. Although they did not aim to develop a shell theory for shells made of soft materials, it is clear that their approach and formulation have effectively laid the necessary foundation for such a theory. This is the starting point for the first approach that we use to investigate the effect of bending stiffness. The constitutive mode that we use contains one disposable parameter that can be fixed by comparing with the exact 3D theory in the small

thickness limit. The advantage of this simple model is that it can potentially be used to describe the entire bulging process at least semi-analytically. It is shown that localized bulging is governed by a system of five non-linear ordinary differential equations. This can be viewed as a dynamical system with the axial variable playing the role of time. The coefficient matrix in its linearization has five real eigenvalues. The bifurcation condition for localized bulging corresponds to the simple fact that it is the condition for the two eigenvalues nearest to zero to coalesce, making zero a triple eigenvalue. This is the case even when the exact 3D theory of non-linear elasticity theory is used, as was shown in the previous chapter. We explored two methods in order to solve this non-linear dynamical system: the shooting method and finite difference method. We note that in the membrane case determination of the fully non-linear bulging solutions is straightforward because the initial values at $Z = 0$ can be determined by solving two algebraic equations and a single integration would yield the fully non-linear bulging solution. In our present case, there are only two integrals for the three unknowns at $Z = 0$. Even with a weakly non-linear solution used as an initial guess, our shooting procedure still failed to produce a valid bulging solution. With the finite difference scheme, we have had more success. We are able to compute fully non-linear bulging solutions when r_∞ is close to its critical value, and they agree well with the weakly non-linear analytical solutions, giving us confidence that our numerical scheme is correct. But as we move further away from the critical point, no convergent solutions could be obtained. Thus, although significant progress has been made in our modelling of the bending stiff effects, the work is not fully completed. We note that our difficulties are all related to the fact that localized bulging solutions are homoclinic orbits mathematically and the latter usually exist in a narrow parameter regime between periodic solutions and unbounded solutions.

Our final chapter is devoted to the derivation of an exact bifurcation condition for localized bulging with the use of the exact 3D theory of non-linear elasticity. We made a thorough study on the effect of bending stiffness on the initiation pressure. However, the price to pay when using this exact theory is that characterization of the weakly non-linear and fully non-linear bulging solutions would become extremely difficult. In this sense, the approaches employed in the last two chapters complement each other very nicely.

The research carried out in this thesis can be extended in a number of directions. Firstly, we shall complete our calculations of the fully non-linear bulging solutions using both the shooting method and the finite difference scheme. Secondly, the approach used in Chapter 4 can be explored further by considering more elaborate models for the second term representing the effect of bending stiffness. The ultimate goal would be a comprehensive shell theory for soft materials. Finally, arteries are not exactly isotropic hyperelastic materials. They are multi-layered and fibre-reinforced. Significant advances have been made in recent years on the constitutive modelling of arteries. Mathematical modelling of the initiation of aneurysms in arteries would ultimately also have to use such more realistic models.

A Expression of $\gamma(r_\infty)$

$$
\begin{aligned}
\gamma(r_\infty) \;=\; & -((z_\infty(\frac{z_\infty(2c-w_1^{(\infty)}+r_\infty w_{11}^{(\infty)})^2}{-2c(-1+r_\infty)-w_1^{(\infty)}+z_\infty w_{12}^{(\infty)}}-(\frac{1}{z_\infty}2cr_\infty^2((2r_\infty-2r_\infty^2 \\
& +z_\infty^2)w_{22}^{(\infty)}-\frac{1}{z_\infty}2cr_\infty^3((2r_\infty-2r_\infty^2+z_\infty^2)w_{22}^{(\infty)}+z_\infty^2)w_2^{(\infty)}+(-1+r_\infty) \\
& (2c(-1+r_\infty)+w_1^{(\infty)}-z_\infty w_{12}^{(\infty)}))-\frac{1}{z_\infty}cr_\infty^2w_1^{(\infty)}((2r_\infty-2r_\infty^2+z_\infty^2)w_{22}^{(\infty)} \\
& +(-1+r_\infty)(2c(-1+r_\infty)+w_1^{(\infty)}-z_\infty w_{12}^{(\infty)}))+cr_\infty^2w_{12}^{(\infty)}((2r_\infty-2r_\infty^2 \\
& +z_\infty^2)w_{22}^{(\infty)}+(-1+r_\infty)(2c(-1+r_\infty)+w_1^{(\infty)}-z_\infty w_{12}^{(\infty)}))+(2cr_\infty^2((2r_\infty \\
& -2r_\infty^2+z_\infty^2)w_2^{(\infty)}+(-1+r_\infty)(2c(-1+r_\infty)+w_1^{(\infty)}-z_\infty w_{12}^{(\infty)})) \\
& w_{122}^{(\infty)})/(z_\infty 22^{(\infty)}-(4cr_\infty^3((2r_\infty-2r_\infty^2+z_\infty^2)w_{22}^{(\infty)}+(-1+r_\infty)(2c(-1 \\
& +r_\infty)+w_1^{(\infty)}-z_\infty w_{12}^{(\infty)}))w_{122}^{(\infty)})/(z_\infty w_{22}^{(\infty)})+(2cr_\infty^4((2r_\infty-2r_\infty^2+z_\infty^2) \\
& w_{22}^{(\infty)}+(-1+r_\infty)(2c(-1+r_\infty)+w_1^{(\infty)}-z_\infty w_{12}^{(\infty)}))w_{122}^{(\infty)})/(z_\infty w_{22}^{(\infty)}) \\
& -(cr_\infty^2w_1^{(\infty)}((2r_\infty-2r_\infty^2+z_\infty^2)w_{22}^{(\infty)}+(-1+r_\infty)(2c(-1+r_\infty)+w_1^{(\infty)} \\
& -z_\infty w_{12}^{(\infty)}))122^{(\infty)})/(z_\infty w_{22}^{(\infty)})+(cr_\infty^3w_1^{(\infty)}((2r_\infty-2r_\infty^2+z_\infty^2)w_{22}^{(\infty)} \\
& +(-1+r_\infty)(2c(-1+r_\infty)+w_1^{(\infty)}-z_\infty w_{12}^{(\infty)}))w_{122}^{(\infty)})/(z_\infty w_{22}^{(\infty)}) \\
& +\frac{1}{w_{22}^{(\infty)}}cr_\infty^2w_{12}^{(\infty)}((2r_\infty-2r_\infty^2+z_\infty^2)w_{22}^{(\infty)}+(-1+r_\infty)(2c(-1+r_\infty) \\
& +w_1^{(\infty)}-z_\infty w_{12}^{(\infty)}))w_{122}^{(\infty)}-\frac{1}{w_{22}^{(\infty)}}cr_\infty^3w_{12}^{(\infty)}((2r_\infty-2r_\infty^2+z_\infty^2)w_{22}^{(\infty)} \\
& +(-1+r_\infty)(2c(-1+r_\infty)+w_1^{(\infty)}-z_\infty w_{12}^{(\infty)}))w_{122}^{(\infty)})/ \\
& -(cz_\infty w_{22}^{(\infty)}w_1^{(\infty)}(-2c+w_1^{(\infty)}-r_\infty w_{11}^{(\infty)}))/ \\
& (-2c(-1+r_\infty)-w_1^{(\infty)}+z_\infty w_{12}^{(\infty)})+(2z_\infty^3(w_{22}^{(\infty)})^2w_1^{(\infty)}(-2c+w_1^{(\infty)}-r_\infty w_{11}^{(\infty)}))/ \\
& (-2c(-1+r_\infty)-w_1^{(\infty)}+z_\infty w_{12}^{(\infty)})+(2cz_\infty w_{22}^{(\infty)}(2c-w_1^{(\infty)}+r_\infty w_{11}^{(\infty)}))/ \\
& (2c(-1+r_\infty)+w_1^{(\infty)}-z_\infty w_{12}^{(\infty)})-(6cr_\infty z_\infty w_{22}^{(\infty)}(2c-w_1^{(\infty)}+r_\infty w_{11}^{(\infty)}))/
\end{aligned}
$$

$$(2c(-1+r_\infty)+w_1^{(\infty)}-z_\infty w_{12}^{(\infty)})+(6cr_\infty^2 z_\infty w_{22}^{(\infty)}(2c-w_1^{(\infty)}+r_\infty w_{11}^{(\infty)}))/$$
$$(2c(-1+r_\infty)+w_1^{(\infty)}-z_\infty w_{12}^{(\infty)})-(2cr_\infty^3 z_\infty w_{22}^{(\infty)}(2c-w_1^{(\infty)}+r_\infty w_{11}^{(\infty)}))/$$
$$(2c(-1+r_\infty)+w_1^{(\infty)}-z_\infty w_{12}^{(\infty)})-(4cr_\infty^3 z_\infty (w_{22}^{(\infty)})^2(2c-w_1^{(\infty)}+r_\infty w_{11}^{(\infty)}))/$$
$$(2c(-1+r_\infty)+w_1^{(\infty)}-z_\infty w_{12}^{(\infty)})+(4cr_\infty z_\infty^3 (w_{22}^{(\infty)})^2(2c-w_1^{(\infty)}+r_\infty w_{11}^{(\infty)}))/$$
$$(2c(-1+r_\infty)+w_1^{(\infty)}-z_\infty w_{12}^{(\infty)})+(2cr_\infty z_\infty w_{22}^{(\infty)} w_1^{\infty}(2c-w_1^{(\infty)}+r_\infty w_{11}^{(\infty)}))/$$
$$(2c(-1+r_\infty)+w_1^{(\infty)}-z_\infty w_{12}^{(\infty)})-(cr_\infty^2 z_\infty w_{22}^{(\infty)} w_1^{(\infty)}(2c-w_1^{(\infty)}+r_\infty w_{11}^{(\infty)}))/$$
$$(2c(-1+r_\infty)+w_1^{(\infty)}-z_\infty w_{12}^{(\infty)})+(cr_\infty z_\infty^2 w_{22}^{(\infty)}(2c-w_1^{(\infty)}+r_\infty w_{11}^{(\infty)})w_{112}^{(\infty)})/$$
$$(2c(-1+r_\infty)+w_1^{(\infty)}-z_\infty w_{12}^{(\infty)})-(2cr_\infty^2 z_\infty^2 w_{22}^{(\infty)}(2c-w_1^{(\infty)}+r_\infty w_{11}^{(\infty)} w_{112}^{(\infty)})/$$
$$(2c(-1+r_\infty)+w_1^{(\infty)}-z_\infty w_{12}^{(\infty)})+(cr_\infty^3 z_\infty^2 w_{22}^{(\infty)}(2c-w_1^{(\infty)}+r_\infty w_{11}^{(\infty)})w_{112}^{(\infty)})/$$
$$(2c(-1+r_\infty)+w_1^{(\infty)}-z_\infty w_{12}^{(\infty)})-(2r_\infty z_\infty^4 (w_{22}^{(\infty)})^2(2c-w_1^{(\infty)}+r_\infty w_{11}^{(\infty)})w_{112}^{(\infty)})/$$
$$(2c(-1+r_\infty)+w_1^{(\infty)}-z_\infty w_{12}^{(\infty)})+\frac{1}{z_\infty}r_\infty^2(2c(-1+r_\infty)+w_1^{(\infty)}-z_\infty w_{12}^{(\infty)})$$
$$(cz_\infty w_{12}^{(\infty)}-cr_\infty z_\infty w_{12}^{(\infty)}+2cr_\infty w_{122}^{(\infty)}-4cr_\infty^2 w_{122}^{(\infty)}+2cr_\infty^3 w_{122}^{(\infty)}+5cz_\infty^2 w_{122}^{(\infty)}$$
$$-5cr_\infty z_\infty^2 w_{122}^{(\infty)}+2z_\infty^3 w_{12}^{(\infty)} w_{122}^{(\infty)}+w_1^{(\infty)}(c(-1+r_\infty)-2z_\infty^2 w_{122}^{(\infty)})-cw_{11}^{(\infty)}$$
$$+2cr_\infty w_{11}^{(\infty)}-cr_\infty^2 w_{11}^{(\infty)}+cz_\infty w_{112}^{(\infty)}-2cr_\infty z_\infty w_{112}^{(\infty)}+cr_\infty^2 z_\infty w_{112}^{(\infty)}+w_{22}^{(\infty)}$$
$$(2cr_\infty-2cr_\infty^2+5cz_\infty^2+2z_\infty^2 w_{11}^{(\infty)}-2z_\infty^3 w_{11}^{(\infty)})-2z_\infty^3 w_{112}^{(\infty)}))-((2c-w_1^{(\infty)}$$
$$+r_\infty w_{11}^{(\infty)}(-\frac{1}{z_\infty}r_\infty(2c(-1+r_\infty)+w_1^{(\infty)}-z_\infty w_{12}^{(\infty)})(z_\infty w_{222}^{(\infty)}(c(-1+r_\infty)$$
$$(-2r_\infty+2r_\infty^2-5z_\infty^2)-2z_\infty^2 w_1^{(\infty)}+2z_\infty^3 w_{12}^{(\infty)})-c(-1+r_\infty)^2(-2c+2cr_\infty$$
$$+w_1^{(\infty)}-z_\infty w_{12}^{(\infty)})-z_\infty^2 w_{122}^{(\infty)})+w_{22}^{(\infty)}(c(-1+r_\infty)(-2r_\infty+2r_\infty^2-z_\infty^2)$$
$$-2z_\infty^4 w_{122}^{(\infty)}))+z_\infty(-((c(-1+r_\infty)r_\infty(w_{22}^{(\infty)}+z_\infty w_{222}^{(\infty)})$$
$$(2c(-1+r_\infty)+w_1^{(\infty)}-z_\infty w_{12}^{(\infty)})((2r_\infty-2r_\infty^2+z_\infty^2)w_{22}^{(\infty)}+(-1+r_\infty)$$
$$(2c(-1+r_\infty)+w_1^{(\infty)}-z_\infty w_{12}^{(\infty)})))/(z_\infty^2 w_{22}^{(\infty)}))-w_{22}^{(\infty)}(c(-1+r_\infty)^2$$
$$(-2z_\infty^2 w_{22}^{(\infty)})(-2c(-1+r_\infty)-w_1^{(\infty)}-(z_\infty^2 w_{122}^{(\infty)}(2c-w_1^{(\infty)}+r_\infty w_{11}^{(\infty)}))/$$
$$(-2c(-1+r_\infty)-w_1^{(\infty)}+z_\infty w_{12}^{(\infty)})+r_\infty z_\infty w_{112}^{(\infty)})))))/$$

$$(2c(-1+r_\infty)+w_1^{(\infty)}-z_\infty w_{12}^{(\infty)})+cr_\infty^2 z_\infty w_{22}^{(\infty)}w_{111}^{(\infty)}$$

$$-2cr_\infty^3 w_{22}^{(\infty)}w_{111}^{(\infty)}+cr_\infty^4 z_\infty w_{22}^{(\infty)}w_{111}^{(\infty)}-2r_\infty^2 z_\infty^3 (w_{22}^{(\infty)})^2 w_{111}^{(\infty)})/$$

$$w_{22}^{(\infty)}(c(-1+r_\infty)^2-2z_\infty^2 w_{22}^{(\infty)}))))/$$

$$(3(\frac{2c^2r_\infty^3}{c(-1+r_\infty)^2-2z_\infty^2 w_{22}^{(\infty)}}-\frac{6c^2r_\infty^4}{c(-1+r_\infty)^2-2z_\infty^2 w_{22}^{(\infty)}}$$
$$+\frac{6c^2r_\infty^5}{c(-1+r_\infty)^2-2z_\infty^2 w_{22}^{(\infty)}}-\frac{2c^2r_\infty^6}{c(-1+r_\infty)^2-2z_\infty^2 w_{22}^{(\infty)}}$$
$$-\frac{3c^2r_\infty^2 z_\infty^2}{c(-1+r_\infty)^2-2z_\infty^2 w_{22}^{(\infty)}}-\frac{3cr_\infty^2 z_\infty^2}{c(-1+r_\infty)^2-2z_\infty^2 w_{22}^{(\infty)}}$$
$$+\frac{6c^2r_\infty^3 z_\infty^2}{c(-1+r_\infty)^2-2z_\infty^2 w_{22}^{(\infty)}}+\frac{6cr_\infty^3 z_\infty^2}{c(-1+r_\infty)^2-2z_\infty^2 w_{22}^{(\infty)}}$$
$$-\frac{3c^2r_\infty^2 z_\infty^2}{c(-1+r_\infty)^2-2z_\infty^2 w_{22}^{(\infty)}}-\frac{3cr_\infty^2 z_\infty^2}{c(-1+r_\infty)^2-2z_\infty^2 w_{22}^{(\infty)}}$$
$$-\frac{3c^2r_\infty^4 z_\infty^2}{c(-1+r_\infty)^2-2z_\infty^2 w_{22}^{(\infty)}}-\frac{3cr_\infty^4 z_\infty^2}{c(-1+r_\infty)^2-2z_\infty^2 w_{22}^{(\infty)}}$$
$$-\frac{cr_\infty^2 z_\infty w_2^{(\infty)}}{c(-1+r_\infty)^2-2z_\infty^2 w_{22}^{(\infty)}}-\frac{2cr_\infty^3 z_\infty w_2^{(\infty)}}{c(-1+r_\infty)^2-2z_\infty^2 w_{22}^{(\infty)}}$$
$$-\frac{cr_\infty^4 z_\infty w_2^{(\infty)}}{c(-1+r_\infty)^2-2z_\infty^2 w_{22}^{(\infty)}}+\frac{2c^3r_\infty^2}{w_{22}^{(\infty)}(c(-1+r_\infty)^2-2z_\infty^2 w_{22}^{(\infty)})}$$
$$+\frac{2c^2r_\infty^2}{w_{22}^{(\infty)}(c(-1+r_\infty)^2-2z_\infty^2 w_{22}^{(\infty)})}-\frac{8c^3r_\infty^3}{w_{22}^{(\infty)}(c(-1+r_\infty)^2-2z_\infty^2 w_{22}^{(\infty)})}$$
$$+\frac{12c^3r_\infty^4}{w_{22}^{(\infty)}(c(-1+r_\infty)^2-2z_\infty^2 w_{22}^{(\infty)})}+\frac{12c^3r_\infty^4}{w_{22}^{(\infty)}(c(-1+r_\infty)^2-2z_\infty^2 w_{22}^{(\infty)})}$$
$$-\frac{8c^3r_\infty^5}{w_{22}^{(\infty)}(c(-1+r_\infty)^2-2z_\infty^2 w_{22}^{(\infty)})}-\frac{8c^2r_\infty^5}{w_{22}^{(\infty)}(c(-1+r_\infty)^2-2z_\infty^2 w_{22}^{(\infty)})}$$
$$+\frac{2c^3r_\infty^6}{w_{22}^{(\infty)}(c(-1+r_\infty)^2-2z_\infty^2 w_{22}^{(\infty)})}+\frac{2c^2r_\infty^6}{w_{22}^{(\infty)}(c(-1+r_\infty)^2-2z_\infty^2 w_{22}^{(\infty)})}$$
$$-\frac{2c^3r_\infty^2}{w_{22}^{(\infty)}(c(-1+r_\infty)^2-2z_\infty^2 w_{22}^{(\infty)})}+\frac{4cr_\infty^3 z_\infty^2 w_{22}^{(\infty)}}{c(-1+r_\infty)^2-2z_\infty^2 w_{22}^{(\infty)}}$$
$$+\frac{4cr_\infty^4 z_\infty^2 w_{22}^{(\infty)}}{c(-1+r_\infty)^2-2z_\infty^2 w_{22}^{(\infty)}}-\frac{2cr_\infty^2 z_\infty^4 w_{22}^{(\infty)}}{c(-1+r_\infty)^2-2z_\infty^2 w_{22}^{(\infty)}}-\frac{2cr_\infty^2 z_\infty^4 w_{22}^{(\infty)}}{c(-1+r_\infty)^2-2z_\infty^2 w_{22}^{(\infty)}}$$

$$-\frac{2c^2r_\infty^2z_\infty^3w_1^{(\infty)}w_{22}^{(\infty)}}{c(-1+r_\infty)^2-2z_\infty^2w_{22}^{(\infty)}}+\frac{4c^2r_\infty^2z_\infty^2w_1^{(\infty)}}{c(-1+r_\infty)^2-2z_\infty^2w_{22}^{(\infty)}}-\frac{4cr_\infty^3z_\infty^2w_1^{(\infty)}}{c(-1+r_\infty)^2-2z_\infty^2w_{22}^{(\infty)}}$$
$$-\frac{2c^2r_\infty^2w_1^{(\infty)}}{w_{22}^{(\infty)}(c(-1+r_\infty)^2-2z_\infty^2w_{22}^{(\infty)})}+\frac{6c^2r_\infty^3w_1^{(\infty)}}{w_{22}^{(\infty)}(c(-1+r_\infty)^2-2z_\infty^2w_{22}^{(\infty)})}$$
$$-\frac{6c^2r_\infty^4w_1^{(\infty)}}{w_{22}^{(\infty)}(c(-1+r_\infty)^2-2z_\infty^2w_{22}^{(\infty)})}+\frac{2c^2r_\infty^5w_1^{(\infty)}}{w_{22}^{(\infty)}(c(-1+r_\infty)^2-2z_\infty^2w_{22}^{(\infty)})}$$
$$-\frac{4cr_\infty^2z_\infty^3w_{12}^{(\infty)}}{c(-1+r_\infty)^2-2z_\infty^2w_{22}^{(\infty)}}+\frac{4cr_\infty^3z_\infty^2w_{12}^{(\infty)}}{c(-1+r_\infty)^2-2z_\infty^2w_{22}^{(\infty)}}$$
$$+\frac{2c^2r_\infty^2z_\infty w_{12}^{(\infty)}}{w_{22}^{(\infty)}(c(-1+r_\infty)^2-2z_\infty^2w_{22}^{(\infty)})}-\frac{6c^2r_\infty^3z_\infty w_{12}^{(\infty)}}{w_{22}^{(\infty)}(c(-1+r_\infty)^2-2z_\infty^2w_{22}^{(\infty)})}$$
$$+\frac{6c^2r_\infty^4z_\infty w_{12}^{(\infty)}}{w_{22}^{(\infty)}(c(-1+r_\infty)^2-2z_\infty^2w_{22}^{(\infty)})}-\frac{2c^2r_\infty^5z_\infty w_{12}^{(\infty)}}{w_{22}^{(\infty)}(c(-1+r_\infty)^2-2z_\infty^2w_{22}^{(\infty)})}))).$$

References

[1] Afendikov, A.L. and T.J.Bridges (2001). Instability of the Hocking- Stewartson pulse and its implications for three-dimensional Poiseuille flow. *Proceedings: Mathematical, Physical and Engineering Sciences* 457(2006), 257-272.

[2] Akkas, N. (1990). Aneurysms as a biomechanical instability problem. *In:F. Mosora(ed.), Biomechanical Transport Processes, Plenum Press* 303 C 311.

[3] Alexander, H. (1971). The tensile instability of an inflated cylindrical membrane as affected by an axial load. *International Journal of Mechanical Sciences* 13, 87-95.

[4] Alhayni, A.A., J.A. Giraldo, J. Rodríguez, and J. Merodio (2013). Computational modelling of bulging of inflated cylindrical shells applicable to aneurysm formation and propagation in arterial wall tissue. *Finite elements in Analysis and Design* 73, 20-29.

[5] Alhayni, A.A., J.A. Giraldo, and J. Rodríguez and, J. Merodio (2014). Competition between radial expansion and axial propagation in bulging of inflated cylinders with application to aneurysm propagation in arterial wall tissue. *International Journal of Engineering and Science* 85, 74-89.

[6] Antman, S.S. (2005). *Non linear problems of elasticity* Berlin: Springer-Verlag.

[7] Ascher, U., R.M.M. Mattheij, and R.D. Russell (1988). *Numerical Solution of Boundary Value Problems for Ordinary Differential Equations*, Prentice-Hall.

[8] Berdichevsky, V.L. (1970). *Variational equation of continuum mechanics. In problem of solid mechanics.* V. Novozhilov 60th birthday anniversary volume.

[9] Bertram, A. (2008). *Elasticity and Plasticity of Large Deformations (Second edition).* Berlin: Springer-Verlag.

[10] Blyth, M.G. and C. Pozrikidis (2004). Solution space of axisymetric capsules enclosed by elastic membranes. *European Journal of Mechanics* 23, 877-892.

[11] Bridges, T.J. (1999). The Orr-Sommerfeld equation on a manifold. *Proceedings of Royal Society of London* A 455, 3019-3040.

[12] Boulanger, P. and M. Hayes, (2001). Finite Amplitude Waves in Mooney- Rivlin and Hadamard Materials, in Topics in Finite Elasticity. *International Center for Mechanical Sciences* 424, 131-167.

[13] Carroll, M.M. (1987). Pressure maximum behaviour in inflation of incompressible elastic hollow spheres and cylinders. *Quarterly of Applied Mathematics* 45, 141-154.

[14] Chater, E. and J.W. Hutchinson (1984). On the propagation of bulges and buckles. *ASME Journal of Applied Mechanics* 51, 269-277.

[15] Chadwick, P. (1999). *Continuum Mechanics: Concise Theory and Problems* (Second edition) Dover Publications.

[16] Ciarlet, P.G. (1997). *Mathematical elasticity, Volume II, Theory of plates*, North-Holland.

[17] Delfino, A., N. Stergiopulos, J.E. Moore, and J. Meister (1997). Residual strain effects on the stress field in a thick wall finite element model of the human carotid bifurcation. *Journal of Biomechanics* 30, 777-786 777786.

[18] Destrade, D., A.N. Annaidh and Coman (2009). Bending instabilities of soft tissues, *International Journal of Solid and Structures* 46, 4322-4330.

[19] Duclaux, V., F. Gallaire, and C. Clanet (2010). A fluid mechanical view on abdominal aortic aneurysms. *Journal of Fluid mechanics* 664, 5-32.

[20] Erbay, H.A. and H. Demiray (1995). Finite axisymmetric deformations of elastic tubes, An approximate method. *Journal of Engineering Mathematics* 29, 451-472.

[21] Ericksen, J.L. (1975). Equilibrium of bars. *Journal of Elasticity* 5, 191-201.

[22] Friedrichs, K.O. (1955a). Asymptotic phenomena in mathematical physics. *Bulletin of the American Mathematical Society* 61, 485-504.

[23] Forsythe, G.E. and W.A. Wasow (1964). *Finite difference method for partial differential equations*. Wiley, New York, pp. 444.

[24] Fu, Y.B., S.P. Pearce, and K.K. Liu (2008). Post-bifurcation analysis of a thin-walled hyperelastic tube under inflation. *International Journal of Non-Linear Mechanics* 43(8), 697-706.

[25] Fu, Y.B. (2001). Perturbation methods and non-linear stability analysis. In Y.B. Fu and R.W. Ogden (Eds.). *Non-linear Elasticity: Theory and Applications* pp. 345-391. Cambridge University Press.

[26] Fu, Y.B. and Y.X. Xie (2010). Stability of localised bulging in inflated membrane tubes under volume control. *International Journal of Engineering Sciences* 48, 1242-1252.

[27] Fu, Y.B. and S.P. Pearce (2010). Characterisation and stability of localised bulging/ necking in inflated membrane tubes. *IMA Journal of Applied Mathematics* 75, 581-602.

[28] Fu, Y.B., G.A. Rogerson, and Y.T. Zhang (2011). Initiation of aneurysms as a

mechanical bifurcation phenomenon. *International Journal of Non-Linear Mechanics* 75, 581-602.

[29] Fu, Y.B. and Y.X. Xie (2012). Effects of imperfections on localised bulging in inflated tubes. *Philosophical Transactions of the Royal Society of London* A370, 1896-1911.

[30] Fu, Y.B. and A.T. Ilichev (2010). Solitary waves in fluid filled elastic tubes: existence, persistence and the role of axial displacement. *IMA Journal of Applied Mathematics* 75(2), 257-268.

[31] Fu Y.B. and A.T. Ilichev (2015). At Localized standing waves in a hyperelastic membrane tube and their stabilization by a mean flow. *Journal of Mathematics and Mechanics of Solids* 1-17.

[32] Fu Y.B. and Pour S.P. M.S. (2002). WKB methods with repeated roots and its application to the buckling analysis of an everted cylindrical tube. *SIAM Journal of Applied Mathematics* 62,1856-1876.

[33] Fu Y.B., J.L. Liu, and G. Francisco, (2016). Localized bulging in an inflated cylindrical tube of arbitrary thickness - the effect of bending stiffness. *Journal of the Mechanics and Physics of Solids.* DOI: 10.1016/j.jmps.2016.02.027

[34] Fung, Y.C., K. Froneck, and P. Patitucci (1979). Pseudoelasticity of arteries and the choice of its mathematical expression. *American Journal of Physiology* 237, H620-H631.

[35] Fung, Y. (1993). *Biomechanics: Mechanical Properties of Living Tissues.* Springer.

[36] Gasser, T.C., R.W. Ogden, and G.A. Holzapfel (2006). Hyperelastic modelling of

arterial layers with distributed collage fibre orientations. *Journal of Royal Society* 3, 15-351.

[37] Gent, A.N. (1996). A new constitutive relation for rubber. *Rubber chemistry and technology* 69(1), 59-61.

[38] Gent, A.N. (2005). Elastic instabilities in rubber. *International Journal of Non-liner Mechanics* 40, 165-175.

[39] Goldenveize, A.L. (1961). *Theory of thin elastic shells.* Pergamon Press.

[40] Goncalves, P.B., D. Pamplona, and S.R.X. Lopes (2008). Finite deformations of an initially stressed cylindrical shell under internal pressure. *International Journal of Mechanical Sciences* 50(1), 92-103.

[41] Green, A.E. (1963). Boundary layer equations in the linear theory of thin elastic shells. *Proceedings of the Royal Society of London. Mathematical and Physical Sciences* 269(1339), 481-491.

[42] Gurtin, M.E., and A.I. Murdoch (1975). A continuum theory of elastic material surfaces. *Archive of Rational Mechanics and Analysis* 57, 291-323.

[43] Haughton, D.M. and R.W. Ogden (1979a). Bifurcation of inflated circular cylinders of elastic material under axial loading-I. Membrane theory for thin walled tubes. *Journal of the Mechanics and Physics of Solids* 27, 179-212.

[44] Haughton, D.M. and R.W. Ogden (1979b). Bifurcation of inflated circular cylinders of elastic material under axial loading-II. Membrane theory for thick walled tubes. *Journal of the Mechanics and Physics of Solids* 27. 489-512.

[45] Heil, M (1996). The stability of cylindrical shells conveying viscous flow. *Journal*

of Fluids and Structures 10, 173-196.

[46] Heil M. and T.J. Pedley (1995). Large axisymmetric deformation of a cylindrical shell conveying a viscous flow. *Journal of Fluids and Structures* 9, 237-256.

[47] Heil M. and T.J. Pedley (1996). Large post-buckling deformations of cylindrical shells conveying viscous flow. *Journal of Fluids and Structures* 10, 565-599.

[48] Hildebrand, F.B. (1974). *Introduction to numerical analysis*, Tata-McGraw Hill, New Delhi, pp. 669

[49] Holzapfel, G.A. (2000). *Non-linear Solid Mechanics: A Continuum Approach for Engineering*. WileyBlackwell.

[50] Horgan, C.O. and G. Saccomandi (2002). Constitutive modelling of rubber-like and biological materials with limiting chain extensibility. *Mathematics and Mechanics of Solids* 7, 353-371.

[51] Horgan, C.O. and G. Saccomandi (2003). A description of arterial wall mechanics using limiting chain extensibility constitutive models. *Biomechanics and Modelling in Mechanobiology*1 4, 251-266.

[52] Humphrey, J.D. and K.R. Rajagopal (2004). A constrained mixture model for growth of the abdominal aortic aneurysm. *Biomechan Model Mechanobiol* 3, 98-113.

[53] Humphrey, J.D., J.F. Eberth, W.W. Dye, and G.R.L. (2009). Fundamental role of axial stress in compensatory adaptations by arteries. *Journal of Biomechanics* 42(1), 1-8.

[54] Kanner, L.M. and C.O. Horgan (2007). Elastic instabilities for strain -stiffening rubber- like spherical and cylindrical thin shells under inflation. *International Journal*

of Non-Linear Mechanics 42(2), 204-215.

[55] Kaplunov, J.D., L.Y. Kossovich, and E.V. Nolde (1998). *Dynamics of thin-walled elastic bodies*, (Academic Press).

[56] Kirchgassner, K. (1982), Wave solutions of reversible system and applications. *Journal of Differential Equations* 45, 113-127.

[57] Kolos, V. (1965). Methods of refining the classical theory of bending and extension of plates. *Journal of Applied Mathematics and Mechanics* 29, 914-925.

[58] Koiter, W.T (1996). On the non-linear theory of thin elastic shells. . *Kon. Ned. Akad. Wetensch.* B 69, 1-54.

[59] Koiter, W.T. and J.G. Simmonds (1973).Foundations of shell theory, in Applied Mechanics, *Proceedings of the 13th International Congress of Theoretical and Applied Mechanics, Moscow, Springer- Verlag, Berlin* 150-176.

[60] Kyriakides, S. and Y.C. Chang (1990). On the inflation of a long elastic tube in the presence of axial load. *International journal of Solid structure* 26, 975-991.

[61] Kyriakides, S. and Y.C. Chang (1991). The initiation and propagation of a localized instability in an inflated elastic tube. *International journal of Solid structure* 27(9), 1113-1137.

[62] Lasheras, J.C. (2007). The biomechanics of arterial aneurysms. *The annual review of Fluid Mechanics* 39, 293-319.

[63] Learoyd, B.M. and M.G. Taylor (1966). Alternations with age in the viscoelastic properties of human arterial walls. *Circulation Research* 18(3), 278.

[64] Le K.C. (1999). *Vibrations of shells and rods.* Springer.

[65] Libai, A. and J.G. Simmonds (1998). *The Non-linear Theory of Elastic Shells*. Cambridge University Press, Cambridge.

[66] Liu, Y.P., C. Li, K.K. Liu, and A.C.K. Lai (2006). The deformation of an erythrocyte under the radiation pressure by optical stretch. *Journal of Biomechanical Engineering* 128, 830.

[67] Mallock, A. (1891). Note on the instability of India-rubber tubes and balloons when distended by fluid pressure. *Proceedings of the Royal Society of London* A 49, 458-463.

[68] Mangan, R. and M. Destrade (2015). Gent models for the inflation of spherical balloons. *International Journal of Non-linear Mechanics* 68, 52-58.

[69] McGloughlin, T.(ed.) (2011). *Biomechanics and mechanobiology of aneurysms*. Studies in Mechanobiology, tissue Engineering and Biomaterials 7.

[70] Mielke, A. (1991). *Hamiltonian and Lagrangian Flows on Center Manifolds, with Applications to Elliptic Variational Problems*. Springer-Verlag (Lecture Notes in Mathematics volume 1489), Berlin.

[71] Mitchell, A. R., and D.F. Griffiths (1980). *The finite difference method in partial differential equations*. Wiley-Inter science publication, Chichester, Wiley.

[72] M̈uller, I. and P.P. Strehlow (2004). *Rubber and Rubber Balloons: Paradigms of Thermodynamics*, Springer-Verlag.

[73] Nagatou K. (2003). Mathematics for eigenvalue problem. *Bulletin of the Japan society for Industrial and Applied Mathematics*. 13(3), 58-71.

[74] Ng, B.S. and W.H. Reid (1985). The compound matrix method for ordinary

differential systems. *Journal of Computational Physics* 58(2), 209-228.

[75] Noether, E. (1971). Invariant variation problems. *Transport theory and Statistical.*Physics 1, 186-207.

[76] Ogden, R.W. (1972). Large deformation isotropic elasticity-on the correlation of theory and experiment for incompressible rubber like solids. *Proceedings of the Royal Society of London. Series A, Mathematical and Physical Sciences* 326, 565-584.

[77] Ogden, R.W. (1997). *Non-linear elastic deformations.* Dover Publications.

[78] Ogden, R.W. (2011). Non-linear Mechanics of soft solids including Biological Tissues. Lecture notes Chapter 5, 37-40.

[79] Ogden, R.W., D.J. Steigmann, and D.M. Haughton (1997). The effect of elastic surface coating on the finite deformation and bifurcation of a pressurized circular annulus. *Journal of Elasticity* 47, 121-145.

[80] Pamplona, D.C., P.B. Goncalves, and S.R.X. Lopes (2006). Finite deformations of cylindrical membrane under internal pressure. *International journal of Mechanical Sciences* 48, 683-696.

[81] Pamplona, D.C., and C.R. Calladine, (1993). The mechanics of axially symmetric liposomes. *Journal of Biomechanical Engineering* 115, 149.

[82] Pego, R.L. and M.I. Weinstein, (1992) Eigenvalues, and instabilities of solitary waves. *Royal Society of London* 340, 47-92.

[83] Pozrikidis, C. (2001). Interfacial dynamics for stokes flow. Journal for Computations Physics.

[84] Rodríguez-Martnez, J.A., J. Femandez-Saez, and R. Zaera (2015). The role of

constitutive relation in the stability of hyper- elasticspherical membranes subjected to dynamic inflation. *International Journal of Engineering and Science* 93, 31-45.

[85] Selvadurai, A.P.S.(2006). Deflections of a Rubber Membrane, *Journal of the Mechanics and Physics of Solids* 54(6), 1093-1119.

[86] Shi J. and G.F. Moita (1996). The post-critical analysis of axisymmetric hyperelastic membranes by the finite element method Computer Methods in Applied Mechanics Engineering 135 265 281 doi: 10.1016/0045-7825(96)01047-X.

[87] Spencer, A.J.M. (1980). *Continuum mechanics.* Longman Mathematical Texts.

[88] Steigmann, D.J. and R.W. Ogden (1997). Plane deformations of elastic solids with intrinsic boundary elasticity. *Journal of Mathematical, Physical and Engineering Sciences* 453, 853-877.

[89] Steigmann, D.J. and R.W. Ogden (1999). Elastic surface–substrate interactions. *Journal of Mathematical, Physical and Engineering Sciences* 455, 437-474.

[90] Steigmann, D.J. (2012). Extension of Koiter's linear shell theory to materials exhibiting arbitrary symmetry. *Journal of Engineering Sciences* 51, 216 -232.

[91] Varga, O.H. (1966). *Stress-strain behaviour of elastic materials: selected problems of large deformations* Inter-science Publishers.

[92] Vorp, D.A. (2007). Biomaechanics of abdominal aortic aneurysm. *Journal of Biomech* 40, 1887-1902.

[93] Watton, P.N, N.A. Hill, and M.A. Heil (2004). A mathematical model for the growth of the abdominal aortic aneurysms. *Journal of Biomechan Model Mechanobiol* 3, 98-113.

[94] Yamaki, N. (1969). *Buckling of circular cylindrical shells under external pressure.* Reports of the Institute of High Speed Mechanics 20, 35-55.

[95] Yamaki, N. (1984). *Elastic Stability of Circular Cylindrical Shells.* North-Holland, Amsterdam.

[96] Yin, W.L. (1977). Non-uniform inflation of a cylindrical elastic membrane and direct determination of the strain energy function. *Journal of Elasticity* 7(3), 265-282.